Chain-end modification of polymer-iodide synthesized via organocatalyzed living radical polymerization and its application in functional materials

Chen CHEN

SCHOOL OF PHYSICAL AND MATHEMATICAL SCIENCES

2019

Chain-end modification of polymer-iodide synthesized via organocatalyzed living radical polymerization and its application in functional materials

Chen CHEN

SCHOOL OF PHYSICAL AND MATHEMATICAL SCIENCES

A thesis submitted to the Nanyang Technological
University in partial fulfilment of the requirement for the
degree of Doctor of Philosophy

2019

Statement of Originality

I hereby certify that the work embodied in this thesis is the result of original research done by me except where otherwise stated in this thesis. The thesis work has not been submitted for a degree or professional qualification to any other university or institution. I declare that this thesis is written by myself and is free of plagiarism and of sufficient grammatical clarity to be examined. I confirm that the investigations were conducted in accord with the ethics policies and integrity standards of Nanyang Technological University and that the research data are presented honestly and without prejudice.

18 October 2019

Date

Chen CHEN

Supervisor Declaration Statement

I have reviewed the content and presentation style of this thesis and declare it of sufficient grammatical clarity to be examined. To the best of my knowledge, the thesis is free of plagiarism and the research and writing are those of the candidate’s except as acknowledged in the Author Attribution Statement. I confirm that the investigations were conducted in accord with the ethics policies and integrity standards of Nanyang Technological University and that the research data are presented honestly and without prejudice.

18 October 2019

. . . .
Date

A Goto

. . . .
Assoc. Prof. Atsushi Goto

Authorship Attribution Statement

This thesis contains material from 3 papers published in the following peer-reviewed journals in which I am listed as an author.

Chapter 2 is published as C. Chen, L. Xiao, and A. Goto, Comprehensive Study on Chain-End Transformation of Polymer−Iodides with Amines for Synthesizing Various Chain-End Functionalized Polymers. *Macromolecules* **49**, 9425-9440 (2016). DOI: 10.1021/acs.macromol.6b02291.

The contributions of the co-authors are as follows:

- Assoc. Prof. A. Goto provided the initial project.
- I performed the experimental work and analysis (for PBA and PSt) at the Division of Chemistry and Biological Chemistry, School of Physical and Mathematical Sciences, Singapore.
- Dr. L. Xiao performed the experimental work and analysis (for PMMA) at the Division of Chemistry and Biological Chemistry, School of Physical and Mathematical Sciences, Singapore.
- Assoc. Prof. A. Goto and Dr. L. Xiao provided guidance in the interpretation of the experimental data.
- I prepared the manuscript draft. Assoc. Prof. A. Goto edited and finalized the manuscript.

Chapter 3 is published as C. Chen, C.-G. Wang, L. Xiao, and A. Goto, Photo-selective chain end transformation of polyacrylate-iodide using cysteamine and its application to facile single-step preparation of patterned polymer brushes. *Chemical Communication* **54**, 13738-13742 (2018). DOI: 10.1039/C8CC08157C. This work is reproduced by permission of The Royal Society of Chemistry.
https://pubs.rsc.org/en/content/articlelanding/2018/cc/c8cc08157c#!divAbstract

The contributions of the co-authors are as follows:

- I proposed the initial project and preformed all the experimental work and analysis.

- Dr. C.-G. Wang, Dr. L. Xiao and Assoc. Prof. A. Goto provided guidance in the interpretation of the experimental data.
- I prepared the manuscript draft; Dr. C.G. Wang refined the draft and Assco. Prof. A. Goto finalized the manuscript.

Chapter 4 is published as C. Chen, C.-G. Wang, W. Guan and A. Goto, A photo-selective chain-end modification of polyacrylate-iodide and its application to patterned polymer brush Synthesis. In press. *Polymer Chemistry* (2019). DOI: 10.1039/c9py01431d. This work is reproduced by permission of The Royal Society of Chemistry.
https://pubs.rsc.org/

The contributions of the co-authors are as follows:

- I proposed the initial project and preformed all the experimental work and analysis.
- Dr. C.-G. Wang, and Assoc. Prof. A. Goto provided guidance in the interpretation of the experimental data.
- W. Guan assisted with the preparation of the polyacrylate-iodide and initiator-immobilized silicon wafer.
- I prepared the manuscript draft; Dr. C.-G. Wang refined the draft and Assco. Prof. A. Goto finalized the manuscript.

18 October 2019
. . . .
Date

. . . .
Chen CHEN

Abstract

Chain-end modification methods of polymer-iodide (polymer-I), which was synthesized via an organocatalyzed controlled radical polymerization, were established in this Thesis. Chain-end functionalized polymers and chain-end reduced polymers were prepared selectively and quantitatively. These methods found useful applications in patterned polymer brushes, chain-end patterned polymer brushes, and rewritable polymer brushes syntheses.

Chapter 1 is the general introduction reviewing the synthesis of chain-end functionalized polymers via several controlled radical polymerization methods and the applications of those polymers. Polymer brushes on solid surfaces, chain-end functionalized polymer brushes, and patterned polymer brushes were also introduced for their useful applications in smart surface materials and biomedical materials. The aims and motivations for developing new chain-end modification methods in this thesis were explained.

In Chapter 2, a chain-end functionalization method of polymer-I was developed by using primary amines (NH_2R) to generate polymer-NHR, where functional groups may be contained in the R moiety. Several functional groups such as OH, phenyl, SH, alkyl, and triethoxysilyl groups were successfully attached at the polymer chain end via a substitution reaction of polymer-I with NH_2R. Two representative polymers, i.e., poly(butyl acrylate) and polystyrene, were comprehensively studied and the reaction mechanism was also probed through matrix-assisted laser desorption/ionization time-of-flight mass spectrometry (MALDI-TOF-MS) analysis. The chain-end functionalization was quantitative and easy to operate, which is attractive as a platform technique to produce various chain-end functionalized polymers.

In Chapters 3 and 4, novel selective chain-end modification methods were developed using biocompatible cysteamine or combining primary amines with formic acid. By switching UV light on and off, hydrogen-terminated polymer (polymer-H) and various chain-end functionalized polymers were selectively produced, respectively. The photo-induced selective

modification was amenable to a range of functional groups. The selective chain-end modification methods were applied to fabricate chain-end patterned polymer brushes.

In Chapter 5, rapid and quantitative chain-end modification methods were developed using thiols (RSH, where the R moiety can contain functional groups). Various functional groups such as COOH, alkyl, SH, alkenyl, OH, and phenyl groups were successfully introduced at the polymer chain end through the substitution reaction of polymer-I with RSH. The quantitative conversion was attained rapidly, i.e., in 10 min. By using $HSCH_2CH_2SH$, thiol-terminated polymers (polymer-SCH_2CH_2SH) were prepared. The thiol-functionalization was applied to obtain thiol-terminated polymer brushes on the surface, which was further applied to rewritable polymer brush surface.

Acknowledgements

I would like to thank my supervisor Assoc. Prof. Atsushi Goto for his kindness guidance and help during the 4 years. He is always patient in correcting my mistakes, providing advices for my experiments, supporting me when I was facing difficulties, and encouraging me when I made progress, and so on. He is always supporting me when I got new ideas and I benefited a lot from his strictness towards research. I am grateful for the opportunity to do a poster presentation in a conference. I experienced a wonderful time in his group and what I learned here will truly help me in my future career.

I also want to thank my thesis advisory committee members, Prof. Alexander M. van Herk and Assoc. Prof. Naohiko Yoshikai. They are always giving me valuable suggestion for my projects.

I appreciate all my labmates. Specially, I want to thank Dr. Longqiang Xiao, Dr. Chen-Gang Wang, Norman Koo Tze Wei and Guan Wenxun for their great suggestion and help on my research projects. And I also want to thank Zheng Jie, Dr. Xu Liu, and Sarkar Jit for their encouragement when I was facing troubles.

Nanyang Technological University (NTU) provides me excellent research condition and the Singapore Government provides me the scholarship. I really appreciate that.

I am grateful for my family and friends for their companies during the last 4 years. Especially, I would like to thank my roommates, Wang Zhiwei and Yang Haibo. At last, I would like to thank my parents and sister for their understanding and unreserved support.

Table of Contents

Abstract 1

Acknowledgements 3

Abbreviations 7

Chapter 1 Introduction 9

1.1 Controlled radical polymerization 9

1.2 Chain-end functionalized polymers 11

1.3 Synthesis of chain-end functionalized polymers via CRP 13

1.4 Aim of Chapter 2 14

1.5 Polymer brushes on the surface 15

1.6 Patterned polymer brushes 17

1.7 Aims of Chapters 3, 4 and 5 18

References 22

Chapter 2 Comprehensive study on chain-end transformation of polymer-iodides with amines for synthesizing various chain-end functionalized polymers 26

2.1 introduction 27

2.2 Results and Discussion 29

Preparation and Characterization of Polymer-Iodides 29

Chain-End Transformation of PBA-I with $NH_2CH_2CH_2Ph$ 35

Chain-End Transformation to Alkyl and $Si(OEt)_3$ Groups 39

Chain-End Transformation to SH Group 40

Chain-End Transformation to OH Group 42

Chain-End Transformation to NH_2 Group 44

Chain-End Transformation of PSt-I with Several Amines 46

2.3 Conclusion 50

2.4 Experimental 51

References.. 54

Chapter 3 Photo-selective chain end transformation of polyacrylate-iodide using cysteamine and its application to facile single-step preparation of patterned polymer brushes 56

3.1 introduction 57

3.2 Results and Discussion 60

3.3 Conclusion 72

3.4 Experimental 73

References.. 78

Chapter 4 A photo-selective chain-end modification of polyacrylate-iodide and its application to patterned polymer brush synthesis 80

4.1 introduction 81

4.2 Results and Discussion 83

Preparation of PBA-I 83

Selective chain-end modification of PBA-I using formic acid and $NH_2CH_2CH_2Ph$ 83

Mechanism study 87

Expansion of chain-end functionality and polymer scopes 90

Chain-end patterned polymer brushes 93

4.3 Conclusion 100

4.4 Experimental 101

References.. 108

Chapter 5 Chain-end modification of polymer iodide using thiols and the applications to patterned polymer brushes and rewritable polymer brushes ... 110

5.1 Introduction ... 110

5.2 Results and Discussion ... 113

5.2.1 Chain-end functionalization of polymer-I using thiols ... 113

5.2.2 Chain-end reduction of polymer-I using thiols ... 116

5.2.3 Hetero-coupling via thiol-disulphide exchange reaction ... 122

5.2.4 Rewritable polymer brushes on the surface ... 126

5.3 Conclusion ... 129

5.4 Experimental ... 130

References ... 137

Chapter 6 Conclusions ... 138

Abbreviations

CRP	Controlled radical polymerization
NMP	Nitroxide mediated polymerization
ATRP	Atom transfer radical polymerization
RAFT	Reversible addition-fragmentation chain transfer polymerization
RCMP	Reversible complexation mediated polymerization
T_g	Glass transition temperature
Đ	Polydispersity index
LCST	Lower critical solution temperature
UCST	Upper critical solution temperature
SSPy	Pyridyldisulphide
MALDI-TOF-MS	Matrix-assisted laser desorption/ionization time-of-flight mass spectrometry
GPC	Gel permeation chromatography
AFM	Atomic force microscope
Polymer-I	Polymer-iodide
Polymer-Br	Polymer-bromide
PBA	Poly(butyl acrylate)
PMMA	Poly(methyl methacrylate)
PMEA	Poly(2-methoxyethyl acrylate)
PNFHA	Poly(*1H*,*1H*,*2H*,*2H*-nonafluorohexyl acrylate)
PEGA	Poly(ethylene glycol) methyl ether acrylate
PSt	Polystyrene
Polymer-SH	Thiol-terminated polymer
Polymer-H	Hydrogen terminated polymer
BA	Butyl acrylate
St	Styrene
MEA	2-methoxyethyl acrylate
NFHA	*1H*,*1H*,*2H*,*2H*-nonafluorohexyl acrylate (NFHA)
CP-I	2-cyanopropyl iodide
BNI	tetrabutylammonium iodide
AIBN	Azobis(isobutyronitrile)
PTH	10-phenylphenothiazine

DCTB	*Trans*-2-[3-(4-tert-butylphenyl)-2-methyl-2-propenylidene]malononitrile
DMF	*N*,*N*-dimethylformamide
THF	Tetrahydrofuran
NaTFA	Sodium trifluoroacetate
AgTFA	Silver trifluoroacetate
EA-I	Ethyl 2-iodopropanoate
EA-Br	Ethyl 2-bromopropanoate
IHE	6-(2-Iodo-2-isobutyloxy)hexyltriethoxysilane
CPM	7-diethylamino-3-(4-maleimidophenyl)-4-methylcoumarin
FITC	Fluorescein 5-isothiocyanate
CPS-SH	7-diethylamino-3-(4-((3-(2-mercaptoethyl)thio)succinimido)phenyl)-4-methylcoumarin
TBA	Tributylamine
TEA	Triethylamine
DTT	DL-dithiothreitol
Irgacure D-2959	2-hydroxy-4’-(2-hydroxyethoxy)-2-methylpropiophenone

Chapter 1 Introduction

Polymer materials are broadly employed in our daily lives and the latest technologies. Radical polymerization is widely employed to produce polymers in both academia and industry because of no requirement of stringent conditions and the amenability to a broad scope of vinyl monomers. Approximately 50% of the commercial polymers (on the value basis) are produced through radical polymerization.[1] However, through conventional radical polymerization, it is difficult to produce polymers with controlled molecular weights, narrow molecular weight distributions, sophisticated architectures, and chain-end functionalities.

1.1 Controlled radical polymerization

To synthesize such well-defined polymers, controlled radical polymerization (CRP), also termed as living radical polymerization or reversible deactivation radical polymerization, has been developed.[2,3] CRP is a useful approach to produce well-defined polymers, resulting in commercial use to produce high-valued materials in, e.g., personal care, surfactant, coating, and dispersant materials.

Scheme 1.1. Reversible activation.

CRP utilizes the reversible generation of a propagating radical (Polymer$^\bullet$) from a dormant species (Polymer-X), where X is a capping agent (Scheme 1.1). The equilibrium is predominantly shifted to Polymer-X, generating an excess of Polymer-X and a relatively low concentration of Polymer$^\bullet$ due to the persistent radical effect.[4] Therefore, the growing chains are dominant, and only a minor fraction of the polymer chains are terminated. By repeating the activation/deactivation cycles, all the polymer chains bear nearly the same possibility to grow, generating narrow-distributed (low dispersity) polymers with controlled molecular weight.

Several CRP methods have been developed by utilizing different X. Representative CRP methods include nitroxide mediated polymerization (NMP),[5] atom transfer radical polymerization (ATRP),[6] and reversible addition-fragmentation chain transfer (RAFT) polymerization.[7]

NMP utilizes nitroxides as X and was first reported in 1993 by Georges et al. to prepare well-distributed polystyrenes (PS) (dispersity ($Đ = M_w/M_n$) < 1.5) using 2,2,6,6-tetramethylpiperidinyl-1-oxy (TEMPO) as a nitroxide,[8] where M_w and M_n are the weight-average and number-average molecular weights, respectively. Upon increasing temperature, Polymer$^\bullet$ is reversibly generated from Polymer-X (Scheme 1.2). NMP was initially amenable to styrenics. With the development of NMP, several nitroxides with different substituents (R_1 and R_2) have been synthesized[5] and encompassed the monomer scope to acrylates, acrylic acid, acrylamides, methacrylates, dienes and other functionalized monomers.[5, 9-11]

Scheme 1.2. Reversible activation of NMP.

ATRP employs halogen (X = Br or Cl) as X and was firstly reported by Sawamoto et al. and Matyjaszewski et al. in 1995.[12,13] ATRP utilizes transition metal complexes (M^nX/L) as the catalysts to cleave the C-X (X = Br or Cl) bond of Polymer-X, generating Polymer$^\bullet$ (Scheme 1.3). Cu is the most widely used, and other transition metals such as Os, Fe, Mo, and Ru are also efficiently utilized.[14-16] ATRP has been extensively used due to the use of simple initiator (alkyl halides (R-Br or R-Cl)) and its amenability to various monomers such as methacrylates, acrylates, styrene, and acrylamides.[17-19] The use of transition metals limits the application of ATRP in biomedical materials, for example. To address this issue, low-catalyst-loading ATRP systems such as activators regenerated electron transfer (ARGET) ATRP, supplemental activator and reducing agent (SARA) ATRP and electronically mediated ATRP (*e*ATRP) have been developed,[20-22] providing industrially favored and environmentally benign techniques. Photo-induced ATRP has also been established by using iridium complexes and more recently, organic photo-redox catalysts, such as 10-phenylphenothiazine (PTH).[23,24]

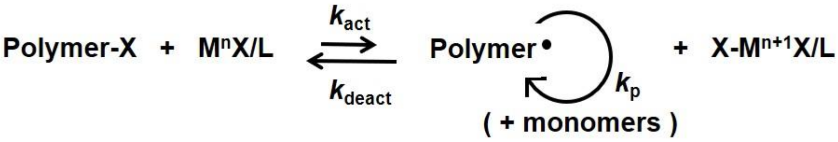

Scheme 1.3. Reversible activation of ATRP.

RAFT polymerization, which was firstly published in 1998 by Rizzardo and Moad et al.,[25] uses thiocarbonylthio compounds (Z-C(=S)-SR) to control the polymerization process, where R is the leaving alkyl group and the Z is the stabilized group. Such compounds include xanthates (Z = OR), dithioesters (Z = alkyl or aryl), dithiocarbamates (Z = NR_1R_2), and trithiocarbonates (Z = SR), affording a broad scope of amenable monomers.[7,26-28] RAFT polymerization is based on the addition-fragmentation equilibria (Scheme 1.4). The polymers obtained from RAFT polymerization possess a thiocarbonylthio group at the propagating chain end.

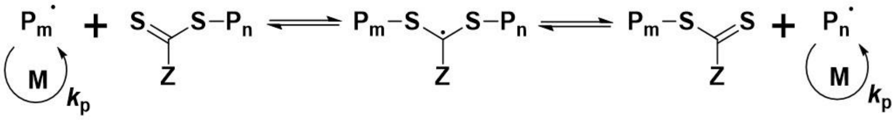

Scheme 1.4. Reversible activation of RAFT polymerization.

1.2. Chain-end functionalized polymers

Chain-end functionalized polymers have attracted considerable attention to creating advanced materials.[29] Taking advantage of the functional groups at the chain end, the polymers can undergo coupling reactions to build blocks and can be employed as stimuli-responsive polymeric materials.

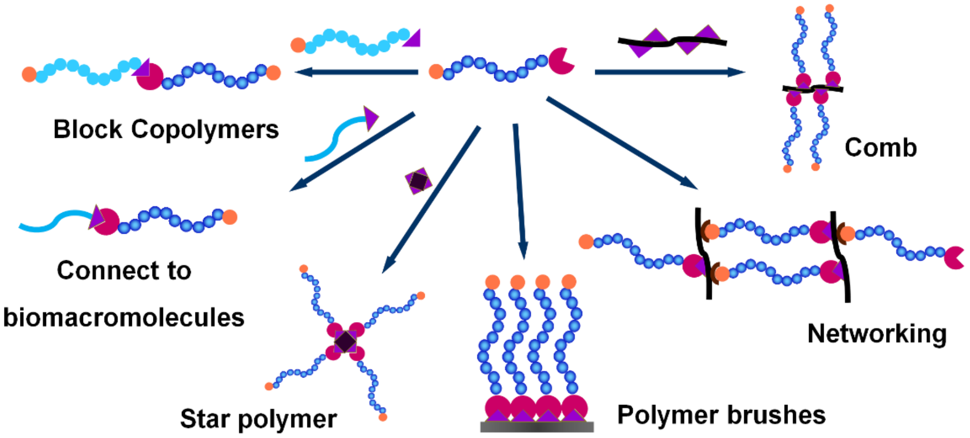

Figure 1.1. Polymer with complex architectures via chain-end functionalized polymers

Chain-end functionalized polymers have been employed to build blocks to obtain complex architectures (Figure 1.1).[29] Chain-end functionalized polymers can attach with another macromolecule to generate block copolymers and with biomolecules to generate bio-conjugates.[30-32] Polymers with complex architectures such as comb, star, and network structures can also be synthesized.[33,34] Chain-end functionalized polymers have also been tailored on solid surfaces, such as gold, silicon, and glass substrates, providing smart surface materials.[34,36]

Stimuli-responsive polymer materials are also obtainable from polymers with stimuli-responsive functional groups such as azobenzene, ferrocene, spiropyran, and donor-acceptor Stenhouse adducts at the chain end.[37-39] Under external stimuli such as temperature, light, pH, and redox potential, the chain-end functional groups undergo intermolecular or intramolecular reaction or rearrangement, resulting in the change in the chain-end physical properties.[40-42] This change has been employed to tune the polymer assembly structures such as micellar and supramolecular structures. Another approach on stimuli-responsive polymers is to attach linkable groups such as azide, alkynyl, vinyl and thiol functionalities at the chain ends, which can connect with another polymer chain with different physical properties from the pre-synthesized polymer chain such as glass transition temperature (T_g), and lower and upper critical solution temperature (LCST and UCST). The assembly of such block copolymer can undergo morphological transformation upon temperature changes.[43-45]

1.3. Synthesis of chain-end functionalized polymers via CRP

CRP utilizes an initiator R-X, where R is an alkyl group. R-X generates a polymer (R-Polymer-X) with R at the initiating chain end and X at the growing chain end. The exact uniform chemical structure and high chain-end fidelity of the prepared R-Polymer-X are crucial for synthesizing chain-end functionalized polymers. There have been a variety of strategies developed for producing chain-end functionalized polymers using CRP.[29,46]

The functional groups can be introduced at the initiating and growing chain ends (Scheme 1.5). In the former case, we may use functionalized initiators with functional groups at the R group (Scheme 1.5a). This method is widely used in all CRP techniques. A number of functional initiators have been designed to yield initiating-chain-end functionalized polymers. The functional groups include OH, COOH, NH_2, NR_1R_2, amide, acetal, succinimide, alkyne, and pyridyldisulphide (SSPy) groups and even more complicated fullerene group.[29,45]

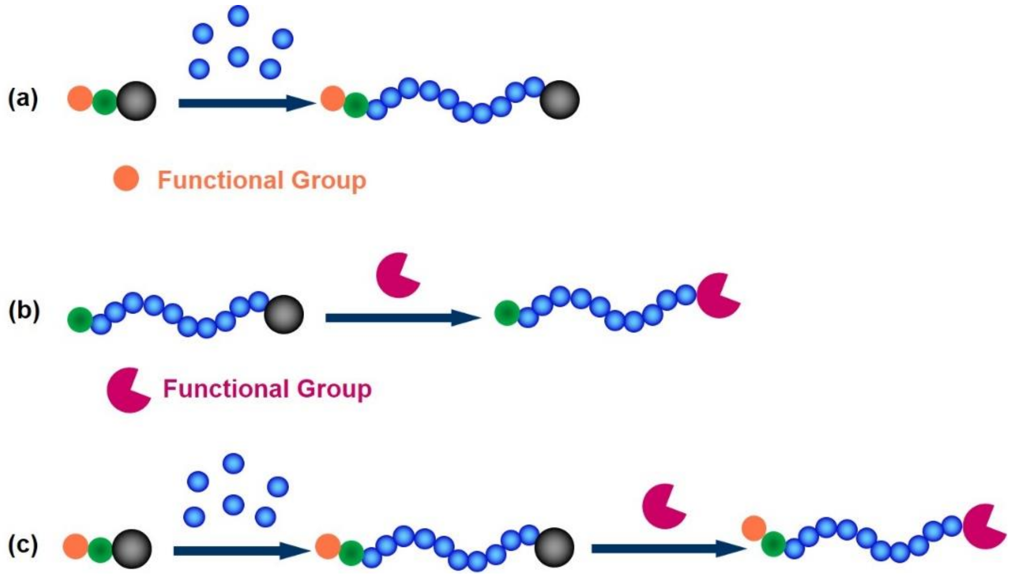

Scheme 1.5. Chain-end functionalization strategies. (a) using functional initiator; (b) post-modification; (c) preparation of telechelic polymers

In the latter case, we may use the post-modification of the growing-chain-end X (Scheme 1.5b). The polymers obtained via NMP and RAFT polymerization have been transformed to OH (NMP and RAFT polymerization),[47,48] SH (RAFT polymerization)[49] and unsaturated olefin-terminated (NMP and RAFT polymerization)[50,51] polymers, for example, but have relatively rarely been used for the post-modification because of the limited reactivity of X.

The polymers obtained via ATRP have been widely used in the post-modification.[29,46] The polymers possess halogens (C-Br and C-Cl chain ends) that are highly reactive in various reactions to be transformed to functional groups. Substitution with nucleophiles such as thiols, amines, azide, and thiourea quantitatively generated SH, OH, NH_2, amide, COOH and N_3 chain-end polymers.[46,52,53] N_3-chain-end polymers were connected with other (macro)molecules containing alkyne group via copper-catalyzed azide-alkyne cycloaddition in a “click” manner to obtain stimuli-responsive polymers, for example.[44]

1.4 Aim of Chapter 2

Our group has developed an organocatalyzed CRP utilizing an iodide as a X and an organic molecule as a catalyst, yielding polymer-iodide (Polymer-I) possessing an iodide at the growing chain end.[54-57] Mechanistically, polymer-I reacts with the catalyst to yield a polymer-I···catalyst complex through a halogen-bonding, which subsequently reversibly generates the propagating polymer$^\bullet$ (Scheme 1.6). The polymerization is termed reversible complexation mediated polymerization (RCMP). Organic molecules such as organic salts and amines are used as catalysts. RCMP is attractive, for it is metal-free, odor-free, and amenable to various monomers such as methacrylates, acrylates, styrene, and acrylonitrile and a range of polymer structures such as star, (multi)blocks, combs and network structures. Photo-induced RCMP has also been developed using light-absorbing catalysts, enabling the synthesis of patterned polymer brushes on solid surfaces.[56]

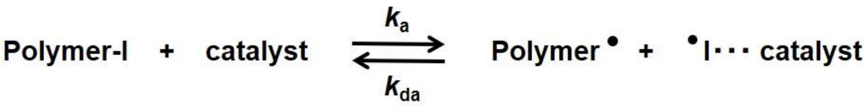

Scheme 1.6. Reversible activation of RCMP

In Chapter 2, we developed a facile chain-end functionalization method of Polymer-I using commercially available primary amines (NH_2R). Through the substitution reaction of Polymer-I with NH_2R, various chain-end functionalized polymers (polymer-NHR) are quantitatively synthesized where the R moiety can contain a functional group. The reaction of NH_2R with polymer-bromide (Polymer-Br) synthesized by ATRP was previously studied. Hydroxyl-terminated polymer was synthesized via the substitution reaction of Polymer-Br and $NH_2(CH_2)_4OH$.[52,53] Since the weaker bonding of C-I compared to C-Br, Polymer-I obtained from RCMP is more reactive than Polymer-Br, leading to a fast chain-end functionalization. In this chapter, we comprehensively studied two important polymers, poly(butyl acrylate) and polystyrene. Six different primary amines with alkyl, hydroxyl, thiol, phenyl, amino, and triethoxysilyl groups were used to synthesize a range of chain-end functionalized polymers. Both RCMP and this chain-end modification method are free from metal, which may find promising biomedical applications.

1.5 Polymer brushes on the surface

The surface of a material is of great importance in materials sciences and engineering. Grafting polymer chains to a solid surface can significantly tune the physical and chemical properties.[58] Polymer brushes are thin polymeric coatings where the polymer chains are anchored on the solid surfaces at one chain end. There are two major methods to fabricate polymer brushes, i.e., the grafting-to method[59,60] and the grafting-from method.[61-63] In the grafting-to method, pre-synthesized chain-end functionalized polymers are attached on solid surfaces via either physisorption or chemisorption (covalent bonding) (Figure 1.2a). This method is a self-repression process, due to the steric repulsion between the polymer chains to be grafted and the already grafted chains, which limits the preparation of thick and dense polymer brushes. Furthermore, with an increase of molecular weight (polymer chain length), the reactivity between chain-end functional group and the complementary group on the surface prominently decreases, resulting in a sharp decrease in the attainable graft density.

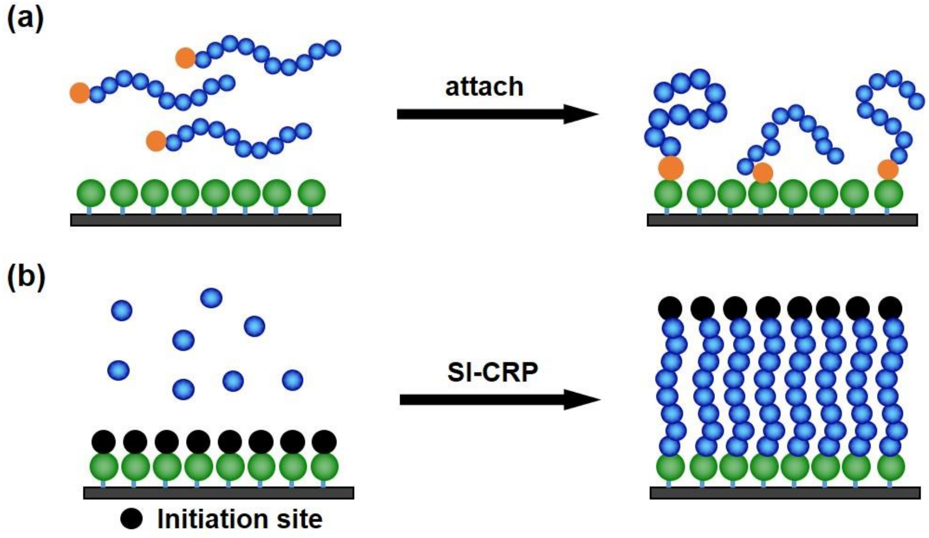

Figure 1.2. Polymer brushes syntheses via (a) grafting-to and (b) grafting-from methods

The grafting-from method, also termed as surface-initiated polymerization, is a bottom-up strategy, in which the polymerization is performed from the initiating sites immobilized on solid surfaces (Figure 1.2b). Polymer brushes with high surface occupancy are accessible using surface-initiated living polymerization, such as ionic polymerization, ring-opening polymerization, and ring-opening metathesis polymerization. Among all the polymerization techniques, surface-initiated CRP has been most frequently employed to fabricate polymer brushes on various solid substrates such as metal, silicon and organic substrates, for its compatibility with organic and water media as well as the amenability to various monomers.[63,64] Surface-initiated CRP allows the fabrication of polymer brushes with designed architecture, graft density, and brush thicknesses, which has been applied in anti-fouling, anti-bacterial, stimuli-responsive, and adhesive surfaces, for example.[64,65]

Polymer brushes synthesized through surface-initiated CRP possess active X groups at the chain ends, which have been transformed to functional groups that will be located on the outermost surface. The chain-ends of polymer brushes synthesized via surface-initiated ATRP, RAFT polymerization and NMP have been successfully transformed to biomolecules such as collagen, heparin, horseradish peroxidase, and chicken immunoglobulin, providing charming applications towards biomedical materials such as cell adhesion, antithrombogenic surfaces, and protein immobilization.[61,66-68] Chain-end bromide of polymer brushes synthesized via surface-initiated ATRP has been converted into an azide group. Various functional groups can be subsequently introduced at the outermost surface of the polymer brush, providing functional surface materials.[69]

1.6 Patterned polymer brushes

Patterned polymer brushes (Figure 1.3) on surfaces have been created using lithography techniques.[70] Patterned polymer brushes find a variety of applications such as light-emitting diodes (LEDs), organic electronics, biomedical materials, antifouling coatings, and optical materials.[71,72]

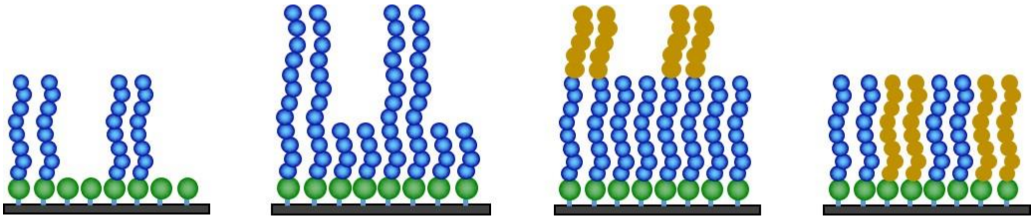

Figure 1.3. Examples of patterned polymer brushes

In one approach, CRP initiators are attached on the surface in patterned manners, followed by polymerization.[70] In another approach (Figure 1.4), the initiators are uniformly attached, and the photo-controlled CRP is carried out using patterned photomasks to obtain patterned polymer brushes. Photo-controlled ATRP using iridium photo-redox catalysts and organic photo-redox catalysts such as 10-phenylphenothiazine (PTH) has successfully been used to obtain patterned polymer brushes.[73]

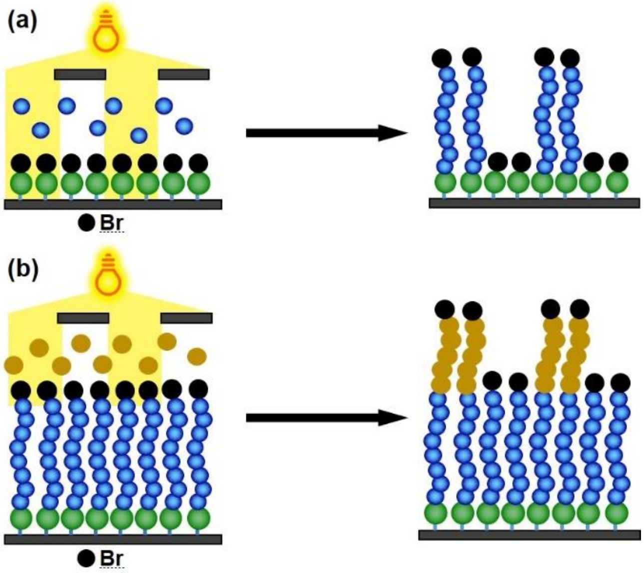

Figure 1.4. Patterned (a) homopolymer and (b) block copolymer brushes synthesized via PTH catalyzed ATRP

1.7 Aims of Chapters 3, 4 and 5

Selective reactions are practical in polymer synthesis and organic synthesis. Under different external stimuli, the reaction will proceed under different pathways to generate different products from the same reactants.

In this thesis, we developed selective chain-end modification methods of Polymer-I, producing chain-end functionalized polymers and hydrogen-terminated polymer. At different experimental conditions, i.e., under UV irradiation or at dark, the chain-end iodide of Polymer-I was selectively converted to a functional group and a simple hydrogen, respectively. The reaction was tolerant to oxygen and moisture, which is an advantage towards practical use. As a useful application, we for the first time fabricated chain-end patterned polymer brushes by taking advantage of our methods.

Previously, patterned polymer brushes were prepared by controlling the polymer growth (Figure 1.4), where the chain ends were uniform. In this thesis, we pioneered to furnish chain-end patterned polymer brushes, which possess different functionalities at the polymer chain ends located at the outermost surface of the polymer brushes. This novel chain-end patterned polymer brush may be useful for, e.g., molecular recognition and biomolecular arrays.

In Chapter 3, we developed a novel selective modification approach of the polymer chain end by using cysteamine ($NH_2CH_2CH_2SH$), which can react with Polymer-I through two different pathways with and without photo irradiation. By controlling the light on and off, hydrogen- and thiol-terminated polymers were selectively obtained quantitatively. This novel selective modification method was also employed in the modification of the chain ends of concentrated polymer brushes giving the unique chain-end patterned polymer brushes (Figure 1.5).

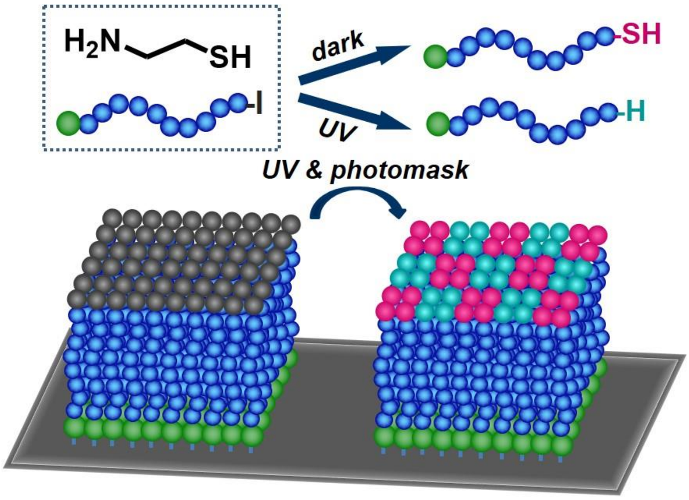

Figure 1.5. Selective chain-end modification using cysteamine and its application on chain-end patterned polymer brush synthesis

In Chapter 4, we widened the scope of the functional groups from the only thiol to various functionalities such as hydroxyl, alkynyl, and triethoxysilyl groups by co-using formic acid and primary amines with various functionalities. Polymer-I was converted to polymers with proton and various functionalities at the chain end with and without photo irradiation, respectively. This selective chain-end modification was employed to fabricate chain-end patterned polymer brushes with different functional groups. The obtained alkyne chain-end patterned polymer brush was reacted with external molecules, successfully altering the surface properties (Figure 1.6).

Figure 1.6. Selective chain-end modification of Polymer-I using formic acid to various chain-end functionalized polymers and Polymer-H, and its application on chain-end patterned polymer brush synthesis.

In chapters 2-4, chain-end modification methods were developed using the substitution between Polymer-I and primary amines. In Chapter 5, we utilized primary thiols instead of primary amines. Polymer-I reacted with functional thiols (RSH) in the presence of a base, yielding chain-end functionalized polymers (Polymer-SR), where R can contain various functional groups. The reaction of RSH with polymer-bromide (Polymer-Br) prepared by ATRP was previously studied to prepare Polymer-SR. Because the C-Br is stronger than the C-I bond, a long reaction time (more than 10 h) was necessary for the quantitative conversion of Polymer-Br to Polymer-SR. In our studied system, Polymer-I was converted to Polymer-SR quantitatively in a much faster manner (within 10 min), which is an attractive feature. Various functional thiols are commercially available, and a range of chain-end functionalized polymers can be synthesized. Thiol-terminated polymer (Polymer-SH) was also prepared using a dithiol HS-R-SH, which was reversibly attached on solid surfaces giving rewritable polymer brushes as an interesting application (Figure 1.7).

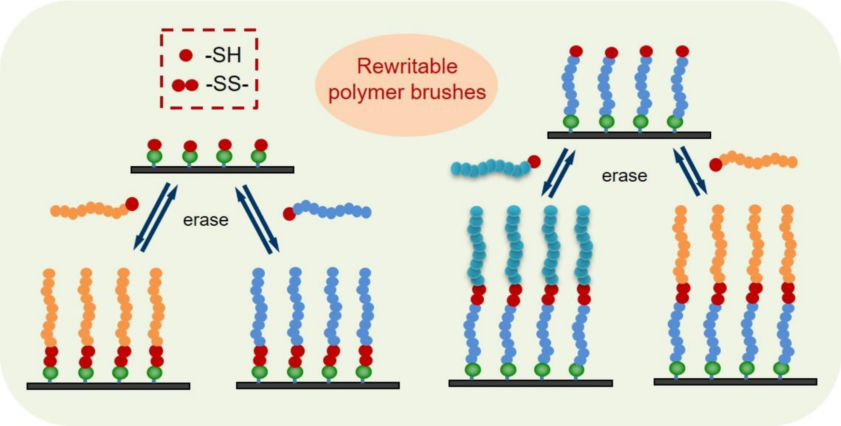

Figure 1.7. Rewritable polymer brushes on the surface

Polymer-I was also converted to thermally and optically stable Polymer-H by using thiol as a good hydrogen donor. Polymer-I was quantitatively converted to Polymer-H in a rapid manner (~ 10 min) under UV irradiation. This UV-induced chain-end reduction was also employed to furnish patterned polymer brushes on the surface (Figure 1.8).

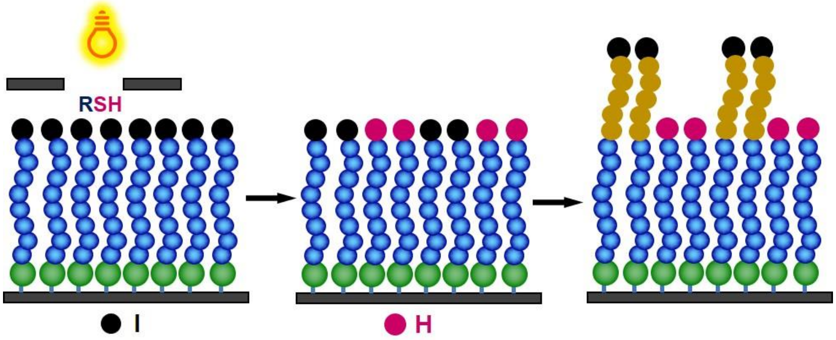

Figure 1.8. Patterned polymer brushes synthesis via spatially chain-end reduction

1.8 References

1. Matyjaszewski, K.; Davis, T. P. *Handbook of Radical Polymerization*, John Wiley & Sons, New Jersey, (2002).
2. Matyjaszewski, K.; Spanswick, J. Controlled/living radical polymerization. In *Handbook of Polymer Synthesis*, CRC Press 2004; pp 907-954.
3. Matyjaszewski, K.; Spanswick, J. *Mater. Today* **2005,** *8*, 26-33.
4. Fischer, H. *Chem. Rev.* **2001**, *101*, 3581.
5. Nicolas, J.; Guillaneuf, Y.; Lefay, C.; Bertin, D.; Gigmes, D.; Charleux, B. *Prog. Polym. Sci.* **2013**, *38*, 63−235.
6. Matyjaszewski, K.; Tsarevsky, N. V. *J. Am. Chem. Soc.* **2014**, *136*, 6513−6533.
7. Keddie, D. J.; Moad, G.; Rizzardo, E.; Thang, S. H. *Macromolecules* **2012**, *45*, 5321−5342.
8. Georges, M. K.; Veregin, R. P. N.; Kazmaier, P. M.; Hamer, G. K. *Macromolecules* **1993,** *26*, 2987-2988.
9. Nicolas, J.; Charleux, B.; Guerret, O.; Magnet, S. *Angew. Chem. Int. Ed.* **2004**, *43*, 6186-6189.
10. Grassl, B.; Clisson, G.; Khoukh, A.; Billon, L. *Eur. Polym. J.* **2008**, *44*, 50-58.
11. Grubbs, R. B. *Polym. Rev.* **2011,** *51*, 104-137.
12. Wang, J.-S.; Matyjaszewski, K. *J. Am. Chem. Soc.* **1995,** *117*, 5614-5615.
13. Kato, M.; Kamigaito, M.; Sawamoto, M.; Higashimura, T. *Macromolecules* **1995,** *28*, 1721-1723.
14. Wang, Y.; Matyjaszewski, K. *Macromolecules* **2010**, *43*, 4003-4005.
15. Le Grognec, E.; Claverie, J.; Poli, R. *J. Am. Chem. Soc.* **2001**, *123*, 9513-9524.
16. Plichta, A.; Li, W.; Matyjaszewski, K. *Macromolecules* **2009**, *42*, 2330-2332.
17. Matyjaszewski, K. *Macromolecules* **2012**, *45*, 4015-4039.
18. Siegwart, D. J.; Oh, J. K.; Matyjaszewski, K. *Prog. Polym. Sci.* **2012**, *37*, 18-37.
19. Matyjaszewski, K.; Xia, J. *Chem. Rev.* **2001**, *101*, 2921-2990.
20. Jakubowski, W.; Min, K.; Matyjaszewski, K. *Macromolecules* **2006**, *39*, 39-45.
21. Zhang, Y.; Wang, Y.; Matyjaszewski, K. *Macromolecules* **2011**, *44*, 683-685.
22. Chmielarz, P.; Fantin, M.; Park, S.; Isse, A. A.; Gennaro, A.; Magenau, A. J.; Sobkowiak, A.; Matyjaszewski, K. *Prog. Polym. Sci.* **2017**, *69*, 47-78.
23. Treat, N. J.; Sprafke, H.; Kramer, J. W.; Clark, P. G.; Barton, B. E.; Read de Alaniz, J.; Fors, B. P.; Hawker, C. J. *J. Am. Chem. Soc.* **2014**, *136*, 16096-16101.

24. Fors, B. P.; Hawker, C. J. *Angew. Chem., Int. Ed.* **2012**, *51*, 8850.

25. Chiefari, J.; Chong, Y. K.; Ercole, F.; Krstina, J.; Jeffery, J.; Le, T. P. T.; Mayadunne, R. T. A.; Meijs, G. F.; Moad, C. L.; Moad, G.; Rizzardo, E.; Thang, S. H. *Macromolecules* **1998,** *31*, 5559-5562.

26. Boyer, C.; Bulmus, V.; Davis, T. P.; Ladmiral, V.; Liu, J.; Perrier, S. *Chem. Rev,* **2009**, *109*, 5402-5436.

27. Moad, G.; Rizzardo, E.; Thang, S.H. *Aust. J. Chem.* **2006**, *59*, 669-692.

28. Boyer, C.; Stenzel, M. H.; Davis, T. P. *J. Polym. Sci. Part A: Polym. Chem*. **2011**, *49*, 551-595.

29. Tasdelen, M. A.; Kahveci, M. U.; Yagci, Y. *Prog. Polym. Sci.* **2011**, *36*, 455−567.

30. Nicolas, J.; Mantovani, G.; Haddleton, D. M. *Macromol. Rapid Commun.* **2007**, *28*, 1083−1111.

31. Dehn, S.; Chapman, R.; Jolliffe, K. A.; Perrier, S. *Polymer Reviews* **2011**, *51*, 214–234.

32. Golas, P. L.; Matyjaszewski, K. *Chem. Soc. Rev.* **2010**, *39*, 1338−1354.

33. Yagci, Y.; Tasdelen, M. A. *Prog. Polym. Sci.* **2006**, *31*, 1133–70.

34. Bernaerts, K. V.; Du Prez, F. E. *Prog. Polym. Sci.* **2006**, 31, 671–722.

35. Jiang, H.; Xu, F.-J. *Chem. Soc. Rev.* **2013**, *42*, 3394–3426.

36. Escorihuela, J.; Marcelis, A. T. M.; Zuilhof, H. *Adv. Mater. Interfaces* **2015**, *2*, 1500135.

37. Wang, G.; Zhu, X.; Zhenping, C.; Zhu, J. *J. Polym. Sci. Part A: Polym. Chem.* **2005**, *43*, 2358-2367.

38. Klajn, R. *Chem. Soc. Rev*. **2014**, *43*, 148-184.

39. Helmy, S.; Leibfarth, F. A.; Oh, S.; Poelma, J. E.; Hawker, C. J.; Read de Alaniz, J. *J. Am. Chem. Soc.* **2014**, *136*, 8169-8172.

40. Bigot, J.; Charleux, B.; Cooke, G.; Delattre, F.; Fournier, D.; Lyskawa, J.; Sambe, L.; Stoffelbach, F.; Woisel, P. *J. Am. Chem. Soc.* **2010**, *132*, 10796-10801.

41. York, A. W.; Kirkland, S. E.; McCormick, C. L. *Adv. Drug Deliv. Rev*. **2008**, *60*, 1018-1036.

42. Stuart, M. A. C.; Huck, W. T.; Genzer, J.; Müller, M.; Ober, C.; Stamm, M.; Sukhorukov, G. B.; Szleifer, I.; Tsukruk, V. V.; Urban, M.; Winnik, F. *Nat. Mater.* **2010**, *9*, 101.

43. Reuther, J. F.; Siriwardane, D. A.; Kulikov, O. V.; Batchelor, B. L.; Campos, R.; Novak, B. M. *Macromolecules* **2015**, *48*, 3207-3216.

44. Zhuang, J.; Gordon, M. R.; Ventura, J.; Li, L.; Thayumanavan, S. *Chem. Soc. Rev.* **2013**, *42*, 7421-7435.

45. Klaikherd, A.; Nagamani, C.; Thayumanavan, S. *J. Am. Chem. Soc.* **2009**, *131*, 4830-4838.

46. Lunn, D. J.; Discekici, E. H.; Read de Alaniz, J.; Gutekunst, W. R.; Hawker, C. J. *J. Polym. Sci. Part A: Polym. Chem.* **2017**, *55*, 2903-2914.

47. Lepoittevin, B.; Perrot, X.; Masure, M.; Hemery, P. *Macromolecules* **2001**, 34, 425–429.

48. Dietrich, M.; Glassner, M.; Gruendling, T.; Schmid, C.; Falkenhagen, J.; Barner-Kowollik, C. *Polym. Chem.* **2010**, *5*, 634–644.

49. Moad, G.; Chong, Y. K.; Postma, A.; Rizzardo, E.; Thang, S. H. *Polymer* **2005**, *46*, 8458–8468.

50. Harth, E.; Hawker, C. J.; Fan, W.; Waymouth, R. M. *Macromolecules* **2001**, *34*, 3856–3862.

51. Postma, A.; Davis, T. P.; Evans, R. A.; Li, G. X.; Moad, G.; O'Shea, M. S. *Macromolecules* **2006**, *39*, 5293–5306.

52. Coessens, V.; Matyjaszewski, K. *Macromol. Rapid Commun.* **1999**, *20*, 127−134.

53. Zhang, H.; Jiang, X.; van der Linde, R. *Polymer* **2004**, *45*, 1455−1466.

54. Goto, A.; Ohtsuki, A.; Ohfuji, H.; Tanishima, M.; Kaji, H. *J. Am. Chem. Soc.* **2013**, *135*, 11131−11139.

55. Ohtsuki, A.; Lei, L.; Tanishima, M.; Goto, A.; Kaji, H. *J. Am. Chem. Soc.* **2015**, *137*, 5610−5617.

56. Wang, C.-G.; Chen, C.; Sakakibara, K.; Tsujii, Y.; Goto, A. *Angew. Chem. Int. Ed.* **2018**, *130*, 13692−13696.

57. Liu, X.; Wang, C.-G.; Goto, A. *Angew. Chem. Int. Ed.* **2019**, *131*, 5654−5659.

58. Chen, W.-L.; Cordero, R.; Tran, H.; Ober, C. K. *Macromolecules* **2017**, *50*, 4089-4113.

59. Tsukruk, V. V. *Prog. Polym. Sci.* **1997**, *22*, 247-311.

60. Brandani, P.; Stroeve, P. *Macromolecules* **2003**, *36*, 9492-9501.

61. Barbey, R.; Lavanant, L.; Paripovic, D.; Schüwer, N.; Sugnaux, C.; Tugulu, S.; Klok, H.-A. *Chem. Rev.* **2009**, *109*, 5437-5527.

62. Tsujii, Y.; Ohno, K.; Yamamoto, S.; Goto, A.; Fukuda, T.: Structure and properties of high-density polymer brushes prepared by surface-initiated living radical polymerization. In *Surface-initiated polymerization I*; Springer, 2006; pp 1-45.

63. Baskaran, D.; Mays, J. W.; Bratcher, M. S. *Angew. Chem. Int. Ed.* **2004**, *43,* 2138-2142.

64. Zoppe, J. O.; Ataman, N. C.; Mocny, P.; Wang, J.; Moraes, J.; Klok, H. A. *Chem. Rev.* **2017,** *117*, 1105-1318.

65. Feng, C.; Huang, X. *Acc. Chem. Res.* **2018**, *51*, 2314-2323.

66. Xu, F. J.; Li, Y. L.; Kang, E. T.; Neoh, K. G. *Biomacromolecules* **2005**, *6*, 1759.

67. Wuang, S. C.; Neoh, K. G.; Kang, E.-T.; Pack, D. W.; Leckband, D. E. *Adv. Funct. Mater.* **2006**, *16*, 1723..

68. Jhaveri, S. B.; Beinhoff, M.; Hawker, C. J.; Carter, K. R.; Sogah, D. Y. *ACS Nano* **2008**, *2*, 719.

69. Lee, B. S.; Lee, J. K.; Kim, W.-J.; Jung, Y. H.; Sim, S. J.; Lee, J.; Choi, I. S. *Biomacromolecules* **2007**, *8*, 744.

70. Nie, Z.; Kumacheva, E. *Nat. Mater.* **2008**, *7*, 277-290.

71. Shimoda, T.; Morii, K.; Seki, S.; Kiguchi, H. *Mrs Bulletin* **2003**, *28*, 821-827.

72. Singh, T. B.; Sariciftci, N. S. *Annu. Rev. Mater. Res.* **2006**, *36*, 199-230.

73. Fors, B. P.; Hawker, C. J. *Angew. Chem., Int. Ed.* **2012**, *51*, 8850−8853.

74. Discekici, E. H.; Pester, C. W.; Treat, N. J.; Lawrence, J.; Mattson, K. M.; Narupai, B.; Toumayan, E. P.; Luo, Y.; McGrath, A. J.; Clark, P. G.; Read de Alaniz, J. *ACS Macro Lett.* **2016**, *5*, 258-262.

Chapter 2 Comprehensive Study on Chain-End Transformation of Polymer-Iodides with Amines for Synthesizing Various Chain-End Functionalized Polymers

Abstract

Chain-end functionalized polymers (Polymer-NHR) were successfully synthesized through the reaction of a polymer-iodide (Polymer-I) with a primary amine (NH_2R), where the R moiety contains a functional group. This reaction was comprehensively studied for two different polymers, i.e., poly(butyl acrylate) and polystyrene, and six different functional amines with phenyl, alkyl, triethoxysilyl, SH, OH, and NH_2 functionalities, and the detailed reaction mechanisms were probed by using matrix-assisted laser desorption/ionization time-of-flight mass spectrometry (MALDI-TOF-MS). This chain-end transformation reaction is easy to perform, amenable to various polymers and functional amines, and also quantitative and selective in many cases. This synthetic technique may serve as a useful platform method for synthesizing various chain-end functionalized polymers.

2.1 Introduction

Chain-end functionalized polymers are employed in many applications.[1] They can be connected to other polymers and are widely used as building blocks for synthesizing block copolymers and topological polymers such as star, comb, and network polymers. They can be connected to small molecules and biomolecules and also on solid surfaces to generate polymer brushes on surfaces. Such connection can be via chemical and physical bonding. External stimuli such as heat, light, moisture, pH, catalysts, and enzymes can trigger the connection and also the disconnection of the polymers. Thus, chain-end functionalized polymers can create advanced stimuli-responsive materials, where structures can be controllably constructed and deconstructed by external stimuli.

Functional groups can be attached at the initiating and terminating (growing) polymer chain ends. Living radical polymerization (LRP) enables the rational design of polymers possessing well-defined initiating and growing chain ends. LRP utilizes the reversible activation of a dormant species (Polymer-X) to a propagating radical (Polymer$^\bullet$) (Scheme 2.1a).[2-5] We may design functional initiating dormant species and/or conduct post chain-end transformation of the capping agents X to functional groups for obtaining various chain-end functionalized polymers.

We developed organocatalyzed LRP using iodine as X and organic molecules as catalysts (Scheme 2.1b).[6,7] This is the first LRP using organic catalysts. Attractive features of this LRP include no use of special capping agents or expensive catalysts. This LRP is metal-free, easy to operate, and amenable to a wide range of monomers and polymer structures. The obtained polymer (polymer-iodide (Polymer-I)) has iodine at its growing chain end. In this work, we attempted to transform iodine to functional groups to synthesize chain-end functionalized polymers. Polymer-I was reacted with a primary amine (NH_2R) (through a substitution reaction) to generate polymer-NHR, where the R moiety can contain a functional group. We synthesized various chain-end functionalized polymers using various functional amines.

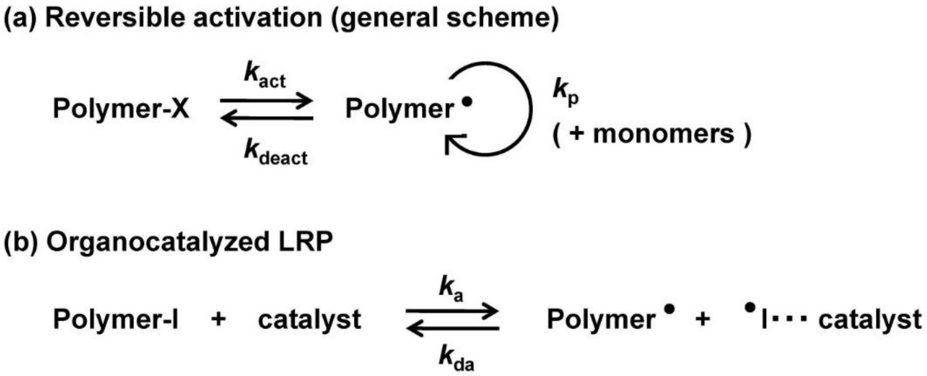

Scheme 2.1. Reversible activation: (a) General scheme and (b) Organocatalyzed LRP.

The reaction with NH_2R was utilized for the chain-end transformation of polymer-bromide (Polymer-Br)[8-10] prepared by atom transfer radical polymerization (ATRP).[3] Chain-end functionalized polymers with an OH functionality were successfully obtained from Polymer-Br (polyacrylate and polystyrene) using $NH_2(CH_2)_4OH$.[8,10] Polymer-I (studied in the present work) should be more reactive than Polymer-Br, because the carbon-iodine bond is weaker than the carbon-bromine bond, and hence faster reaction is expected. In the present work, we did not limit our study to the OH functionality for the two polymers. Instead, we comprehensively studied this reaction for two important polymers, poly(butyl acrylate) (PBA) and polystyrene (PSt), and six different functional amines, and synthesized a range of chain-end functionalized polymers. The chain-end functionalization of poly(methyl methacrylate) by using the primary amine was also studied by Dr. L. Xiao (as mentioned in Authorship Attribution Statement), but it was not introduced in this Chapter. The mechanistic details were also probed. The combination of organocatalyzed LRP and this post chain-end transformation may serve as a useful technique for preparing chain-end functionalized polymers.

2.2 Results and Discussion

Table 2.1. Preparation and Characterization of Polymer-I.

entry	Polymer-I	Polymerization Condition	Conv (%)	M_n	$M_{n,theo}$	$Đ$	Iodine chain-end fidelity (%)
1	PBA-I (polymer **1**)	$[BA]_0/[CP\text{-}I]_0/[Bu_4NI]_0$ = 8000/80/320 (mM) at 110 °C for 6 h	36.7	5200	4900	1.36	
		after purification	–	5300	–	1.36	>95%
2	PSt-I (polymer **7**)	$[St]_0/[CP\text{-}I]_0/[AIBN]_0/[Bu_4NI]_0$ = 8000/160/60/40 (mM) at 80 °C for 9 h	85.0	4200	4500	1.25	
		after purification	–	4500	–	1.21	90%

Preparation and Characterization of Polymer-Iodides. Table 2.1 summarizes the synthetic conditions, number-average molecular weight M_n, and polydispersity index ($Đ$) (M_w/M_n, where M_w is the weight-average molecular weight) of the polymer-iodides, i.e., PBA-I, and PSt-I used in the following chain-end transformation. These polymer-iodides were synthesized in the polymerizations of BA, St, and MMA using 2-cyanopropyl iodide (CP-I (Figure 2.1)) as an initiating alkyl iodide and tetrabutylammonium iodide (Bu_4NI) as a catalyst.[7] For St, a small amount of azobis(isobutyronitrile) (AIBN) was added to increase the polymerization rate. The polymer chains generated from both AIBN and CP-I bear the 2-cyanopropyl (CP) group. The polymerizations were intentionally stopped at relatively small M_n values (= 4200-5200) to retain the high chain-end fidelity of iodine. The polymers were purified by reprecipitation and subsequently by preparative GPC to remove trace amounts of small molecules such as monomers, catalysts, and possible impurities. The obtained polymers possess the CP group at the initiating chain-end and iodine at the growing chain-end and are termed polymer **1** (PBA-I) (Scheme 2.2), and polymer **7** (PSt-I) (Scheme 2.3).

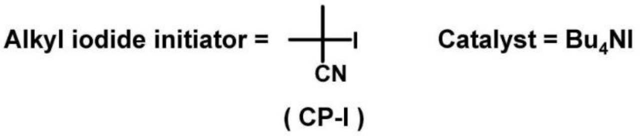

Figure 2.1. Structures of alkyl iodide initiator and catalyst used in this work.

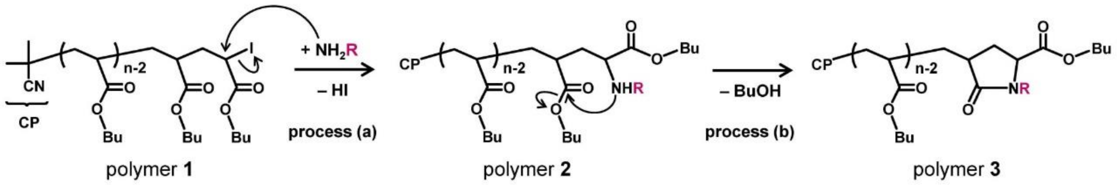

R	n	Theoretical mass		
		polymer **1**	polymer **2**	polymer **3**
$(CH_2)_2Ph$	21	2907.70	2900.88	2826.81
$(CH_2)_2SH$			2856.82	2782.75
$(CH_2)_3Si(OEt)_3$			3000.94	2926.86
$(CH_2)_4CH_3$			2866.90	2792.82
$(CH_2)_2OH$			2840.84	2766.77
$(CH_2)_2NH_2$			2839.86	2765.79
$(CH_2)_4OH$			2868.88	2794.80
$(CH_2)_4NH_2$			2867.89	2793.82

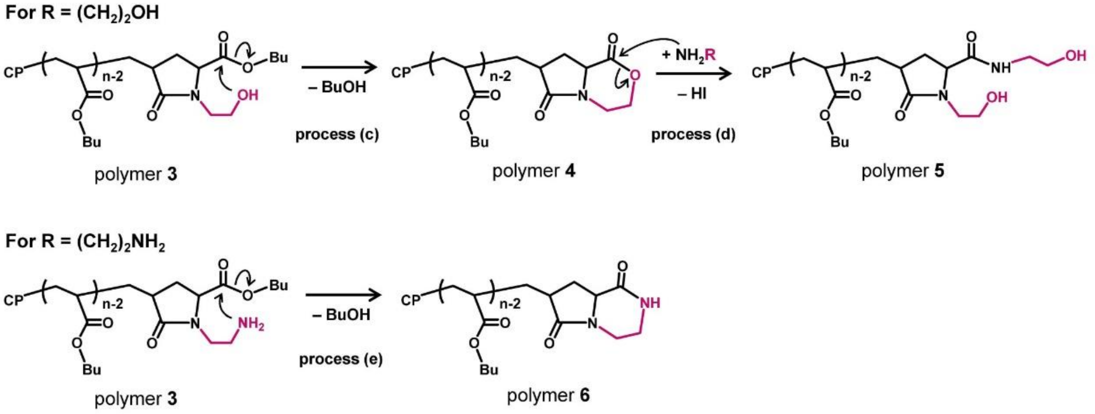

R	n	Theoretical mass		
		polymer **4**	polymer **5**	polymer **6**
$(CH_2)_2OH$	21	2692.70	2753.75	–
$(CH_2)_2NH_2$		–	–	2691.71

Scheme 2.2. Possible processes of chain-end transformation of PBA-I with NH_2R.

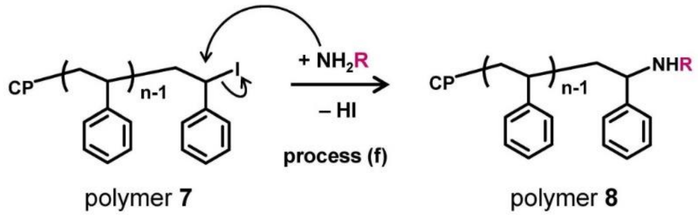

R	n	Theoretical mass	
		polymer **7**	polymer **8**
$(CH_2)_2Ph$	25	2819.51	2812.69
$(CH_2)_2SH$			2768.63
$(CH_2)_3Si(OEt)_3$			2912.74
$(CH_2)_4CH_3$			2778.70
$(CH_2)_2OH$			2752.65
$(CH_2)_2NH_2$			2751.67

Scheme 2.3. Possible Process of Chain-End Transformation of PSt-I with NH_2R.

Figure 2.2 shows the matrix-assisted laser desorption/ionization time-of-flight mass spectrometry (MALDI-TOF-MS) spectra of these polymer-iodides. For the MALDI-TOF-MS sample preparation, we used *trans*-2-[3-(4-*tert*-butylphenyl)-2-methyl-2-propenylidene]malononitrile (DCTB) (for PBA and PSt) or dithranol (for PSt) as a matrix and NaI (for PBA) or CF_3COONa (for PSt) as an additive salt. The studied polymers can possess ^{12}C and ^{13}C atoms. For simplicity, the theoretical molar masses discussed below and the experimental molar masses given in the figures (MALDI-TOF-MS spectra) are those without ^{13}C atom (i.e., with only ^{12}C atoms); unless otherwise specified, those molar masses are compared.

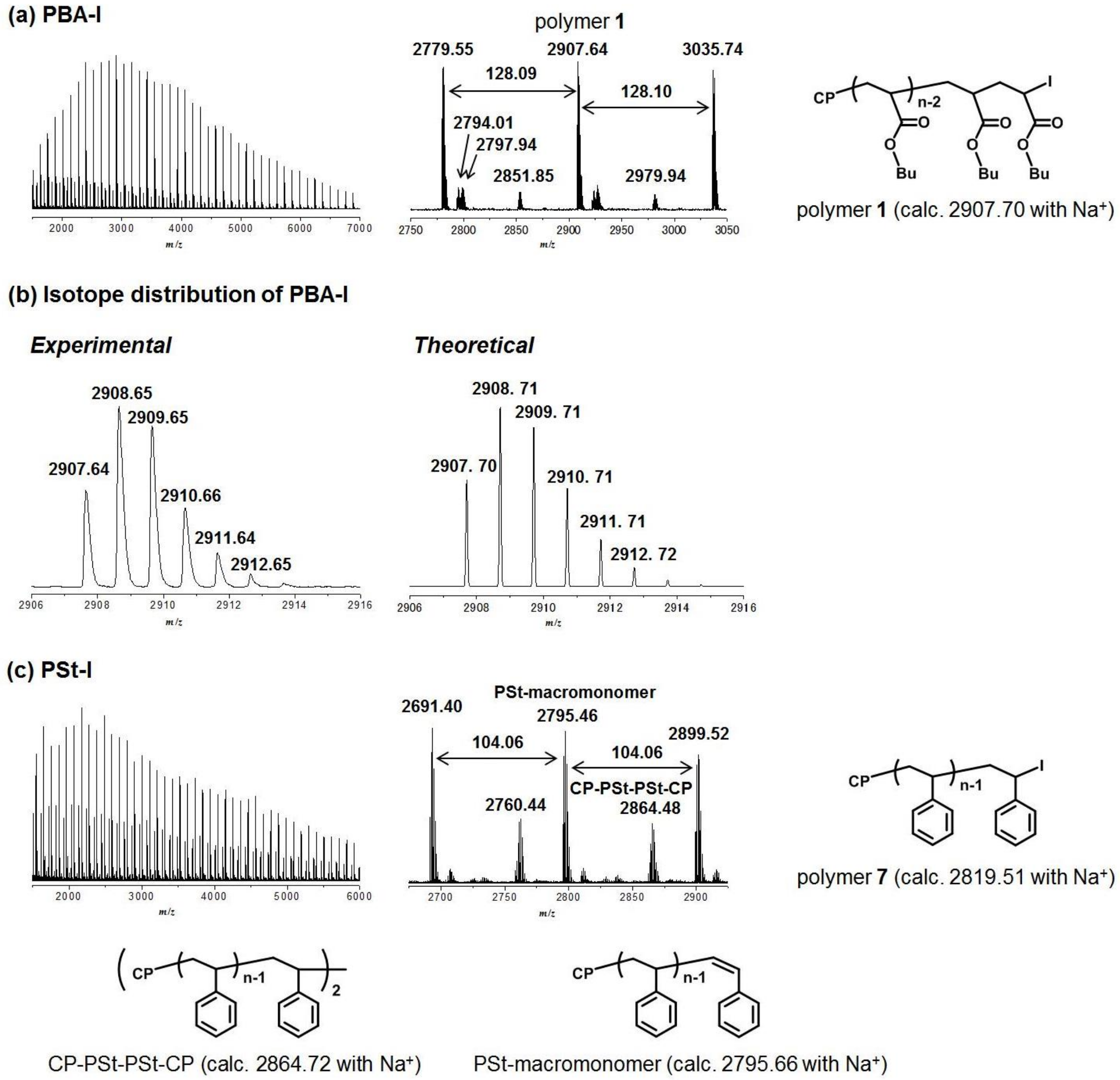

Figure 2.2. MALDI-TOF-MS spectra of (a and b) PBA-I, and (c) PSt-I.

For PBA, the theoretical molar mass (formula weight) of the monomer (BA) unit is 128.0838. The initiating chain end is the CP group whose molar mass is 68.05. The additive cation is Na^+ whose molar mass is 22.99. Let Y be the molar mass of the terminal chain-end group and n be the degree of polymerization. Then, the theoretical molar mass of PBA will be:

$$68.05 + 128.0838 \times n + Y + 22.99 \quad \text{(for PBA)} \tag{1}$$

For polymer **1** (PBA-I), the terminal group is iodine whose molar mass is 126.90.

Figures 2.2a and 2b show the MALDI-TOF-MS spectrum of the obtained PBA-I. Figure 2.2b shows the isotope distribution in the molar mass region of 2906-2916. The experimental molar mass distribution well matched the theoretical one. The far left peak (experimental molar mass = 2907.64) corresponds to the polymer without ^{13}C atom (with all carbon atoms being ^{12}C) whose molar mass is provided in Figure 2.2a. The second peak from the left (experimental molar mass = 2908.65) corresponds to the polymer possessing one ^{13}C atom, and the other peaks (experimental molar mass = 2909.65 and so on) correspond to those possessing two or more ^{13}C atoms.

As shown in Figure 2.2a, the peaks appeared at 128.1 molar mass unit intervals corresponding to the monomer unit. The experimental molar mass (2907.64) well matched the theoretical molar mass (2907.70) with $n = 21$ for polymer **1** as calculated according to eq (1). We observed only a single series of repeated peaks (i.e., only one product) in Figure 2.2a, confirming the high chain-end fidelity of iodine for the obtained PBA-I (>95%).

Three series of minor peaks were also observed at 2851.85, 2797.94, and 2794.01. These species seemed to be generated during the MALDI-TOF-MS analysis and were not originally present in the prepared polymer; the first one (experimental molar mass = 2851.85) seemed to be a species losing C_4H_9I (generating a lactone ring end group) during the MALDI-TOF-MS analysis (theoretical molar mass = 2851.81),[11] and the second one (experimental molar mass = 2797.94) seemed to be a species associated with a water (H_2O) molecule (theoretical molar mass = 2797.62), and the third one (experimental molar mass = 2794.01) remains unclear. In principle, the reactive chain end C-I may also react other nucleophile, such as the solvent (1-butanol or diglyme), but the signals of the corresponding products were not obtained. Because this polymerization is a radical polymerization, a radical-radical termination product CP-PBA-PBA-CP (theoretical molar mass = 2848.85) should be generated during the polymerization. However, the corresponding peak was not clearly detected, suggesting that the amount of the termination product is negligible in this case.

Similarly, the theoretical molar mass of PSt is:

$$68.05 + 104.0626 \times n + Y + 22.99 \quad \text{(for PSt)} \qquad (2)$$

The theoretical molar mass for polymer **7** with n = 25 is 2819.51, but polymer **7** was not observed in the spectrum (Figure 2.2c). The carbon-iodine bond of polymer **7** is so weak that this bond could be cleaved during the MALDI-TOF-MS analysis. Therefore, we observed PSt-macromonomer (theoretical molar mass = 2795.66 and experimental molar mass = 2795.46) with an unsaturated C=C bond generated through the elimination of HI from polymer **7**. This PSt-macromonomer seemed to be generated during the MALDI-TOF-MS analysis.[12-17]

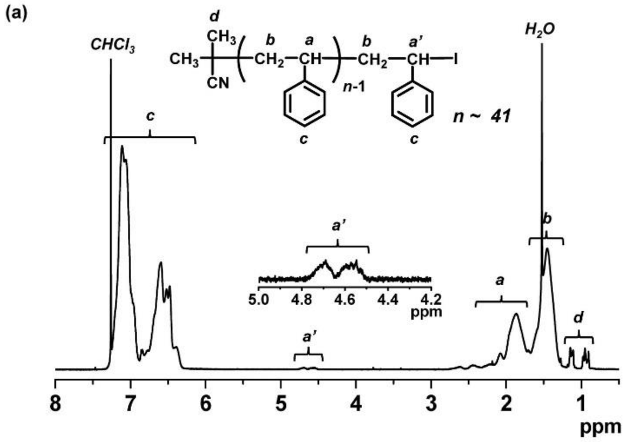

Figure 2.3. ^{1}H NMR spectra ($CDCl_3$) of PSt-I (polymer **7**).

Thus, it was difficult to characterize the obtained PSt-I by MALDI-TOF-MS. To check the iodine-chain-end fidelity, the polymer was analyzed by ^{1}H NMR (Figure 2.3). The spectrum clearly shows signals for the methine proton at the iodine end (4.5-4.8 ppm: peak a') and the methyl protons at the CP chain end (0.8-1.2 ppm: peak d). This polymer could contain polymer **7** bearing one CP group and one iodine and also a radical-radical termination product bearing two CP groups. Assuming that these two species are present, based on the peak area (peaks a' and d), we calculated the fraction of polymer **7** to be 90% (with ± 5% experimental error), confirming the high iodine-chain-end fidelity (90%).

The radical-radical termination product CP-PSt-PSt-CP (theoretical molar mass = 2864.72 and experimental molar mass = 2864.48) was observed by MALDI-TOF-MS (Figure 2.2c), and the peak ratio of CP-PSt-PSt-CP and PSt-macromonomer (hence polymer **7**) was 30/70. This ratio is much larger than the actual ratio (10/90) determined by ^{1}H NMR (Figure 2.3a). This large discrepancy would be because the ionization of polymer **7** accompanies the reaction of polymer **7** to PSt-macromonomer and is less effective than the ionization of CP-PSt-PSt-CP which accompanies no reaction.

Chain-End Transformation of PBA-I with $NH_2CH_2CH_2Ph$. We studied the chain-end transformation of PBA-I (polymer **1**) with $NH_2CH_2CH_2Ph$. We heated PBA-I (M_n = 5300 and $Đ$ = 1.36) (1 eq) and excess $NH_2CH_2CH_2Ph$ (20 eq) in a mixed solvent of diethylene glycol dimethyl ether (diglyme) (40 wt%) and 1-butanol (40 wt%) (with 20 wt% polymer) at 100 °C for 8 h (Table 2.2 (entry 1)). Diglyme is inexpensive and environmentally friendly and is therefore widely used as a solvent in industry. 1-Butanol is a polar solvent and accelerated the chain-end transformation reaction. After the reaction, the obtained polymer was purified by reprecipitation with methanol/water (50/50 wt%) and was further purified with preparative GPC to remove trace amounts of $NH_2CH_2CH_2Ph$ and other low-molecular-weight species. Some oligomers might also be removed by this purification. Because the removed amount varied among runs, the molecular weight distribution (Figures 2.4 and 2.6-2.14) differed slightly among runs (even when the same polymer-iodide reactant was used).

Table 2.2. Chain-End Transformation of PBA-I (polymer 1) with Amines (NH_2R)

entry	R	Equiv of NH_2R	T (°C)	Solvent	t (h)	Observed polymers (%) (percentages are rough estimate from MALDI-TOF-MS spectra with 10% estimate error)		
						Polymer **2**	Polymer **3**	Others
1	$(CH_2)_2Ph$	20	100	D/B^a	8	0	100	0
2	$(CH_2)_2Ph$	20	100	D/B^a	1	45	55	0
3	$(CH_2)_2Ph$	2	100	D/B^a	24	0	100	0
4	$(CH_2)_3Si(OEt)_3$	20	100	diglyme^b	8	0	100	0
5	$(CH_2)_3Si(OEt)_3$	20	100	diglyme^b	1	50	50	0
6	$(CH_2)_3Si(OEt)_3$	2	100	diglyme^b	24	0	80	20 (unidentified)
7	$(CH_2)_4CH_3$	20	100	D/B^a	8	0	100	0
8	$(CH_2)_4CH_3$	20	100	D/B^a	1	50	50	0
9	$(CH_2)_4CH_3$	2	100	D/B^a	24	0	100	0
10	$(CH_2)_2SH$	20	100	D/B^a	8	0	50	50 (PBA-H)
11	$(CH_2)_2SH$	20	70	D/B^a	8	0	80	20 (PBA-H)
12	$(CH_2)_2SH$	20	25	D/B^a	12	0	100	0
13	$(CH_2)_2OH$	20	100	D/B^a	8	0	0	100 (polymer **5**)
14	$(CH_2)_2OH$	20	100	D/B^a	1	0	80	20 (polymer **5**)
15	$(CH_2)_2OH$	2	100	D/B^a	24	0	100	0
16	$(CH_2)_4OH$	20	100	D/B^a	8	0	100	0
17	$(CH_2)_2NH_2$	20	100	D/B^a	1	0	0	100 (polymer **6**)
18	$(CH_2)_2NH_2$	20	100	D/B^a	0.17	0	30	10 (polymer **1**) 60 (polymer **6**)
19	$(CH_2)_2NH_2$	2	100	D/B^a	1	0	0	100 (polymer **6**)
C1	$Ph(CH_2)_2SH$	20	100	D/B^a	8	0	0	100 (PBA-H)

^{a} polymer **1**/diglyme/1-butanol = 20/40/40 wt%. ^{b} polymer **1**/diglyme = 20/80 wt%.

Scheme 2.2 shows possible mechanisms and products in the chain-end transformation of PBA-I (polymer **1**). Process (a) is the substitution of iodine of polymer **1** with an amine to produce polymer **2**. Process (b) is the intramolecular amidation of polymer **2** to produce polymer **3**, giving a 5-membered ring at the chain end. Scheme 2.2 shows the theoretical molar masses of these polymers (including the molar mass of Na^+ for the MALDI-TOF-MS analysis).

Figure 2.4a shows the MALDI-TOF-MS spectrum. The experimental molar mass (2826.70) matched the theoretical molar mass (2826.81) of polymer **3**. We observed only a single series of repeated peaks (i.e., only one product) and did not observe the reactant polymer **1** (theoretical molar mass = 2907.70). Thus, polymer **1** was successfully converted to polymer **3** in a quantitative manner.

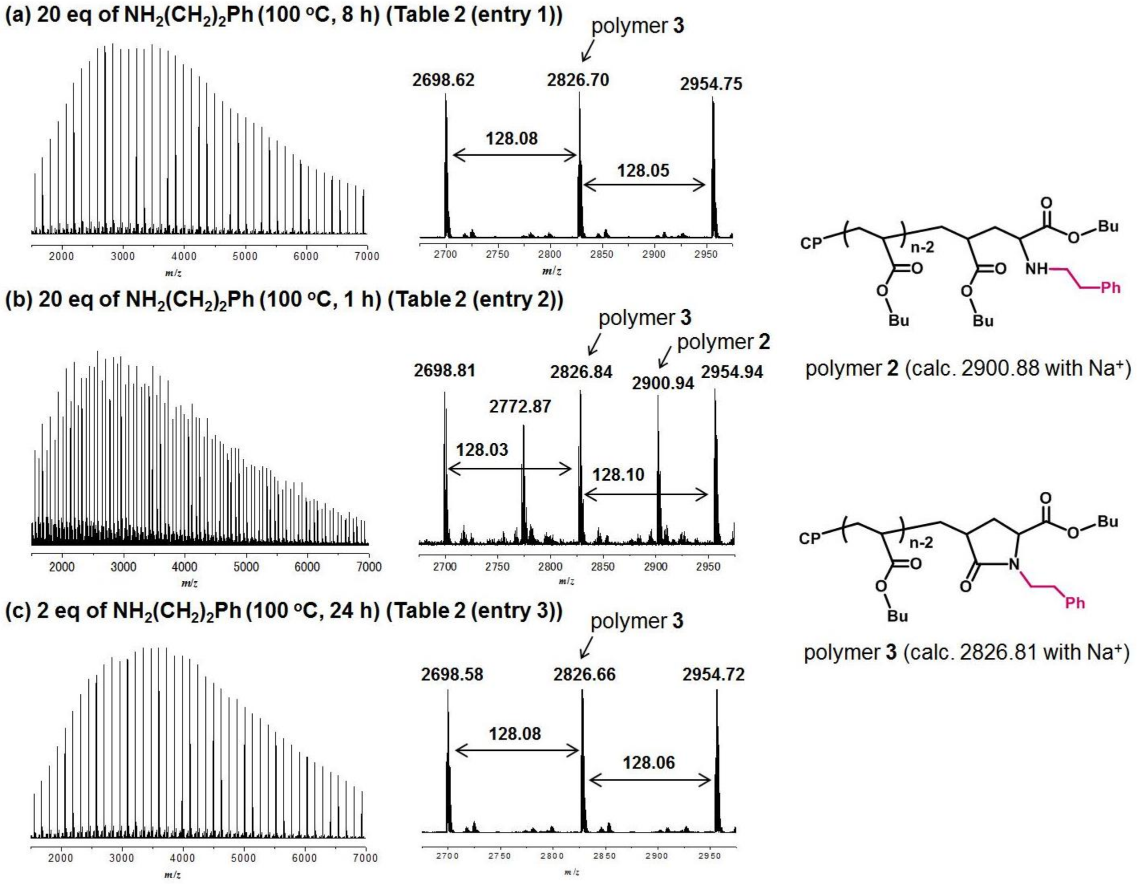

Figure 2.4. MALDI-TOF-MS spectra of polymers obtained via reactions of PBA-I (polymer **1**) with $NH_2(CH_2)_2Ph$ in Table 2.2 (entries 1-3). The reaction conditions are given in the figure .

We also confirmed the inclusion of the NCH_2CH_2Ph moiety in the polymer by ^1H NMR. Figure 2.5 shows the ^1H NMR spectrum. The signal of C_6H_5 (7.2-7.4 ppm) was clearly observed, demonstrating the introduction of the NCH_2CH_2Ph moiety. The chain-end functionality can be estimated from the relative peak areas of C_6H_5 and the monomer units

(OCH_2). We calculated the number of monomer units (= 40) using the M_n determined by GPC and estimated the chain-end functionality to be 105% (with ± 5% experimental error). Thus, the chain-end functionalized polymer was quantitatively obtained.

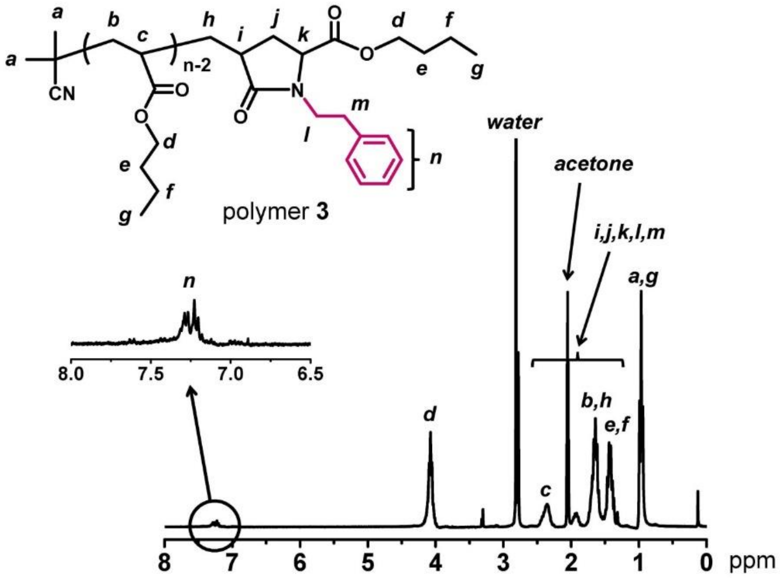

Figure 2.5. ^{1}H NMR spectrum (acetone-d_6) of polymer obtained with a reaction of PBA-I (polymer **1**) with $NH_2(CH_2)_2Ph$ in Table 2.2 (entry 1).

Figure 2.4b shows the MALDI-TOF-MS spectrum of the polymer obtained after a shorter reaction time 1 h instead of 8 h. We observed a mixture of two products, polymer **2** (experimental molar mass = 2900.94 and theoretical molar mass = 2900.88) and polymer **3**. The relative ratio of the peak intensities was approximately 45% for polymer **2** and 55% for polymer **3**. This ratio may not necessarily correspond to the actual product ratio, because the ionization of polymer during the MALDI analysis depends on the polymer structure. In the present case, because the polymer backbones are the same (CP-PBA) and the only difference is the growing chain end, the observed ratio should be close to the actual product ratio. This result demonstrates that polymer **1** is initially transformed to polymer **2**, which then forms polymer **3**, as described in Scheme 2.2.

We reduced the amount of $NH_2CH_2CH_2Ph$ from 20 eq to 2 eq. The stoichiometric amount of amine in this chain-end transformation is 2 eq, because 1 eq of amine attaches to the polymer chain end and the other 1 eq of amine acts as a base to trap HI (hydroiodic acid) generated in this reaction. As Figure 2.4c shows, this stoichiometric amount (2 eq) of amine successfully provided polymer **3** virtually quantitatively, although the reaction took a relatively long time of 24 h. Thus, 2 eq is sufficient to complete the reaction, when the reaction time is long enough. Table 2.2 (entries 1-3) summarizes these three results with $NH_2CH_2CH_2Ph$.

(a) $NH_2(CH_2)_4CH_3$ (100 °C, 8 h) (Table 2 (entry 4))

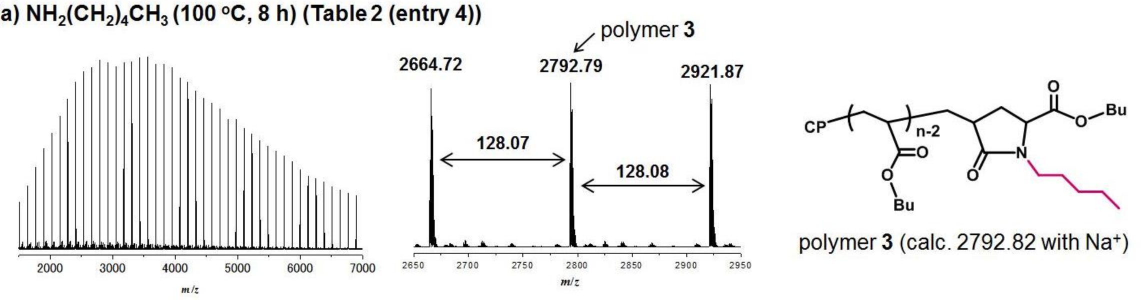

(b) $NH_2(CH_2)_3Si(OEt)_3$ (100 °C, 8 h) (Table 2 (entry 7))

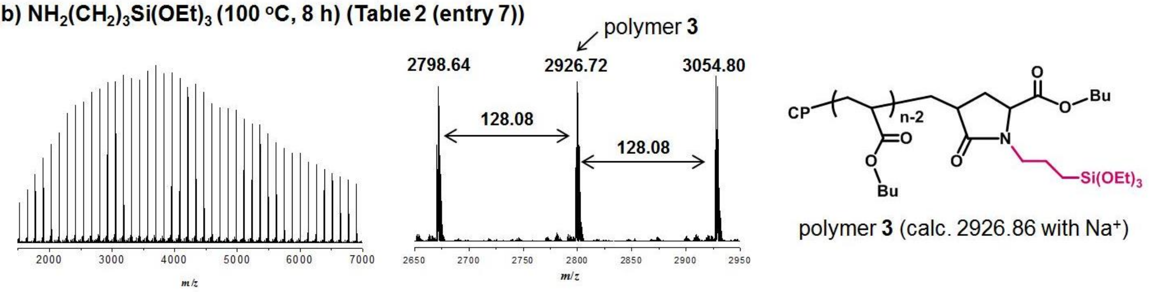

Figure 2.6. MALDI-TOF-MS spectra of polymers obtained through reactions of PBA-I (polymer **1**) with NH_2R in Table 2.2 (entries 4 and 7). The amines are given in the figure.

Chain-End Transformation to Alkyl and $Si(OEt)_3$ Groups. We used $NH_2(CH_2)_4CH_3$ and $NH_2(CH_2)_3Si(OEt)_3$ for the chain-end transformation of PBA-I (polymer **1**). Figure 2.6 shows the MALDI-TOF-MS spectra of the polymers obtained with 20 eq of amine at 100 °C for 8 h. In both cases, polymer **1** was virtually quantitatively converted to polymer **3** with $CH_2(CH_2)_3CH_3$ and $CH_2(CH_2)_2Si(OEt)_3$ groups at the chain end. Table 2.2 (entries 4-9) summarizes the results obtained at different reaction conditions.

Chain-End Transformation to SH Group. $NH_2CH_2CH_2SH$ was used to obtain polymer **3** with a CH_2CH_2SH group. Figure 2.7a shows the MALDI-TOF-MS spectra of the polymer obtained with 20 eq of amine at 100 °C for 8 h. In the detailed molar mass distribution, we observed two products, i.e., polymer **3** (experimental molar mass = 2782.56 and theoretical molar mass = 2782.75) and PBA-H (experimental molar mass = 2781.60 and theoretical molar mass = 2781.81) with a hydrogen atom at the chain end (Figure 2.7d). The theoretical molar mass difference between the two products is 0.94 (2782.75 vs 2781.81 in Figure 2.7d). The observed peak intensity in Figure 2.7a suggests that the product yield was 50% for both polymer **3** and PBA-H.

The SH group in $NH_2CH_2CH_2SH$ is an efficient radical chain transfer group. At the studied high reaction temperature of 100 °C, a small amount of PBA radical ($PBA^\bullet$) would be generated by the thermal dissociation of PBA-I (polymer **1**). $PBA^\bullet$ can react with $NH_2CH_2CH_2SH$ to generate PBA-H and the sulfur-centered radical $NH_2CH_2CH_2S^\bullet$. $NH_2CH_2CH_2S^\bullet$ abstracts iodine from PBA-I to generate $PBA^\bullet$. This radical chain transfer cycle would lead to the observed large amount of PBA-H.

(a) 20 eq of $NH_2(CH_2)_2SH$ (100 °C, 8 h) (Table 2 (entry 10))

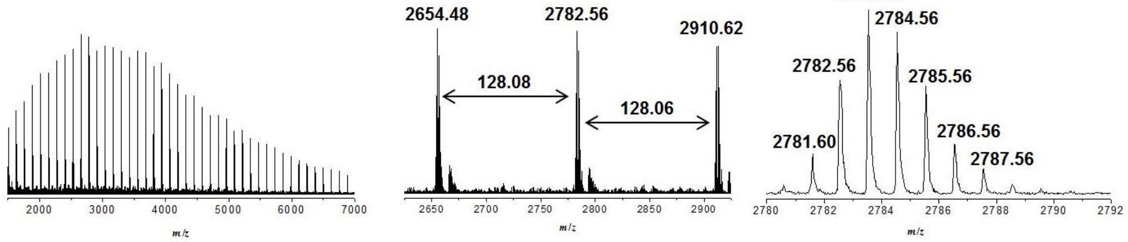

(b) 20 eq of $NH_2(CH_2)_2SH$ (70 °C, 8 h) (Table 2 (entry 11))

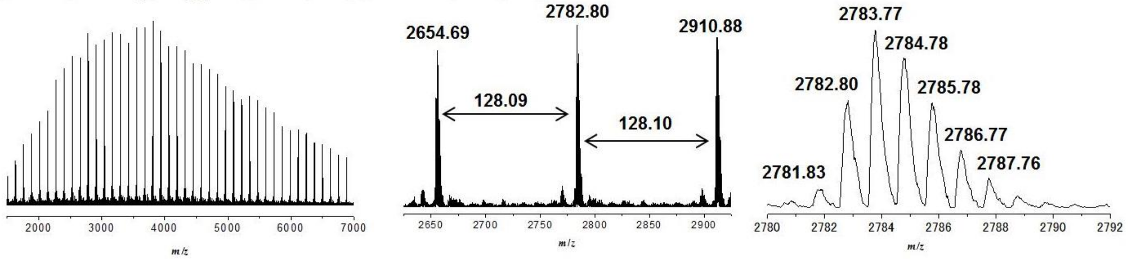

(c) 20 eq of $NH_2(CH_2)_2SH$ (25 °C, 12 h) (Table 2 (entry 12))

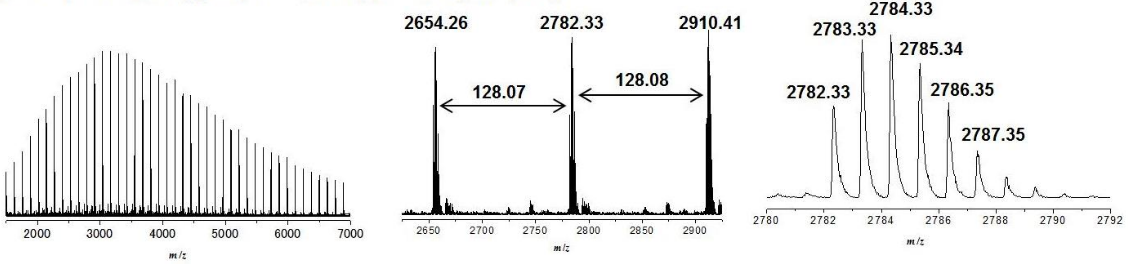

(d) Theoretical mass distribution

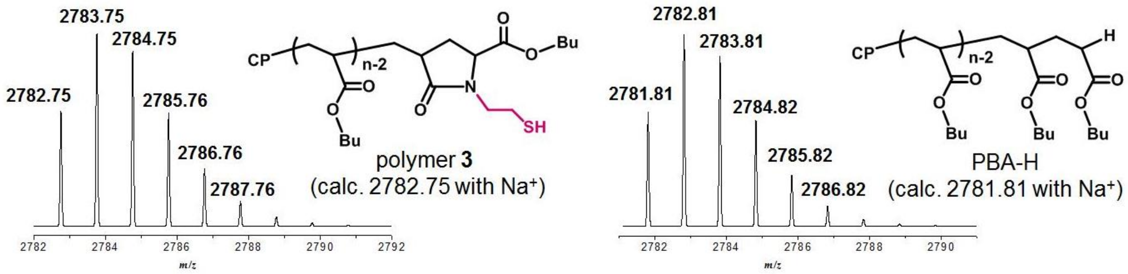

(e) 20 eq of $Ph(CH_2)_2SH$ (100 °C, 8 h) (Table 2 (entry C1))

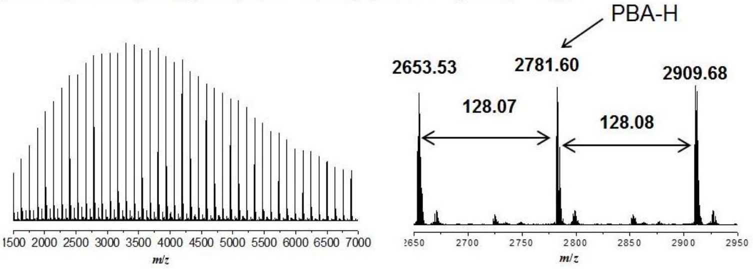

Figure 2.7. MALDI-TOF-MS spectra of polymers obtained with reactions of PBA-I (polymer **1**) with $NH_2(CH_2)_2SH$ and $Ph(CH_2)_2SH$ in Table 2.2 (entries 10-12 and C1). The reaction conditions are given in the figure.

To reduce the amount of PBA-H, we decreased the reaction temperature from 100 °C to 70 °C (Figure 2.7b) and 25 °C (Figure 2.7c). The radical generation (thermal dissociation of PBA-I) was suppressed at these lower temperatures. Thus, we successfully obtained polymer **3** with the SH functionality in a higher yield (80%) at 70 °C and a quantitative yield (100%) at 25°C. A slightly longer time 12 h was required to complete the reaction at 25 °C. An SH-functionalized polymer is difficult to obtain by using an SH containing initiator because the SH group is consumed via the chain transfer during the polymerization. It can only be obtained by post chain-end transformation, and in this regard, the obtained SH functionalized polymer is a unique polymer in the present work.

$NH_2CH_2CH_2SH$ has NH_2 and SH groups. Both groups are nucleophiles and may undergo iodine substitution reactions. Experimentally, only polymer **3** (via the reaction with NH_2) was observed (Figures 2.7a, 2.7b, and 2.7c). Therefore, NH_2 is much more reactive than SH for the substitution reaction,[9] and SH remained as a functional group in the obtained polymer.

We in turn applied this radical chain transfer reaction to the chain-end transformation of polymer **1** to PBA-H using a thiol $PhCH_2CH_2SH$ without the NH_2 group at a high temperature 100 °C for 8 h. In this case, only the chain transfer reaction occurred, and we quantitatively obtained PBA-H (Figure 2.7e). Thus, once the appropriate conditions were selected, the SH functionalized polymer (polymer **3**) (Figure 2.7c) and PBA-H (Figure 2.7e) were selectively obtained.

Chain-End Transformation to OH Group. Figure 2.8a shows the MALDI-TOF-MS spectrum of the polymer obtained with 20 eq of $NH_2CH_2CH_2OH$ at 100 °C for 8 h. The result did not match either polymer **2** or polymer **3**. Scheme 2.2 shows possible additional reactions of polymer **3** for R = CH_2CH_2OH. Similar reactions were experimentally demonstrated for low-mass alkyl bromides and polymer-bromides.[8] Process (c) is the intramolecular esterification of polymer **3** through the terminal OH group to produce polymer **4** with a 6-membered cyclic ester. Process (d) is the ring-opening amidation of polymer **4** through another amine ($NH_2CH_2CH_2OH$) to produce polymer **5** with two OH groups. The result (experimental molar mass = 2753.76) matched polymer **5** (theoretical molar mass = 2753.75). We observed only a single product and hence could selectively attach two OH groups at the chain end.

To attach only one OH group, we reduced the reaction time from 8 h to 1 h for avoiding the processes (c) and (d). We in fact obtained polymer **3** with one OH group in 80% yield but still observed polymer **5** with two OH groups in 20% yield (Figure 2.8b). We then reduced the amount of $NH_2CH_2CH_2OH$ from 20 eq to the stoichiometric amount (2 eq) to attach one OH group (Figure 2.8c). Because of the absence of additional $NH_2CH_2CH_2OH$ (which offered the second OH group), we successfully obtained polymer **3** with one OH group in virtually 100% yield. An alternative method for the selective attachment of one OH group was to use $NH_2(CH_2)_4OH$ with a longer alkyl chain. In this case, polymer **4** included an energetically unfavorable 8-membered cyclic ester and was hardly generated. This method (i.e., the use of $NH_2(CH_2)_4OH$ to attach one OH group) was previously reported for polymer-bromides.[8,10] Figure 2.8d shows the MALDI-TOF-MS result. The spectrum matched polymer **3**, demonstrating the quantitative and selective attachment of one OH group. Thus, we can selectively attach one or two OH groups by selecting appropriate reaction conditions.

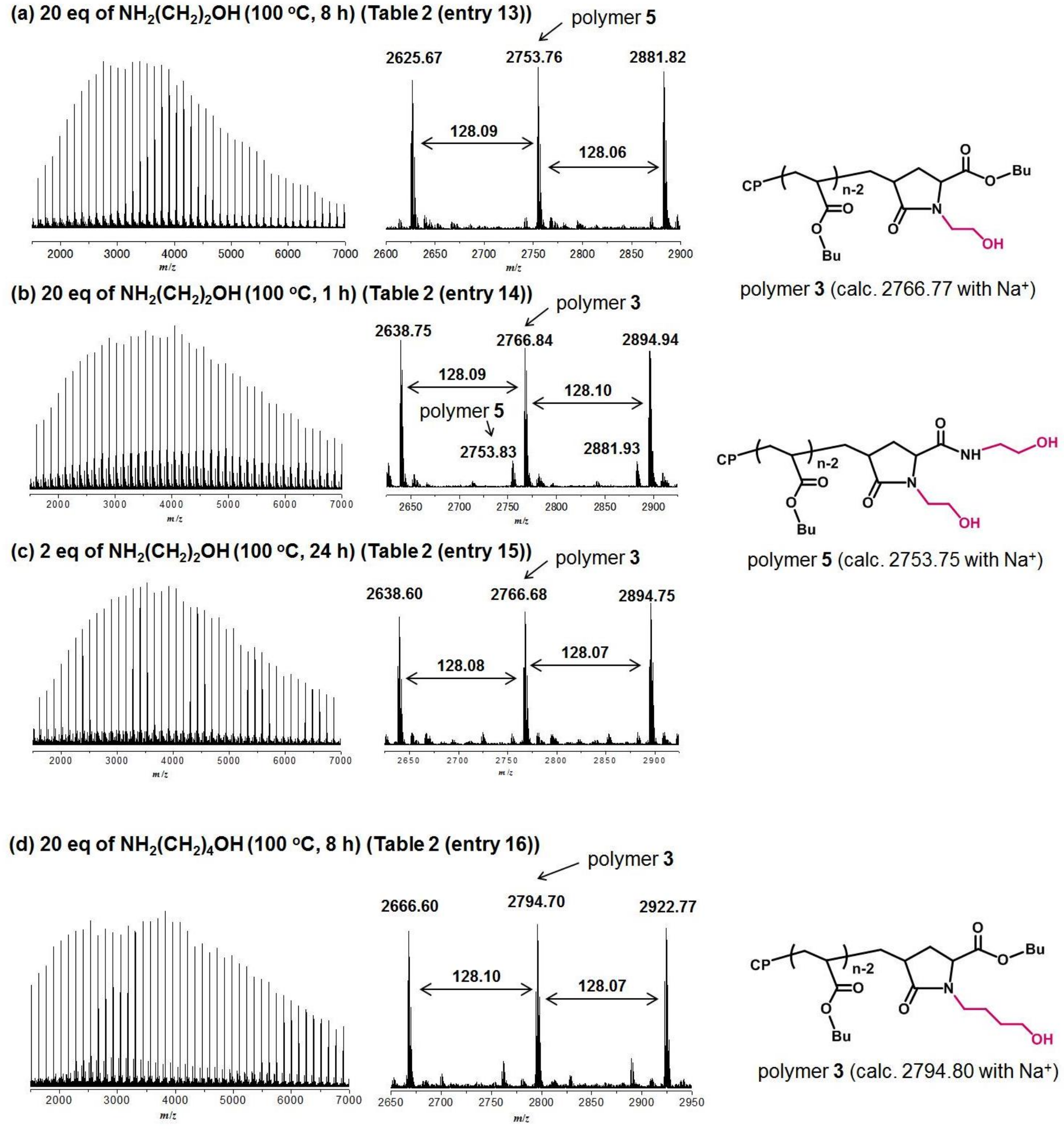

Figure 2.8. MALDI-TOF-MS spectra of polymers obtained with reactions of PBA-I (polymer **1**) with $NH_2(CH_2)_2OH$ and $NH_2(CH_2)_4OH$ in Table 2.2 (entries 13-16). The amines and reaction conditions are given in the figure.

Chain-End Transformation to NH_2 Group. Figure 2.9a shows the MALDI-TOF-MS spectrum of the polymer obtained with 20 eq of $NH_2CH_2CH_2NH_2$ at 100 °C for 1 h. Similar to R = CH_2CH_2OH, the reaction did not stop at polymer **3**. Scheme 2.2 shows a possible further reaction of polymer **3** for R = $CH_2CH_2NH_2$. Process (e) is the intramolecular amidation of polymer **3** through the terminal NH_2 group to produce polymer **6** with a 6-membered cyclic amide. The spectrum (experimental molar mass = 2691.69) matched polymer **6** (theoretical molar mass = 2691.71). Because an amide is more stable than an ester, the subsequent ring-opening of polymer **6** by the attack of another amine ($NH_2CH_2CH_2NH_2$) did not occur. Polymer **6** does not possess an NH_2 functionality and may not be very useful.

(a) 20 eq of $NH_2(CH_2)_2NH_2$ (100 °C, 1 h) (Table 2 (entry 17))

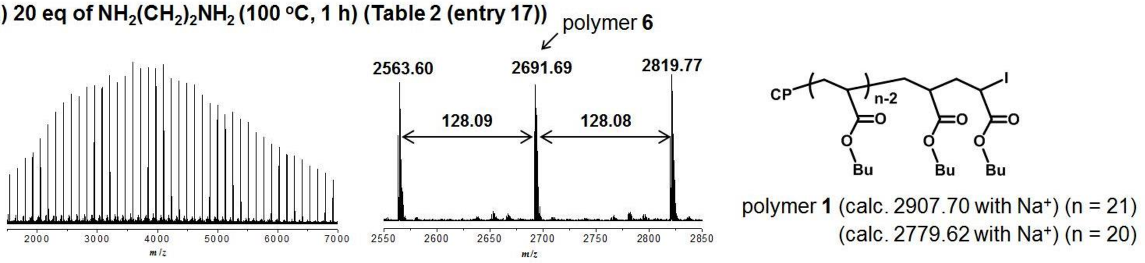

(b) 20 eq of $NH_2(CH_2)_2NH_2$ (100 °C, 10 min) (Table 2 (entry 18))

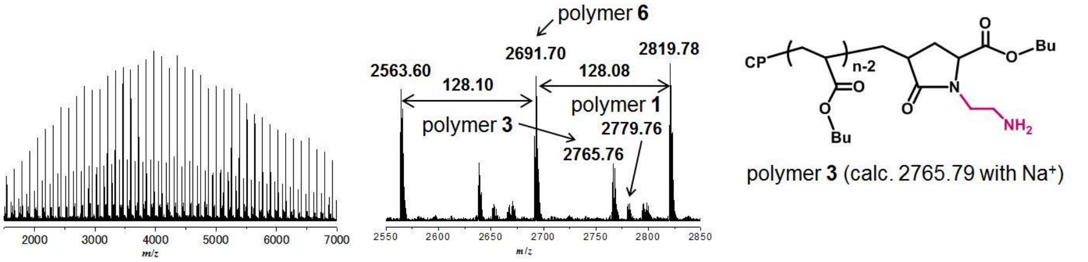

(c) 2 eq of $NH_2(CH_2)_2NH_2$ (100 °C, 1 h) (Table 2 (entry 19))

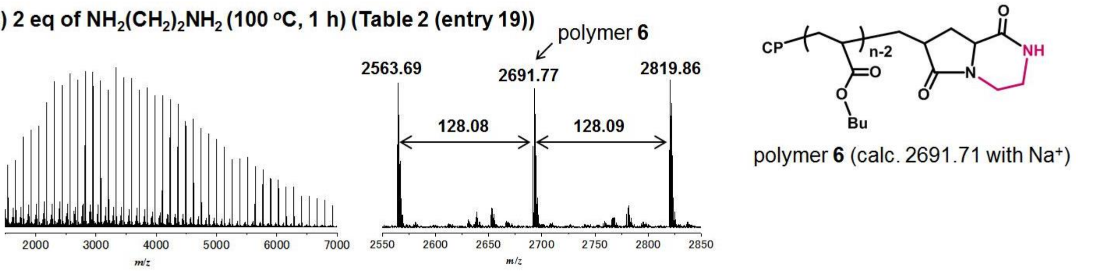

Figure 2.9. MALDI-TOF-MS spectra of polymers obtained with reactions of PBA-I (polymer **1**) with $NH_2(CH_2)_2NH_2$ in Table 2.2 (entries 17-19). The amines and reaction conditions are given in the figure.

To attach an NH_2 group, we reduced the reaction time from 1 h to a very short time 10 min to avoid the process (e). We observed the desired polymer **3** with an NH_2 functionality in 30% yield but still observed polymer **6** (60%) and polymer **1** (10%) (Figure 2.9b). Because we observed both reactant (polymer **1**) and further reacted (polymer **6**) polymers, it could be difficult to selectively stop the reaction at the intermediate polymer **3**. The reduced amount of $NH_2CH_2CH_2NH_2$ was not effective to provide polymer **3** (Figure 2.9c) (as expected). We used

$NH_2(CH_2)_4NH_2$ with a longer alkyl chain to avoid the generation of polymer **6** in the same manner as $NH_2(CH_2)_4OH$. However, we obtained only a mixture of polymer **6** and other unidentified side products and were unable to obtain polymer **3** (Figure 2.10).

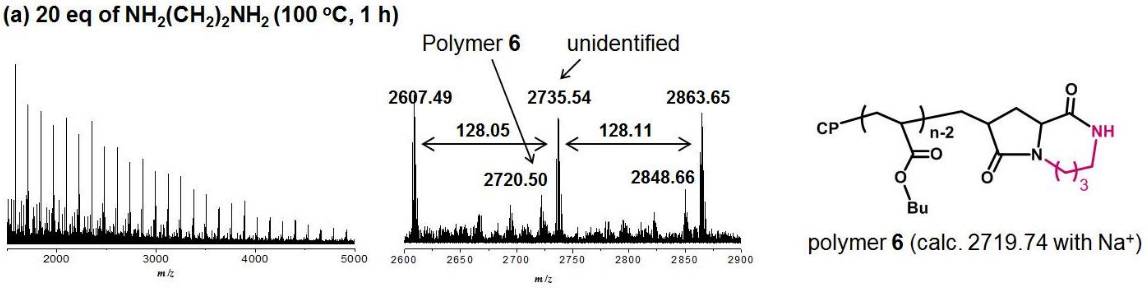

Figure 2.10. MALDI-TOF-MS spectrum of polymer obtained with a reaction of PBA-I (polymer **1**) (1 eq, 20 wt%) with $NH_2(CH_2)_4NH_2$ (20 eq) in diglyme (40 wt%) and 1-butanol (40 wt%) at 100 ^oC for 1 h.

Chain-End Transformation of PSt-I with Several Amines. We studied the chain-end transformation of PSt-I. We heated PSt-I (M_n = 4500 and $Đ$ = 1.21) (polymer **7**) (1 eq) and $NH_2CH_2CH_2Ph$ (5 eq) in *N*,*N*-dimethylformamide (DMF) (80/20 wt% DMF/polymer) at 100 °C for 8 h (Figure 2.11a). Scheme 2.3 shows the possible process and product of this chain-end transformation. Process (f) is the substitution of iodine with an amine to generate polymer **8**. Unlike PBA, PSt has no ester group, and hence polymer **8** undergoes no further reaction (no ring closure). Process (f) (substitution (S_N2) reaction) can compete with the elimination of HI from polymer **7** (elimination (E2) reaction) generating PSt-macromonomer. The substitution reactions of PSt-I with possible nucleophiles (such as moisture, diglyme and 1-butanol) may also happen. The corresponding products were also obtained during MALDI-TOF-MS analysis as minor products. The signals are very weak. Thus in the following discussions, we only focused on the chain-end functionalized PSt, PSt-macromonomer and CP-PSt-PSt-CP.

(a) 5 eq of $NH_2(CH_2)_2Ph$ (100 °C, 8 h) (Table 3 (entry 2))

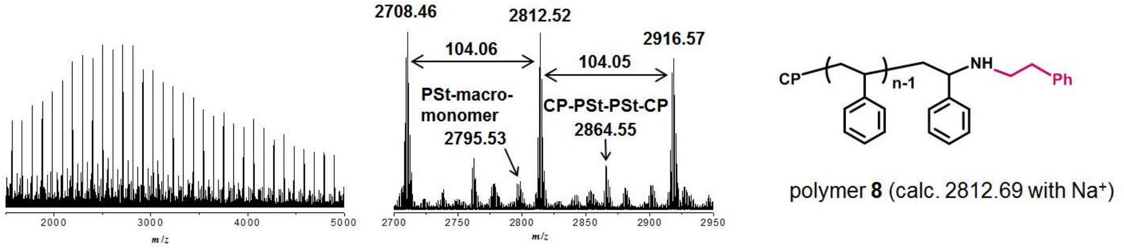

(b) 5 eq of $NH_2(CH_2)_4CH_3$ (100 °C, 8 h) (Table 3 (entry 4))

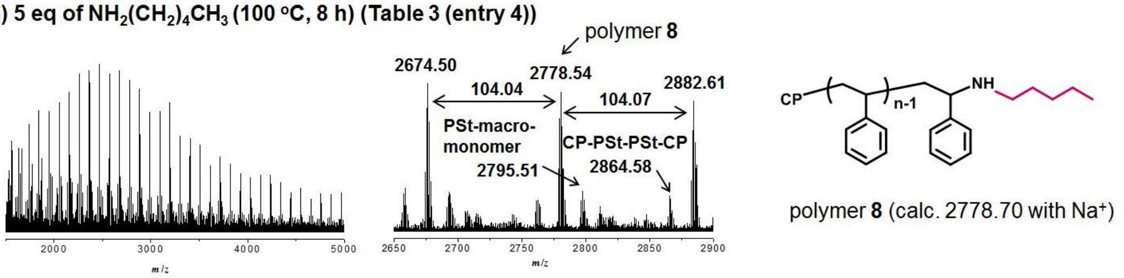

(c) 5 eq of $NH_2(CH_2)_3Si(OEt)_3$ (100 °C, 8 h) (Table 3 (entry 5))

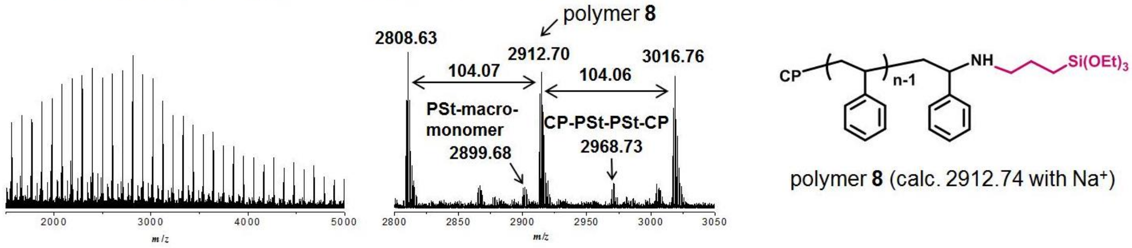

(d) 5 eq of $NH_2(CH_2)_2OH$ (100 °C, 8 h) (Table 3 (entry 7))

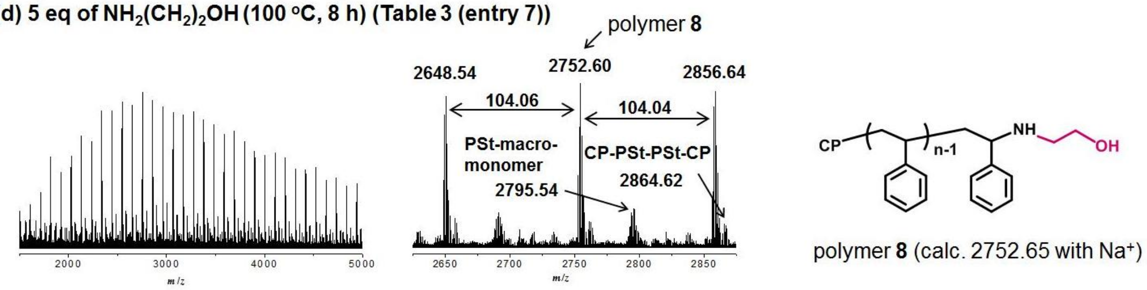

PSt-macromonomer (calc. 2795.66 with Na+)
(calc. 2899.72 with Na+)

CP-PSt-PSt-CP (calc. 2864.72 with Na+)
(calc. 2968.78 with Na+)

Figure 2.11. MALDI-TOF-MS spectra of polymers obtained with reactions of PSt-I (polymer **7**) with NH_2R in Table 2.3 (entries 2, 4, 5, and 7). The amines are given in the figure.

In Figure 2.11a, we observed the desired polymer **8** in 85% fraction and the elimination product PSt-macromonomer in 15% fraction, in addition to the originally contained CP-PSt-PSt-CP impurity. Thus, high selectivity was achieved in DMF. The selectivity was slightly lower when a mixed solvent of diglyme and 1-butanol was used (70% for polymer **8** and 30% for PSt-macromonomer, as shown in Table 2.3 (entry 1)). Thus, DMF was used as the solvent for the PSt experiments. We decreased the reaction temperature from 100 °C to 25 °C, but the selectivity was unchanged (Table 2.3 (entries 2 vs 3)). As shown in Figures 2.11b, 2.11c, and 2.11d, we also obtained polymer **8** with high selectivity (75-85%) for R = $(CH_2)_4CH_3$, $(CH_2)_3Si(OEt)_3$, and $(CH_2)_2OH$.

Table 2.3. Chain-End Transformation of PSt-I (polymer 7) with Amines (NH_2R).

entry	R	Equiv of NH_2R	*T* (°C)	Solvent	*t* (h)	Observed polymers (%) (percentages are rough estimate from MALDI-TOF-MS spectra with 10% estimate error)		
						Polymer **8**	PSt-macromonomer	Others
1	$(CH_2)_2Ph$	5	100	D/B[a]	8	70	30	0
2	$(CH_2)_2Ph$	5	100	DMF[b]	8	85	15	0
3	$(CH_2)_2Ph$	5	25	DMF[b]	12	85	15	0
4	$(CH_2)_4CH_3$	5	100	DMF[b]	8	75	25	0
5	$(CH_2)_3Si(OEt)_3$	5	100	DMF[b]	8	85	15	0
6	$(CH_2)_2SH$	5	100	DMF[b]	8	0	0	100 (unidentified)
7	$(CH_2)_2OH$	5	100	DMF[b]	8	85	15	0
8	$(CH_2)_2NH_2$	5	100	DMF[b]	8	0	0	100 (unidentified)

[a] polymer **7**/diglyme/1-butanol = 20/40/40 wt%. [b] polymer **7**/DMF = 20/80 wt%.

We observed unexpected and unidentified products for R = $(CH_2)_2SH$ and $(CH_2)_2NH_2$ (Figure 2.12). Only a single species was observed in both cases, but they match neither the reactant polymer **7**, the desired product polymer **8**, nor the PSt-macromonomer and PSt-H (with a hydrogen atom at the chain end) byproducts, and remain unidentified. Table 2.3 summarizes the PSt results.

(a) 5 eq of $NH_2(CH_2)_2SH$ (100 °C, 8 h) (Table 3 (entry 6))

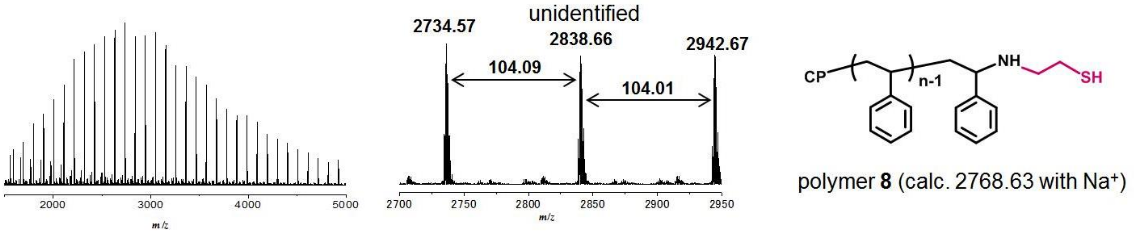

(b) 5 eq of $NH_2(CH_2)_2NH_2$ (100 °C, 8 h) (Table 3 (entry 8))

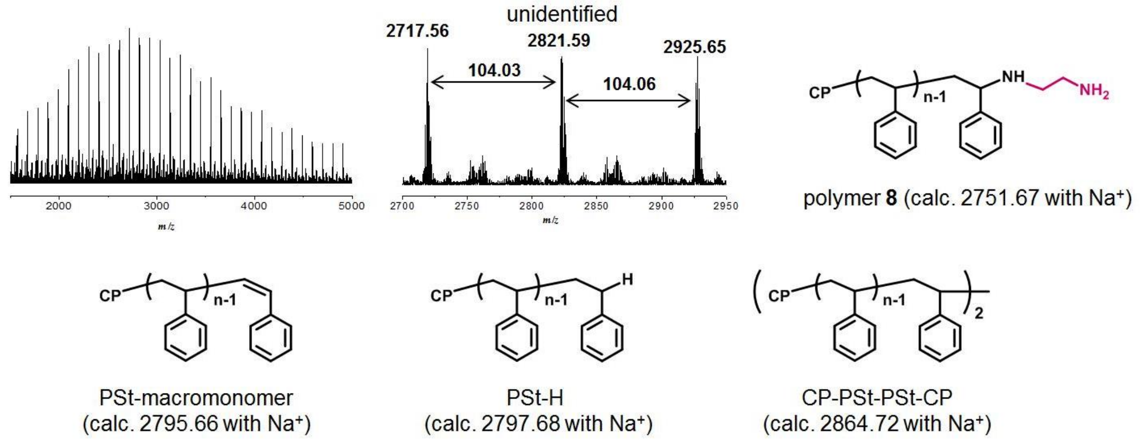

Figure 2.12. MALDI-TOF-MS spectra of polymers obtained with reactions of PSt-I (polymer **7**) with NH_2R in Table 2.3 (entries 6 and 8). The amines are given in the figure.

2.3 Conclusions

Chain-end functionalized polymers were successfully prepared through reactions of polymer-iodides and functional amines. Phenyl, alkyl, $Si(OEt)_3$, SH, and OH functionalities were attached at the chain end, and the reaction mechanisms were elucidated in detail. In addition, through radical chain transfer and CH_3I elimination reactions, hydrogen and lactone chain ends were also obtained. The reactant polymer-iodides can be synthesized by organocatalyzed LRP. The studied chain-end transformation reactions are metal-free, easy to perform, and versatile in wide ranges of polymers and functional groups. The combined use of organocatalyzed LRP and this post chain-end transformation may be useful for synthesizing various chain-end functionalized polymers.

2.4 Experimental

Materials. Styrene (St) (>99%, Tokyo Chemical Industry (TCI), Japan), butyl acrylate (BA) (>99%, TCI), 2-cyanopropyl iodide (CP-I) (>95%, TCI), tetrabutylammonium iodide (Bu_4NI) (>98%, TCI), 2.2′-azobis(2-methylpropionitrile) (AIBN) (98%, Wako Pure Chemical, Japan), 2-phenylethylamine (>98%, TCI), 1-amylamine (>98%, TCI), 3-aminopropyltriethoxysilane (>98%, TCI), 2-aminoethanethiol (>95%, TCI), 2-aminoethanol (>99%, TCI), 4-amino-1-butanol (>98%, TCI), ethylenediamine (>99%, Kanto Chemical, Japan), 1,4-diaminobutane (>98%, TCI), 1,6-diaminohexane (>99%, TCI), 2-phenylethanethiol (>97%, TCI), diethylene glycol dimethyl ether (diglyme) (>99%, TCI), 1-butanol (>99%, Kanto), *N*,*N*-dimethylformamide (DMF) (>99.5%, Kanto), methanol (>99%, International Scientific), tetrahydrofuran (THF) (>99.5%, Kanto), trans-2-[3-(4-t-butylphenyl)-2-methyl-2-propenylidene]malononitrile (DCTB) (>99%, Fluka Chemicals Ltd., UK), dithranol (>98%, Fluka), NaI (>99.5%, Kanto), and sodium trifluoroacetate (NaTFA) (>98%, TCI) were used as received.

Analytical GPC. The GPC analysis was performed on a Shodex GPC-101 liquid chromatograph (Tokyo, Japan) equipped with two Shodex KF-804L mixed gel columns (300 × 8.0 mm; bead size = 7 μm; pore size = 20–200 Å). The eluent was THF at a flow rate of 1.0 mL/min (40 °C). Sample detection and quantification were conducted using a Shodex differential refractometer RI-101 calibrated with known concentrations of polymer in solvent. The monomer conversion was determined from the peak area. The column system was calibrated with standard polystyrenes and poly(methyl methacrylate)s.

Preparative GPC. Polymers were purified with a preparative GPC (LC-9204, Japan Analytical Industry, Tokyo) equipped with JAIGEL 1H and 2H polystyrene gel columns

(600×40 mm; bead size = 16 μm; pore size = 20-30 (1H) and 40-50 (2H) Å). Chloroform was used as eluent at a flow rate of 14 mL/min (room temperature).

NMR. The NMR spectra of the polystyrene (PSt) in Figure 3 were recorded on an AV500 spectrometer (500 MHz) (Bruker, Germany) at ambient temperature; ^{1}H: spectral width 5000.00 Hz, acquisition time 6.554 sec, and pulse delay 1.000 sec. The NMR spectrum of poly(butyl acrylate) (PBA) in Figure 5 was recorded on a BBFO400 spectrometer (400 MHz) (Bruker) at ambient temperature; ^{1}H: spectral width 4000.00 Hz, acquisition time 8.192 sec, and pulse delay 1.000 sec.

MALDI-TOF-MS. The matrix assisted laser desorption/ionization time-of-flight mass spectrometry (MALDI-TOF-MS) spectra were recorded on a JMS-S3000 SpiralTOF (JEOL Ltd., Japan) at an accelerating potential of 20 kV in the positive spiral mode. We prepared the polymer solution (PBA: 10 g/L and PSt: 15 g/L in THF in all cases), matrix solution (DCTB: 10 g/L, or dithranol: 60 g/L, in THF in both cases), and cationization agent solution (NaI: 10 g/L in methanol, or NaTFA: 10 g/L in THF). The MALDI-TOF-MS samples were prepared by the dried droplet method.[1] For the PBA samples, the PBA solution (in THF) and the DCTB solution (in THF) were mixed in a ratio of 1/4 (v/v). First, 5 μL of the NaI solution (in methanol) was deposited on the target plate and dried in the air at room temperature. Second, 5 μL of the mixed PBA/DCTB solution (in THF) was deposited on the same target plate spot and dried in the air at room temperature. The solutions were deposited in this two-step manner, because NaI is not soluble in THF. For the PSt samples, NaTFA was used as a cationization agent which is soluble in THF. The polymer, matrix, and cationization agent solutions (all in THF) were mixed together in ratios of 1/2/1 (v/v/v) for PSt/dithranol (or DCTB)/NaTFA. Then, 5 μL of the mixed solution was deposited on the target plate and dried in the air at room temperature.

Preparation of PBA-I. A mixture of BA (20 g (8 M)), CP-I (80 mM), and Bu_4NI (320 mM) was heated in a 100 mL flask at 110 °C for 6 h under an argon atmosphere with magnetic stirring, yielding a PBA-I with M_n = 5200 and M_w/M_n = 1.36 (monomer conversion = 36.7%) (before purification). The reaction mixture was diluted with THF, and the polymer was reprecipitated in a water/methanol mixture (50/50 wt%). After further purification with preparative GPC, a PBA-I with M_n = 5300 and M_w/M_n = 1.36 was obtained (Table 2.1 (entry 1)).

Preparation of PSt-I. A mixture of St (10 g (8 M)), CP-I (160 mM), AIBN (60 mM), and Bu_4NI (40 mM) was heated in a 100 mL flask at 80 °C for 9 h under an argon atmosphere with magnetic stirring, yielding a PSt-I with M_n = 4200 and M_w/M_n = 1.25 (monomer conversion = 85.0%) (before purification). The reaction mixture was diluted with THF, and the polymer was reprecipitated in methanol. After further purification with preparative GPC, a PSt-I with M_n = 4500 and M_w/M_n = 1.21 was obtained (Table 2.1 (entry 2)).

Chain-End Functionalization. A mixture of a polymer-I (20 wt%), an amine (20 eq or 2 eq), and a solvent (80 wt%) in a reaction tube was capped with a stopcock in the atmospheric air, heated at a prescribed temperature in the dark for a prescribed time with magnetic stirring, and quenched to room temperature. The mixture was diluted by THF, and then the polymer was reprecipitated in a non-solvent (methanol/water (50/50 wt%) for PBA, and methanol for PSt. The polymer was further purified with preparative GPC and dried overnight. The obtained polymer was subjected to MALDI-TOF-MS and ^{1}H NMR analyses.

2.5 References

1. Tasdelen, M. A.; Kahveci, M. U.; Yagci, Y. *Prog. Polym. Sci.* **2011**, *36*, 455−567.
2. Debuigne, A.; Hurtgen, M.; Detrembleur, C.; Jérôme, C.; Barner-Kowollik, C.; Junkers, T. *Prog. Polym.Sci.* **2012**, *37*, 1004−1030.
3. Fairbanks, B. D.; Gunatillake, P. A.; Meagher, L. *Adv. Drug Delivery Rev.* **2015**, *91*, 141−152.
4. Matyjaszewski, K.; Möller, M. *Polymer Science*: A Comprehensive Reference; Elsevier: Amsterdam, 2012.
5. Tsarevsky, N. V.; Sumerlin, B. S. *Fundamentals of Controlled/Living Radical Polymerization*; Royal Society of Chemistry: U.K., 2013.
6. Matyjaszewski, K.; Tsarevsky, N. V. *J. Am. Chem. Soc.* **2014**, *136*, 6513−6533.
7. Ouchi, M.; Terashima, T.; Sawamoto, *M. Chem. Rev.* **2009**, *109*, 4963−5050.
8. Zhang, N.; Samanta, S. R.; Rosen, B. M.; Percec, V. *Chem. Rev.* **2014**, *114*, 5848−5958.
9. Boyer, C.; Corrigan, N. A.; Jung, K.; Nguyen, D.; Nguyen, T.-K.; Adnan, N. N. M.; Oliver, S.; Shanmugam, S.; Yeow, J. *Chem. Rev.* **2016**, *116*, 1803−1949.
10. David, G.; Boyer, C.; Tonnar, J.; Ameduri, B.; Lacroix-Desmazes, P.; Boutevin, B. *Chem. Rev.* **2006**, *106*, 3936−3962.
11. Nicolas, J.; Guillaneuf, Y.; Lefay, C.; Bertin, D.; Gigmes, D.; Charleux, B. *Prog. Polym. Sci.* **2013**, *38*, 63−235.
12. Keddie, D. J.; Moad, G.; Rizzardo, E.; Thang, S. H. *Macromolecules* **2012**, *45*, 5321−5342.
13. Yamago, S. *Chem. Rev.* **2009**, *109*, 5051−5068.
14. Satoh, K.; Kamigaito, M. *Chem. Rev.* **2009**, *109*, 5120−5156.
15. Monteiro, M. J.; Cunningham, M. F. *Macromolecules* **2012**, *45*, 4939−4957.
16. Mastan, E.; Li, X.; Zhu, S. *Prog. Polym. Sci.* **2015**, *45*, 71−101.
17. Zetterlund, P. B.; Thickett, S. C.; Perrier, S.; Bourgeat-Lami, E.; Lansalot, M. *Chem. Rev.* **2015**, *115*, 9745−9800.
18. Chen, M.; Zhong, M.; Johnson, *J. A. Chem. Rev.* **2016**, *116*, 10167−10211.
19. Goto, A.; Fukuda, T. *Prog. Polym. Sci.* **2004**, *29*, 329−385.
20. Goto, A.; Zushi, H.; Hirai, N.; Wakada, T.; Tsujii, Y.; Fukuda, T. *J. Am. Chem. Soc.* **2007**, *129*, 13347−13354.
21. Vana, P.; Goto, A. *Macromol. Theory Simul.* **2010**, *19*, 24−35.

22. Yorizane, M.; Nagasuga, T.; Kitayama, Y.; Tanaka, A.; Minami, H.; Goto, A.; Fukuda, T.; Okubo, M. *Macromolecules* **2010**, *43*, 8703−8705.

23. Goto, A.; Suzuki, T.; Ohfuji, H.; Tanishima, M.; Fukuda, T.; Tsujii, Y.; Kaji, H. *Macromolecules* **2011**, *44*, 8709−8715.

24. Ohtsuki, A.; Goto, A.; Kaji, H. *Macromolecules* **2013**, *46*, 96−102.

25. Ohtsuki, A.; Lei, L.; Tanishima, M.; Goto, A.; Kaji, H. *J. Am. Chem. Soc.* **2015**, *137*, 5610−5617.

26. Goto, A.; Sanada, S.; Lei, L.; Hori, K. *Macromolecules* **2016**, *49*, 2511−2517.

27. Sarkar, J.; Xiao, L.; Goto, A. *Macromolecules* **2016**, *49*, 5033−5042.

28. Goto, A.; Ohtsuki, A.; Ohfuji, H.; Tanishima, M.; Kaji, H. *J. Am. Chem. Soc.* **2013**, *135*, 11131−11139.

29. Coessens, V.; Matyjaszewski, K. *Macromol. Rapid Commun.* **1999**, *20*, 127−134.

30. Snijder, A.; Klumperman, B.; van der Linde, R. *J. Polym. Sci., Part A: Polym. Chem.* **2002**, *40*, 2350−2359.

31. Zhang, H.; Jiang, X.; van der Linde, R. *Polymer* **2004**, *45*, 1455−1466.

32. Lacroix-Desmazes, P.; Severac, R.; Boutevin, B. *Macromolecules* **2005**, *38*, 6299−6309.

33. Lansalot, M.; Farcet, C.; Charleux, B.; Vairon, J. P.; Pirri, R. *Macromolecules* **1999**, *32*, 7354−7360.

34. Nonaka, H.; Ouchi, M.; Kamigaito, M.; Sawamoto, M. *Macromolecules* **2001**, *34*, 2083−2088.

35. Ladavière, C.; Lacroix-Desmazes, P.; Delolme, F. *Macromolecules* **2009**, *42*, 70−84.

36. Kim, K.; Hasneen, A.; Paik, H.; Chang, T. *Polymer* **2013**, *54*, 6133−6139.

37. Chendo, C.; Le, D.; Phan, T. N. T.; Gigmes, D.; Charles, L. *J. Polym. Sci., Part A: Polym. Chem.* **2016**, *54*, 3388−3397.

38. Charles, L. *Mass Spectrom. Rev.* **2014**, *33*, 523−543.

39. Borman, C. D.; Jackson, A. T.; Bunn, A.; Cutter, A. L.; Irvine, D. J. *Polymer* **2000**, *41*, 6015−6020.

40. Ando, T.; Kamigaito, M.; Sawamoto, M. Macromolecules 1997, 30, 4507−4510.

41. Sakashita, K.; Onuma, T.; Noda, T. *Jpn. Patent Application Publication* JP 2014015574, 2014.

Chapter 3 Photo-selective chain end transformation of polyacrylate-iodide using cysteamine and its application to facile single-step preparation of patterned polymer brushes

Abstract

Cysteamine, which is an inexpensive and non-toxic aminothiol, was successfully employed as a photo-selective chain end transformation agent of iodo-terminated polymer chains (polymer-I). Polymer-I was selectively transformed to hydrogen-terminated (polymer-H) and thiol-terminated (polymer-SH) polymers with and without UV irradiation, respectively. This method is applicable to acrylate polymers. This photo-selective reaction offered a single-step preparation of patterned polymer brushes with SH and H chain end functionalities as a unique application.

3.1 Introduction

Selective reactions, in which different products are selectively generated from the same reactant in response to the applied environment, are useful tools in organic and polymer syntheses. Different products are targeted upon different external stimuli such as temperature, light, redox, force, and solvent polarity, enabling unique molecular design by simply switching the external stimuli.[1–6]

Living radical polymerization (LRP),[7–9] also known as reversible-deactivation radical polymerization, is a powerful approach for preparing polymers with narrow molecular weight distribution and well-defined structures. The obtained polymer (polymer-X) possesses a capping agent (X) at the chain end. Chain end functionalized polymers are obtainable via the conversion of X to functional groups.[10–13]

Thiol-terminated polymers can connect with other polymers and biomolecules to create block copolymers, stars, and bio-conjugates,[14–18] and can also be anchored on gold surfaces to generate polymer brushes on the surfaces.[19]

The reactive chain end (capping agent X) of the polymer obtained via LRP often negatively influences the long-term stability and the post polymer possessing. To address this negative aspect, the conversion of X to a simple hydrogen has been achieved through either thermal or photo-induced reduction.[20,21]

Thiol- and hydrogen-terminated polymers (polymer-SH and polymer-H, respectively) were synthesized independently. Recently, an elegant approach was reported on successive conversion of polymer-trithiocarbonate to polymer-SH and subsequently to polymer-H using a photo-redox catalyst and amine and phosphine additives (Scheme 3.1a).[22] Herein, we propose a simple and unique approach for synthesizing polymer-SH and polymer-H selectively under two different external stimuli (Schemes 3.1b).

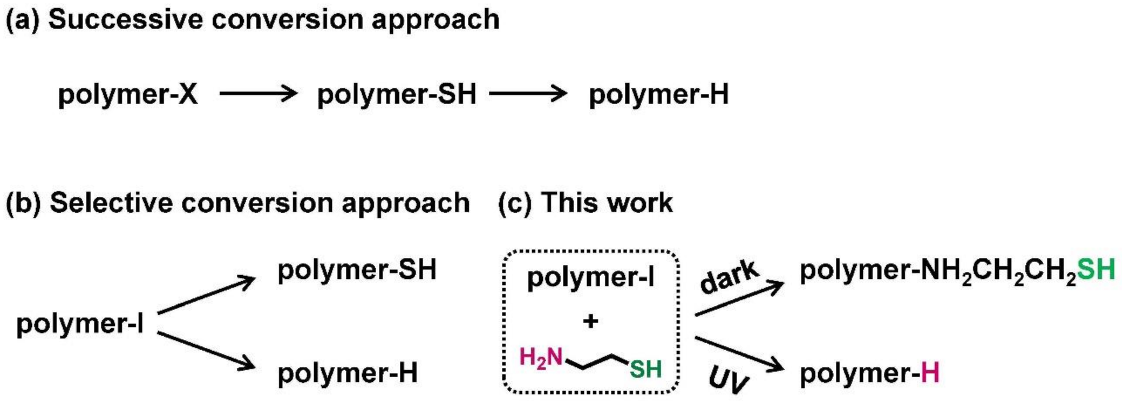

Scheme 3.1. (a) Successive and (b) selective conversion approaches for the synthesis of polymer-SH and polymer-H. (c) This work.

Our group developed an organocatalyzed LRP using alkyl iodides as dormant species (X = iodide) and organic molecules as catalysts.[23–26] The post-modification of the terminal iodide was studied via treatment with primary amines (R-NH_2), yielding chain end functionalized polymers (polymer-NHR) with various functionalities at the R group.[27]

In the present work, we use bifunctional cysteamine ($NH_2CH_2CH_2SH$) containing thiol and primary amino groups as a chain end modification agent (Scheme 3.1c). Cysteamine is biosynthesized in mammals and biocompatible. Without photo irradiation, the chain end iodide reacts with the amino group of cysteamine via substitution reaction, yielding a thiol-terminated polymer-SH (Scheme 3.1c). With the UV irradiation, the carbon-iodide bond is photo-cleaved to generate a carbon-centred radical (polymer$^•$), which undergoes a radical transfer reaction with the thiol group of cysteamine and yields a hydrogen-terminated polymer-H (Scheme 3.1c). Therefore, by switching the UV irradiation on and off, polymer-H and polymer-SH are selectively obtained from the same reactant polymer-I (iodo-terminated polymer). Because the substitution occurs effectively for secondary alkyl chains but not tertiary alkyl chains, this method is useful to acrylate polymers but not methacrylate polymers. This work focuses on acrylate polymers. This approach is selective conversion (Scheme 3.1b) different from successive conversion (Scheme 3.1a). The selective conversion enables a single-step preparation of patterned polymer brushes with SH and H chain end functionalities as a unique application described below. This approach is attractive for the use of only two reactants, *i.e.*, polymer-I and cysteamine without extra catalysts and additives. The non-toxic nature of cysteamine is further attractive for biological applications.

3.2 Results and Discussion

To probe this reaction, we first studied a low-mass model alkyl iodide, *i.e.*, ethyl 2-iodopropanoate (EA-I (Figure 3.1)), which is a unimer model of poly(acrylate)-iodide. We studied a mixture of EA-I (80 mM) and cysteamine (400 mM) with or without UV irradiation (365 (± 10) nm) at room temperature. The solvent was a mixed solvent (dielectric constant ε = 6.0) of toluene-d_8 (ε = 2.4) and methanol-d_4 (ε = 32.7) (w/w = 88/12), in which methanol-d_4 was added to dissolve cysteamine.

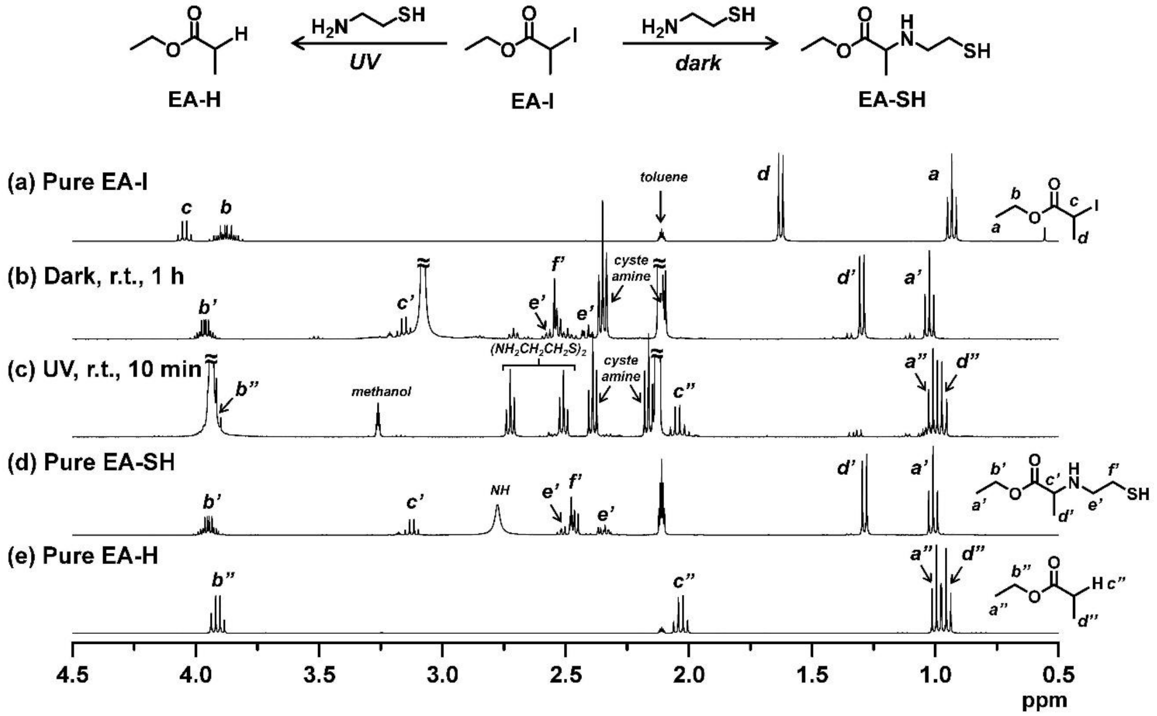

Figure 3.1. ^{1}H NMR (400 MHz) spectra in a mixture of toluene-d_8 and methanol-d_4 (w/w = 88/12). (a) Pure EA-I. (b)(c) A reaction mixture of EA-I (80 mM) and cysteamine (400 mM) (b) without UV after 1 h and (c) with UV (365 (± 10) nm) after 10 min. (d) Pure EA-SH. (e) Pure EA-H.

In a dark condition (without UV) after 1 h, EA-I was virtually quantitatively (> 99%) converted to the substitution product EA-SH (Figures 3.1a, 3.1b, and 3.1d). In contrast, under UV irradiation for 10 min, EA-I was mainly converted to the radical transfer product EA-H (91%) with minor generation of the substitution product EA-SH (9%) (Figures 3.1a, 3.1c, and

3.1e). (While this reaction was optimized, a higher UV intensity and a lower temperature may even suppress the generation of EA-SH.) These results clearly demonstrate high selectivity of the reaction with and without UV irradiation.

Mechanistically, with UV irradiation, EA-I is photo-dissociated to generate $EA^{\bullet}$, which subsequently abstracts a hydrogen from the SH group of cysteamine to generate EA-H and $NHCH_2CH_2S^{\bullet}$. Two molecules of $NHCH_2CH_2S^{\bullet}$ subsequently combine to form a disulfide (as observed at 2.51 and 2.72 ppm in Figure 3.1c). Both with and without UV irradiation, HI was generated, forming a salt (precipitation) with cysteamine. HI changed pH, resulting in slight difference in the NMR chemical shift among the samples (Figure 3.1).

Instead of EA-I, the bromide analogue, *i.e.*, ethyl 2-bromopropanoate (EA-Br), was also studied. However, EA-Br was converted to only EA-SH but not EA-H. EA-SH was also slow to generate (85 % for 1 h). Therefore, the dual (selective) and rapid reactions are unique to the alkyl iodide.

Both of the NH_2 and SH groups of cysteamine are nucleophiles and may undergo substitution with alkyl halides.[28] However, in our studied condition, we observed only the substitution with NH_2 (hence EA-SH as a product), meaning that NH_2 is a much more reactive nucleophile than SH in our condition.

If SH is a nucleophile, the substitution reaction of EA-I with cysteamine generates EA-$SCH_2CH_2NH_2$ with a terminal NH_2 group (EA-NH_2). EA-NH_2 would subsequently readily undergo an intra-molecular amidation to generate a 6-memberred lactam (EA-lactam, Figure 3.2b).

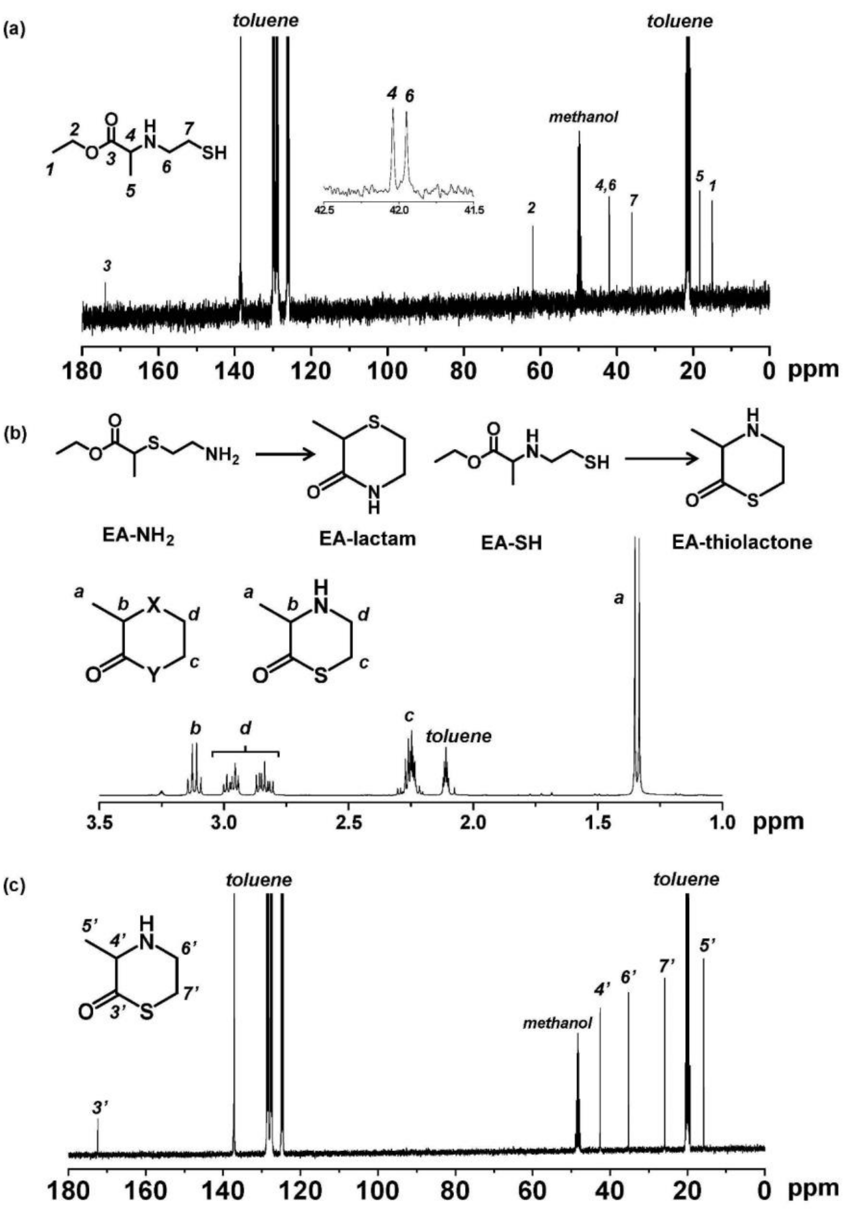

Figure 3.2. NMR spectra in a mixture of toluene-*d*$_8$ and methanol-*d*$_4$ (w/w = 88/12). (a) ^{13}C NMR spectrum of EA-SH. (b and c) ^{1}H and ^{13}C NMR spectra of EA-thiolactone.

For the reaction of EA-I with cysteamine in the dark condition, we observed EA-SH after 1 h. We further prolonged the reaction time from 1 h to 12 h. EA-SH was stable and underwent no further reaction. To this reaction mixture, for a characterization purpose, silica gel was added to induce the ring closure reaction. After the purification by chromatography**,** a product with a 6-membered ring was obtained, which should be either EA-thiolactone or EA-lactam if any (Figure 3.2b). Figure 3.2b shows the ^{1}H NMR spectrum of the 6-membered ring product.

The two split signals (2.79–2.88 ppm and 2.93–3.02 ppm) belong to XCH_2 (protons d), because the axial proton d interacts with the axial proton b (the methyl group is bulkier and equatorial) and the equatorial proton d does not, resulting in the two different chemical shifts (protons d). The non-split signal at 2.22–2.31 ppm belongs to YCH_2 (protons c). In comparison of N and S, the chemical shift of NCH_2 (down-field) should be higher than that of SCH_2 (up-field). This means that XCH_2 (down-field protons d) is NCH_2, and YCH_2 (up-field protons c) is SCH_2. The product obtained must be EA-thiolactone (not EA-lactam), demonstrating that only NH_2 worked as a nucleophile in the studied reaction condition. The ^{1}H NMR and ^{13}C NMR spectra (toluene-d_8/methanol-d_4 (w/w = 88/12)) and the assignment are given in Figures 3.2b and 3.2c.

We then studied polymer systems. Poly(butyl acrylate)-iodide (PBA-I) was prepared via the organocatalyzed LRP of butyl acrylate (BA) with 2-iodo-2-methylpropionitrile (CP-I) as an alkyl iodide initiator and tetrabutylammonium iodide (BNI) as a catalyst (ESI). The PBA-I was purified by reprecipitation and subsequently by preparative GPC to remove trace amounts of impurities. The M_n and dispersity ($Đ = M_w/M_n$) of the purified PBA-I were 2900 and 1.29, respectively, where M_n and M_w are the number-average and weight-average molecular weights, respectively.

Subsequently, polymer-I (1 eq, 20 wt%) and cysteamine (20 eq) were dissolved in a mixed solvent ($\varepsilon = 13.8$) of diglyme ($\varepsilon = 7.2$) and 1-butanol ($\varepsilon = 17.4$) (w/w = 1/1). An excess of cysteamine (20 eq) was used, because the reaction is slower for a polymer (polymer-I) than a low-mass analogue (EA-I). A more polar solvent was used for polymer-I ($\varepsilon = 12.3$) than EA-I ($\varepsilon = 6.0$) to accelerate the substitution reaction. The reaction time was also prolonged to 12 h in the dark condition and 2 h with UV irradiation.

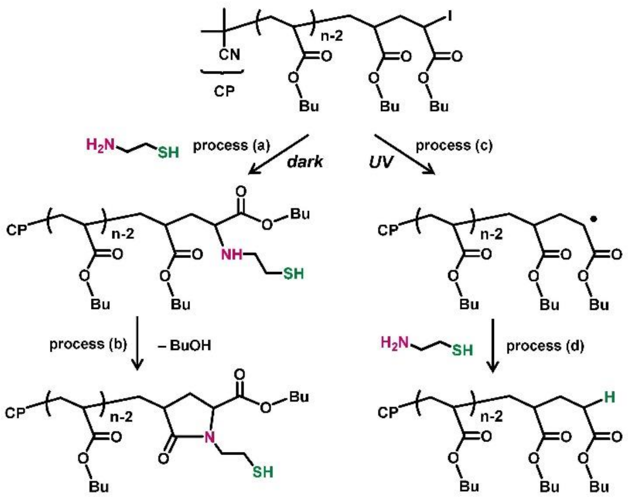

Scheme 3.2. Detailed mechanisms for the selective reactions of PBA-I and cysteamine with and without UV irradiation.

Scheme 3.2 shows the detailed reaction mechanisms. In the dark condition, PBA-I undergoes substitution with NH_2 of cysteamine to generate polymer **1** (process (a) in Scheme 3.2), followed by an intramolecular amidation to generate polymer **2** with a 5-membered ring at the chain end (process (b)). The chain end of Polymer **2** possesses an SH group. Under UV irradiation, PBA-I was photo-dissociated to generate a polymer radical $PBA^{\bullet}$ (process (c)), followed by a radical transfer with SH of cysteamine to generate a hydrogen-terminated PBA-H (process (d)).

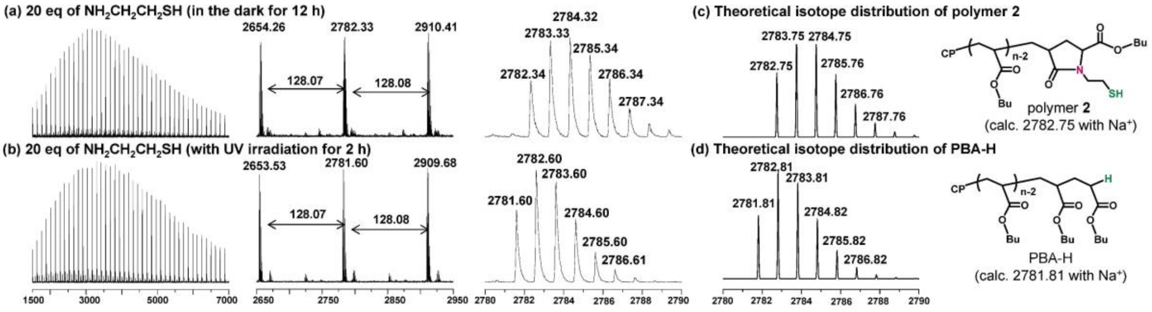

Figure 3.3. MALDI-TOF-MS spectra of products obtained *via* a reaction of PBA-I and cysteamine (a) without UV after 12 h and (b) with UV after 2 h. The theoretical molar mass distributions of (c) polymer **2** and (d) PBA-H with n = 21.

Figure 3.3a shows the matrix-assisted laser desorption/ionization time-of-flight mass spectrometry (MALDI-TOF-MS) spectrum of the product in the dark condition for 12 h. We used trans-2-[3-(4-*tert*-butylphenyl)-2-methyl-2-propenylidene]malononitrile (DCTB) as a matrix and CF_3COONa as an additive salt for the MALDI-TOF-MS analysis. Figure 3.3a (right) shows the isotope distribution (^{13}C distribution) in the molar mass region of 2780–2790. Figure 3.3c shows the theoretical isotope distribution of polymer **2**. The far left peak (experimental molar mass = 2782.34) corresponds to the polymer without ^{13}C atom (only with ^{12}C atoms). The experimental molar mass matches the theoretical molar mass (2782.75). The second peak from the left (experimental molar mass = 2783.33) corresponds to the polymer possessing one ^{13}C atom, and the other peaks (experimental molar mass = 2784.32 and so on) correspond to those possessing two or more ^{13}C atoms. The experimental molar mass distribution (Figure 3.3a (right)) well matched the theoretical one of polymer **2** (Figure 3.3c). We also observed only a single series of repeated peaks (*i.e.*, only one product) (Figure 3.3a (middle)), suggesting a nearly quantitative conversion of PBA-I to polymer **2**. The ^{1}H NMR spectrum (Figure 3.4) also confirmed successful attachment of the CH_2CH_2SH moiety (Figure 3.4b, protons *l* and *m*).

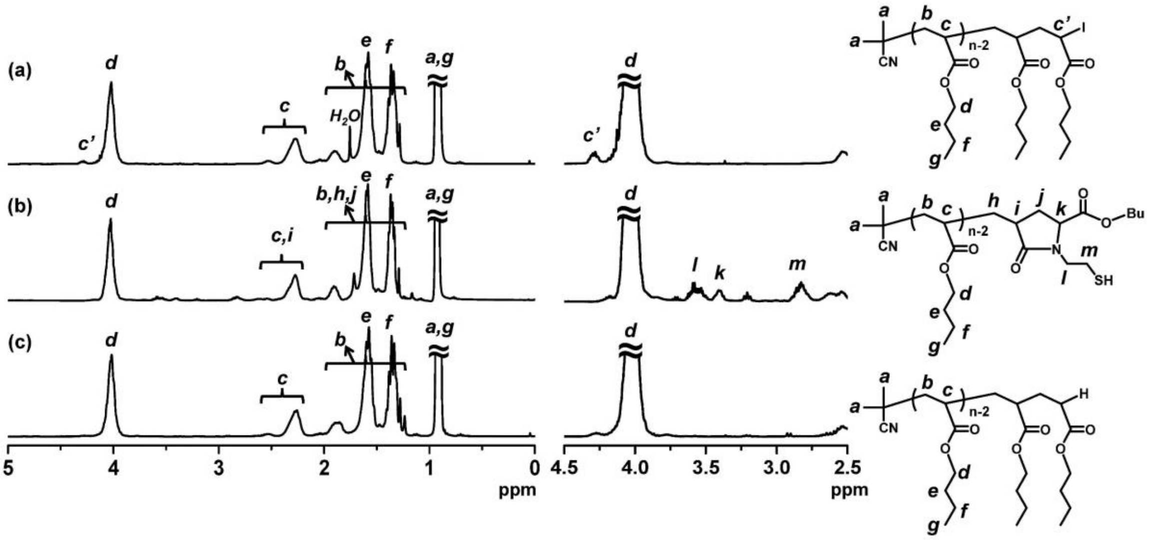

Figure 3.4. ^{1}H NMR (400 MHz) spectra ($CDCl_3$) of (a) PBA-I, (b) PBA-SH (polymer **2**), and (c) PBA-H.

In contrast, under UV irradiation for 2 h, we observed only PBA-H as a single species (Figure 3.3b (middle)). The experimental molar mass (2781.60) (Figure 3.3b (right)) matched the theoretical molar mass of PBA-H (2781.81 (Figure 3.3d)). The difference in the theoretical molar masses of polymer **2** (2782.75 (Figure 3.3c)) and PBA-H (2781.81 (Figure 3.3d)) is only 0.94. Therefore, we look into the peak areas. The theoretical area ratio of the far left and second left peaks of PBA-H (2781.81 and 2782.81 (Figure 3.3d)) is 0.571. The experimental area ratio (0.605) of those peaks (2781.60 and 2782.60 (Figure 3.3b)) was close to the theoretical one. If polymer **2** is also generated, the experimental peak at 2782.60 should increase because the peak of polymer **2** is overlapped. The close matching of the experimental (0.605) and theoretical (0.571) ratios means a nearly quantitative conversion of PBA-I to PBA-H. These results show high selectivity of the reactions with and without UV irradiation.

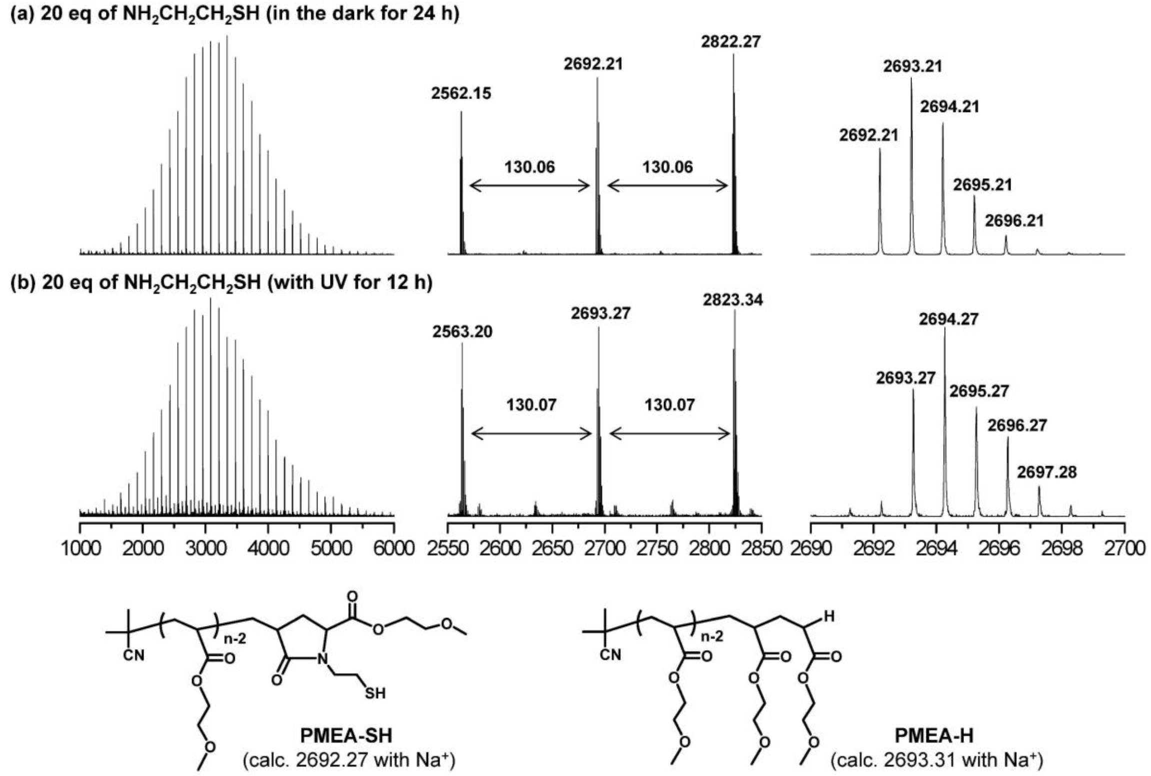

Figure 3.5. MALDI-TOF-MS spectra of the polymers obtained via a reaction of PMEA-I (1 equiv) and cysteamine (20 equiv) (a) without UV after 24 h and (b) with UV after 12 h.

To extend the scope of polymer, we also used this method to other polymers, *i.e.*, poly(2-methoxyethyl acrylate)-iodide (PMEA-I) (M_n = 3000 and $Đ$ = 1.16) and carboxylic acid terminated PMEA-I (HOOC-PMEA-I) (M_n = 3200 and $Đ$ = 1.79). We successfully obtained thiol-terminated polymers (PMEA-SH and HOOC-PMEA-SH) and hydrogen-terminated polymers (PMEA-H and HOOC-PMEA-H) in a selective manner (Figures 3.5 and 3.6).

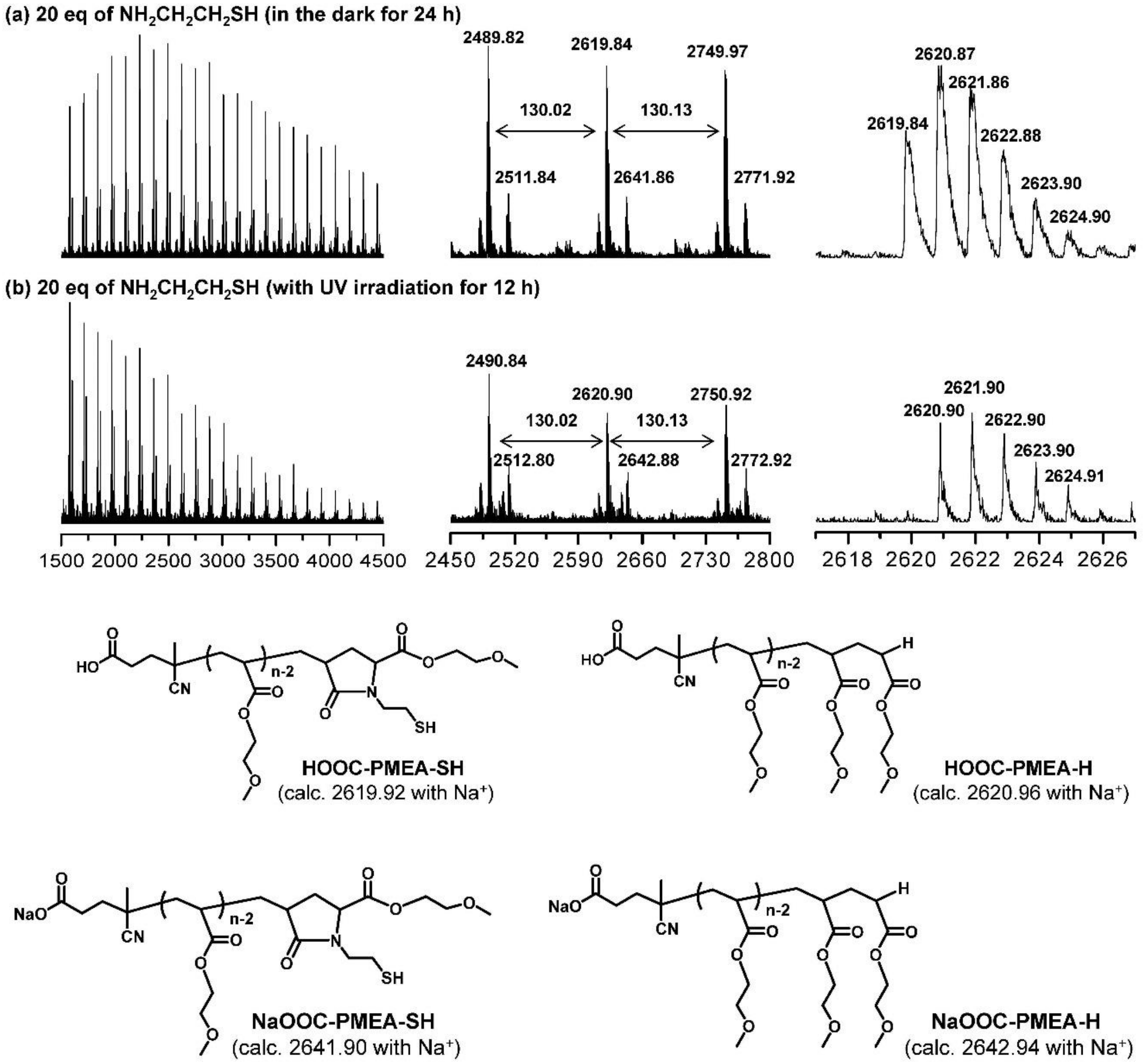

(a) 20 eq of $NH_2CH_2CH_2SH$ (in the dark for 24 h)

(b) 20 eq of $NH_2CH_2CH_2SH$ (with UV irradiation for 12 h)

Figure 3.6. MALDI-TOF-MS spectra of the polymers obtained via a reaction of HOOC-PMEA-I (1 equiv) and cysteamine (20 equiv) (a) without UV after 24 h and (b) with UV after 12 h.

Figure 3.5 shows the MALDI-TOF-MS spectra of the products in the reaction of PMEA-I and cysteamine in the dark condition (24 h) and under UV irradiation (12 h). In the dark condition, PMEA-SH was obtained (Figure 3.5a); the experimental molar mass (2692.21) matched the theoretical molar mass of PMEA-SH (2692.27). Under UV irradiation, PMEA-H was obtained (Figure 3.5b); the experimental molar mass (2693.27) matched the theoretical molar mass of PMEA-SH (2693.31). Figure 3.6 shows the MALDI-TOF-MS spectra of the products in the reaction of HOOC-PMEA-I and cysteamine in the dark condition (24 h) and under UV irradiation (12 h). In the dark condition, HOOC-PMEA-SH was obtained (Figure 3.6a); we observed two series, i.e., HOOC-PMEA-SH (theoretical molar mass = 2619.92) without Na^+ (main peak) and NaOOC-PMEA-SH (theoretical molar mass = 2641.90) with replacement of H^+ with Na^+ (minor peak). Under UV irradiation, HOOC-PMEA-H was obtained (Figure 3.6b); we observed HOOC-PMEA-H (theoretical molar mass = 2620.96) without Na^+ (main peak) and NaOOC-PMEA-H (theoretical molar mass = 2642.94) with replacement of H^+ with Na^+ (minor peak) in the MALDI-TOF-MS spectrum (Figure 3.6b). These results indicate good compatibility with functional groups in this approach.

Table 3.1. M_n and $Đ$ of the non-immobilized polymers generated from CP-I and the thickness and surface occupancy (σ^*) of the obtained PBA brush.

entry	M_n	$Đ$	Dry thickness (nm)	σ^*
1	61,000	1.92	20	0.19
2	139,000	1.80	30	0.11

A unique application was the chain end functionalization of polymer brushes on surfaces. Polymer brushes provide surfaces with advanced mechanical, optical, electrical, and biological properties.[29] Surface-initiated LRP is a powerful method to synthesize concentrated polymer brushes with high surface densities.[30] Because of the steric hindrance of neighbouring chains, polymer chains are forced to be extended and the growing chain ends tend to be localized at the outermost surface of the brush layer. Post chain end modification can afford functionalities at the outermost surface. In the present work, we used selective reactions (not multi-step modification or successive reactions) and prepared patterned polymer brushes with SH and H chain end functionalities in a single step. The single step manner is a unique advantage of this approach.

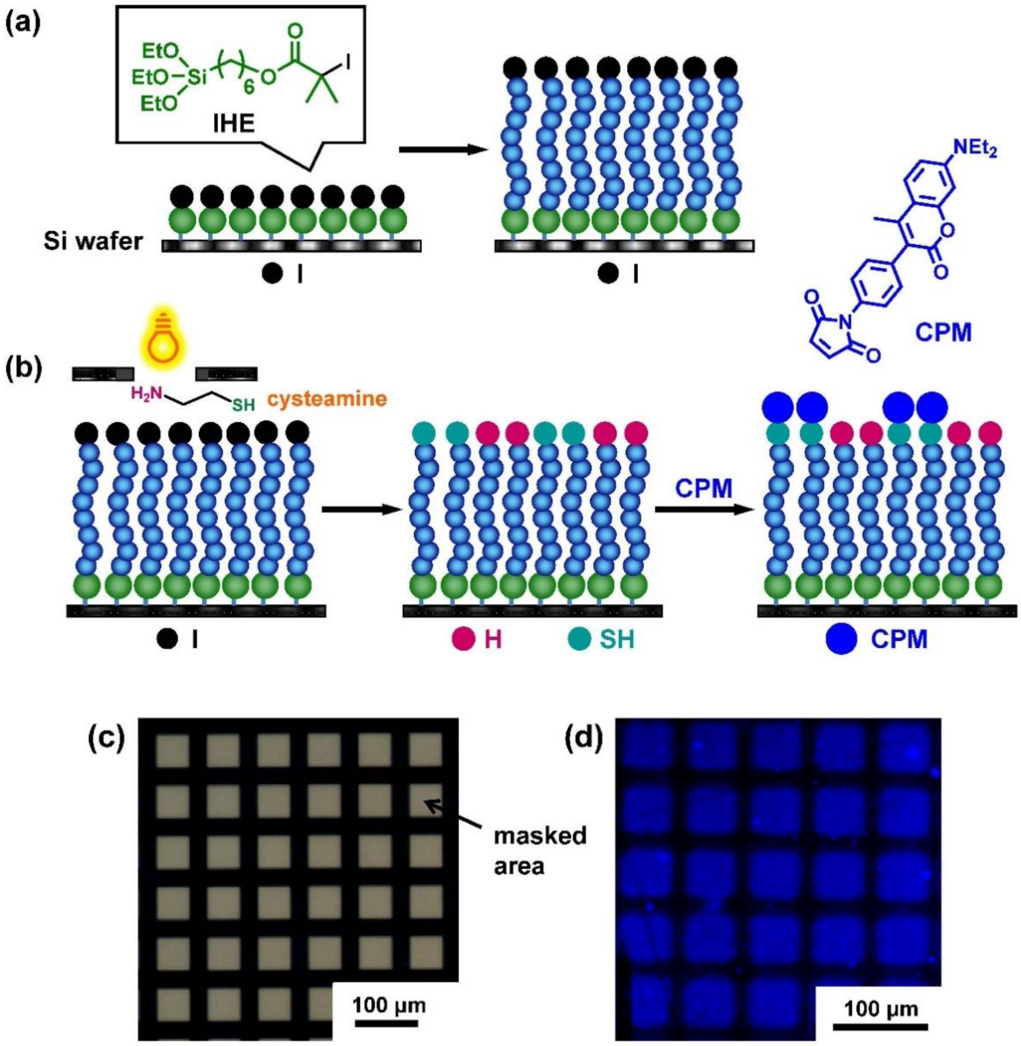

Figure 3.7. (a) Synthesis of PBA-I brush via surface-initiated organocatalyzed LRP. (b) Surface patterning of H and SH chain end functionalized polymer brush and subsequent attachment of CPM. (c) Optical microscope image of the glass photomask. (d) Fluorescence microscope image of CPM-attached patterned PBA brushes.

PBA-I brushes were uniformly fabricated on silicon wafers (without patterning) via surface-initiated organocatalyzed LRP (Figure 3.7a). Concentrated polymer brushes (with surface occupancy (σ*) > 10%) with different thicknesses (20 and 30 nm) were prepared (Table 3.1). A cysteamine solution (5 wt% in diglyme/1-butanol (w/w = 1/1)) was dropped on the polymer brush, which was covered by a cover glass. A glass photomask containing repeating squares (Figure 3.7c) or a copper grid (Figure 3.8a) was placed on the cover glass. After the UV irradiation for 2 h, the chain end iodide was converted to SH in the masked area and to H in the unmasked area (Figure 3.7b). We subsequently labelled SH with a fluorescent maleimide, 7-diethylamino-3-(4-maleimidophenyl)-4-methylcoumarin (CPM), *via* the thiol-maleimide Michael addition (Figure 3.7b). A fluorescence pattern was clearly observed with a fluorescence microscope (Figure 3.7d for 30 nm thick brush with the glass photomask), demonstrating the selective chain end modification on the polymer brush. A similarly clear fluorescence pattern was observed with the copper grid (Figure 3.8b) and for the brushes with different thicknesses (Figure 3.9). These results demonstrate the versatility in photomasks and brush thickness.

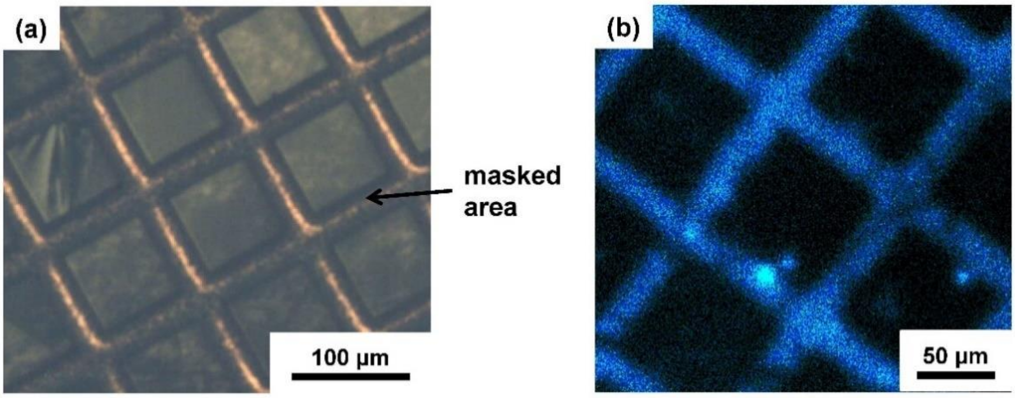

Figure 3.8. (a) Optical microscope image of the copper grid. (b) Fluorescence microscope image of CPM-attached patterned PBA brush (thickness = 30 nm) with use of the copper grid.

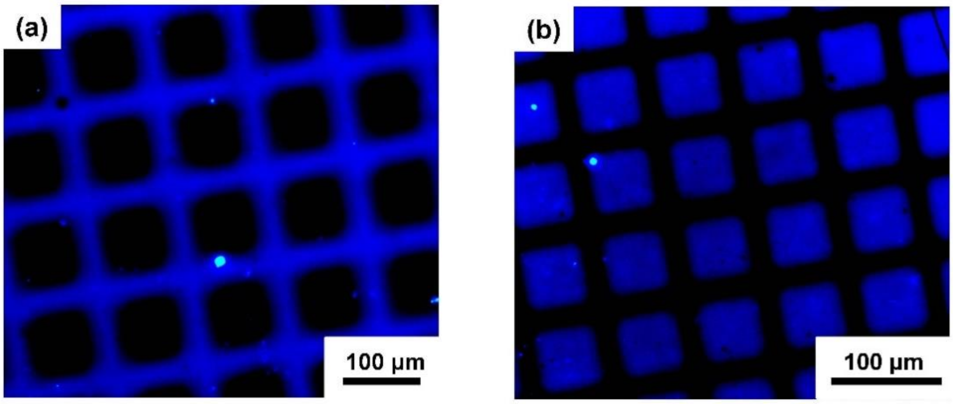

Figure 3.9. Fluorescence microscope images of CPM-attached patterned PBA brushes (thickness = 20 nm) with use of (a) copper grid and (b) glass photomask.

The fabrication of chain-end patterned polymer brushes is attractive. However, it is challenging to quantify the introduced the thiol functionality. In this study, we assumed the reactivity of the reaction at the outermost surface of the polyacrylate-iodide brushes is similar with that of the non-immobilized polyacrylate-iodide. Quantitative analysis of the introduced functional group (thiol) should be proceeded. The introduction of the functional group at the chain-ends of the polymer brushes would lead to a change in contact angle analysis. One possible method is to use the contact angle analysis to monitor the reaction on the surface. The other method is to use the X-ray photoelectron spectroscopy (XPS) to quantify the amounts of the iodide (before the reaction) and the functional group (S element). Then the conversion of polyacrylate-iodide to polyacrylate-SH would be calculated.

3.3 Conclusions

In conclusion, an inexpensive and non-toxic cysteamine was successfully employed as a photo-selective chain end modification agent of polymer-I. By simply switching UV light on and off, polymer-I was selectively transformed to polymer-H and polymer-SH, respectively, in a facile and quantitative manner. A unique application was a single-step preparation of patterned polymer brushes with SH and H chain end functionalities. Patterned surfaces with inert (hydrogen-terminated) and reactive/binding (thiol-terminated) areas may find sensing applications, *e.g.*, for biomolecular and ionic recognitions.

3.4 Experimental

Materials. Ethyl 2-iodopropanoate (EA-I) (> 99%, Tokyo Chemical Industry (TCI), Japan), cysteamine (> 95%, TCI), 2-iodo-2-methylpropionitrile (CP−I) (> 95%, TCI), butyl acrylate (BA) (> 97%, TCI), 2-methoxyethyl acrylate (MEA) (> 98%, TCI), tetrabutylammonium iodide (BNI) (> 98%, TCI), 4,4’-azobis(4-cyanovaleric acid) (V501) (> 75%, Sigma-Aldrich, United States), diethylene glycol dimethyl ether (diglyme) (> 99%, TCI), 1-butanol (> 99%, Kanto Chemical, Japan), iodine (I_2) (> 98%, TCI), tributylamine (TBA) (> 98%, TCI), 7-diethylamino-3-(4-maleimidophenyl)-4-methylcoumarin (CPM) (> 95%, Sigma-Aldrich), ammonia solution (28% in water, TCI), trans-2-[3-(4-t-butylphenyl)-2-methyl-2-propenylidene]malononitrile (DCTB) (> 99%, Fluka Chemicals Ltd., UK), sodium trifluoroacetate (NaTFA) (> 98%, TCI), and tetrahydrofuran (THF) (> 99.5%, Kanto) were used as received. 6-(2-Iodo-2-isobutyloxy)hexyltriethoxysilane (IHE) was provided through the courtesy of Godo Shigen Co., Ltd. (Japan) and was used as received. The glass photomask (Hunan Omnisun Information Material Co., Ltd., China) is polished on both sides with a patterned low reflective chrome film on one side. The photomask was used as received. The Cu grid is carbon-coated on 200 mesh (Ted Pella, USA). The Cu grid was washed by acetone with sonication for 30 min before use.

Analytical GPC. The GPC analysis was performed on a Shodex GPC-101 liquid chromatograph (Tokyo, Japan) equipped with two Shodex KF-804L mixed gel columns (300 × 8.0 mm; bead size = 7 μm; pore size = 20–200 Å). The eluent was THF at a flow rate of 1.0 mL/min (40 °C). Sample detection and quantification were conducted using a Shodex differential refractometer RI-101 calibrated with known concentrations of polymer in solvent. The monomer conversion was determined from the peak area. The column system was calibrated with standard poly(methyl methacrylate)s.

Preparative GPC. Polymers were purified with a preparative GPC (LC-9204, Japan Analytical Industry, Tokyo) equipped with JAIGEL 1H and 2H polystyrene gel columns (600×40 mm; bead size = 16 μm; pore size = 20-30 (1H) and 40-50 (2H) Å). Chloroform was used as eluent at a flow rate of 14 mL/min (room temperature).

NMR. The NMR spectra were recorded on a BBFO400 spectrometer (400 MHz) (Bruker, Germany) at ambient temperature; ^{1}H: spectral width 4000.00 Hz, acquisition time 8.192 sec, and pulse delay 1.000 sec.

MALDI-TOF-MS. The MALDI-TOF-MS spectra were recorded on a JMS-S3000 Spiral-TOF (JEOL Ltd., Japan) at an accelerating potential of 20 kV in the positive spiral mode. We prepared polymer solution (10 g/L in THF), matrix solution (DCTB: 60 g/L in THF), and cationization agent solution (NaTFA: 10 g/L in THF). The polymer solution, the DCTB solution, and the cationization agent solution were mixed in a ratio of 1/2/1 (v/v/v). Then, 5 μL of the mixed solution was deposited on the target plate spot and dried in the air at room temperature.

UV-LED light. The UV-LED light source (C11924-101) (at 365 (± 10) nm), was purchased from Hamamatsu Photonics (Japan). The energy of the radiating light per area (mW/cm^2) (described below) was measured with a power meter (FieldMate, Coherent, USA).

Photo-Selective Reaction of EA-I with Cysteamine. Cysteamine (0.2 mmol, 5 eq) was pre-dissolved in a toluene-d_8/methanol-d_4 (w/w = 88/12) mixed solvent (0.4 mL) because of its slow dissolution. Then, the solution was mixed with a solution of EA-I (0.04 mmol, 1 eq) in a toluene-d_8/methanol-d_4 (w/w = 88/12) mixed solvent (0.1 mL) in a reaction tube (hence 0.5 mL solution in total) and magnetically stirred under UV irradiation (365 nm) for 10 min or without UV irradiation for 1 h at ambient temperature.

Preparation of Purified EA-SH. The reaction mixture of EA-I and cysteamine in the dark condition (without UV irradiation) after 1 h was washed with brine three times and deionized water once. The organic phase was collected and dried under vacuum, giving EA-SH. ^{1}H NMR (toluene-d_8/methanol-d_4 (w/w = 88/12)) is given in Figure 3.1d. ^{13}C NMR (toluene-d_8/methanol-d_4 (w/w = 88/12)) is given in Figure 3.2a.

Preparation of polymer-I (PBA-I and PMEA-I). A mixture of monomer (BA or MEA) (15 g, 50 eq), CP-I (1 eq), and BNI (4 eq) was heated in a 100 mL flask at 110 °C for 5 h under an argon atmosphere with magnetic stirring**.** The reaction mixture was diluted with THF, and the polymer was reprecipitated in a non-solvent (methanol/water mixture (w/w = 1/1) for PBA and hexane for PMEA). The polymer was further purified with preparative GPC.

Preparation of HOOC-PMEA-I. A mixture of MEA (10 g, 100 eq), V501 (3.75 eq), I_2 (1 eq), BNI (1 eq) and diglyme (50 wt%) was heated in a 100 mL flask at 110 °C for 1 h under an argon atmosphere with magnetic stirring**.** The reaction mixture was diluted with THF, and the polymer was reprecipitated in hexane. The polymer was further purified with preparative GPC.

General Procedure of Photo-Selective Reaction for Polymers. A mixture (0.5 g) of polymer-I (1 eq, 20 wt%) and cysteamine (20 eq) in a mixed diglyme/1-butanol (w/w = 1/1) solvent was stirred in a reaction tube at room temperature in the dark condition (for 12 h for PBA and 24 h for PMEA) or under UV irradiation (for 2 h for PBA and 12 h for PMEA). The reaction mixture was diluted by THF, and then the polymer was reprecipitated in a non-solvent (methanol/water mixture (w/w = 1/1) for PBA and hexane for PMEA). The polymer was further purified with preparative GPC.

Preparation of IHE-Immobilized Silicon Wafer. A silicon wafer (0.8 cm × 0.8 cm) was washed with acetone (with sonication for 30 min), chloroform (with sonication for 30 min), and isopropanol (with sonication for 30 min). After drying under nitrogen flow, the wafer was placed in the ozone cleaner and radiated for 30 min. The wafer was immersed in a mixture of IHE, aqueous ammonia solution, and ethanol (1/89/10 (w/w/w)) for one day. The wafer was rinsed with ethanol, sonicated in ethanol for 30 min, and dried under nitrogen flow to give an IHE immobilized silicon wafer.

Preparation of PBA-I Brushes. The IHE-immobilized silicon wafer was heated in a mixture of BA (10 g, 1000 eq), CP−I (1 eq), and BNI (4 eq) in a Schlenk flask at 110 °C under argon atmosphere for 20 h (entry 1 in Table 3.1) and 48 h (entry 2 in Table 3.1). After the polymerization, the wafer was rinsed with acetone, sonicated in acetone for 30 min twice, and dried under nitrogen flow. The thickness of the polymer brush in the dry state was determined by AFM. We scratched the brush and measured the height gap between the scratched and unscratched areas (Figure 3.10). The M_n and $Đ$ of the non-immobilized polymers generated from CP-I (non-immobilized alkyl iodide initiator) and the height and surface occupancy (σ^*) of the obtained PBA brushes are summarized in Table 3.1.

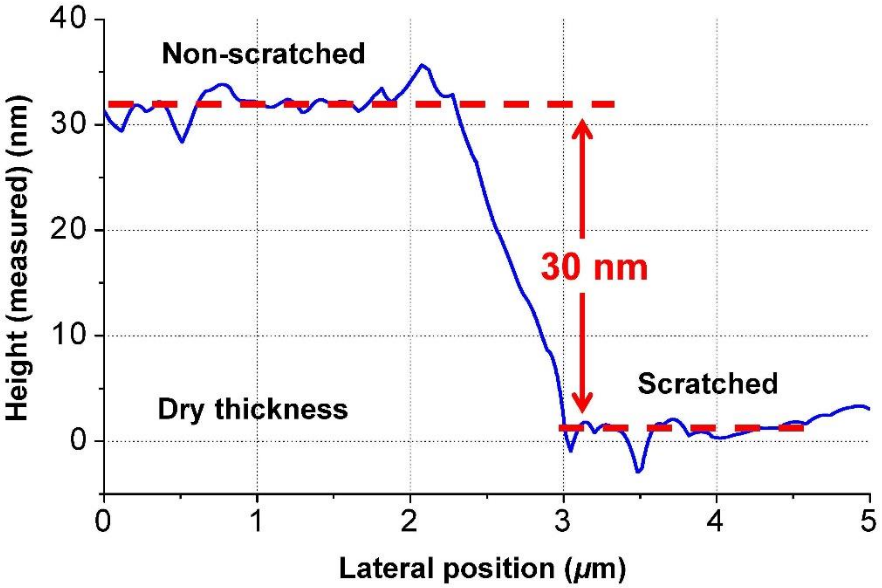

Figure 3.10. AFM height profile in the scratched and non-scratched areas of the obtained brush (Table 3.1, entry 2).

Preparation of Patterned Brushes. A cysteamine solution (5 wt%) in a diglyme/1-butanol (w/w = 1/1) mixed solvent was dropped onto a silicon wafer fabricated with PBA-I brush. Then, a cover glass was placed to form a thin layer of solution between the cover glass and wafer. A photomask was then placed on the cover glass, and UV was irradiated (irradiation power = 900 mW/cm^2) for 2 h. The wafer was cleaned by ultra-sonication in THF for 30 min and dried under nitrogen flow.

Fluorescent Labeling of Thiol Patterned PBA Brushes. The wafer with the thiol patterned PBA brush was immersed in a mixture of CPM (0.5 mg/mL, 1 eq), TBA (2 eq), and DMF in dark at room temperature for 4 h. The wafer was cleaned by ultra-sonication in THF for 30 min and dried under nitrogen flow. The fluorescence picture was taken with Zeiss Observer Z1 (Germany) using the filter set 49 under autoexposure.

3.5 References

1. Discekici, E. H.; Amant, A. H. St.; Nguyen, S. N.; Lee, I.-H.; Hawker, C. J.; Read de Alaniz, J. *J. Am. Chem. Soc.* **2018**, *140*, 5009–5013.

2. Nguyen, N. H.; Levere, M. E.; Kulis, J.; Monteiro, M. J.; Percec, V. *Macromolecules* **2012**, *45*, 4606–4622.

3. Hernández, J. G.; Bolm, C. *J. Org. Chem.* **2017**, ***82***, 4007–4019.

4. Peterson, B. M.; Kottisch, V.; Supej, M. J.; Fors, B. P.; *ACS Cent Sci.* 2018, **4**, 1228–1234.

5. Wang, C. G.; Goto, A. *J. Am. Chem. Soc.* **2017**, *139*, 10551–10560.

6. Zheng, J.; Wang, C.-G.; Yamaguchi, Y.; Miyamoto, M.; Goto, A. *Angew. Chem. Int. Ed.* **2018**, *130*, 1568–1572.

7. Matyjaszewski, K. *Adv. Mater.* **2018**, *30*, 1706441.

8. Keddie, D. J.; Moad, G.; Rizzardo, E.; Thang, S. H. *Macromolecules* **2012**, *45*, 5321–5342.

9. Nicolas, J.; Guillaneuf, Y.; Lefay, C.; Bertin, D.; Gigmes, D.; Charleux, B. *Prog. Polym. Sci.* **2013**, *38*, 63-235.

10. Tasdelen, M. A.; Kahveci, M. U.; Yagci, Y. *Prog. Polym. Sci*. **2011**, *36*, 455–567.

11. Debuigne, A.; Hurtgen, M.; Detrembleur, C.; Jérôme, C.; Barner-Kowollik, C.; Junkers, T. *Prog. Polym. Sci.* **2012**, *37*, 1004−1030.

12. Lunn, D. J.; Discekici, E. H.; Read de Alaniz, J.; Gutekunst, W. R.; Hawker, C. J. *J. Polym. Sci., Part A: Polym. Chem.* **2017**, *55*, 2903–2914.

13. Vinciguerra, D.; Tran, J.; Nicolas, J. *Chem. Commun.* **2018**, *54*, 228−240.

14. Lowe, A. B. *Polym. Chem.* **2010**, *1*, 17–36.

15. Nair, D. P.; Podgórski, M.; Chatani, S.; Gong, T.; Xi, W.; Fenoli, C. R.; Bowman, C. N. *Chem. Mater.* **2014**, *26*, 724−744.

16. Tsarevsky, N. V.; Matyjaszewski, K. *Macromolecules* **2002**, *35*, 9009−9014.

17. Klaikherd, A.; Nagamani, C.; Thayumanavan, S. *J. Am. Chem. Soc.* **2009**, *131*, 4830−4838.

18. Mukherjee, I.; Sinha, S. K.; Datta, S.; De, P. *Biomacromolecules* **2018**, *19*, 2286–2293.

19. Shan, J.; Tenhu, H. *Chem. Commun.* **2007**, *44*, 4580−4598.

20. Coessens, V.; Matyjaszewski, K. *Macromol. Rapid Commun.* **1999**, *20*, 66−70.

21. Mattson, K. M.; Pester, C. W.; Gutekunst, W. R.; Hsueh, A. T.; Discekici, E. H.; Luo, Y.; Schmidt, B. V. K. J.; McGrath, A. J.; Clark, P. G.; Hawker, C. J. *Macromolecules* **2016**, *49*, 8162−8166.

22. Discekici, E. H.; Shankel, S. L.; Anastasaki, A.; Oschmann, B.; Lee, I.-H.; Niu, J.; McGrath, A. J.; Clark, P. G.; Laitar, D. S.; Read de Alaniz, J.; Hawker, C. J.; Lunn, D. J. *Chem. Commun.* **2017**, *53*, 1888−1891.

23. Goto, A.; Ohtsuki, A.; Ohfuji, H.; Tanishima, M.; Kaji, H. *J. Am. Chem. Soc.* **2013**, *135*, 11131−11139.

24. Ohtsuki, A.; Lei, L.; Tanishima, M.; Goto, A.; Kaji, H. *J. Am. Chem. Soc.* **2015**, *137*, 5610−5617.

25. Wang, C.-G.; Hanindita, F.; Goto, A. *ACS Macro Lett.* **2018**, *7*, 263−268.

26. Wang, C.-G.; Chen, C.; Sakakibara, K.; Tsujii, Y.; Goto, A. *Angew. Chem. Int. Ed.* **2018**, *57*, 13504−13508.

27. Chen, C.; Xiao, L.; Goto, A. *Macromolecules* **2016**, *49*, 9425−9440.

28. Anastasaki, A.; Willenbacher, J.; Fleischmann, C.; Gutekunsta, W. R.; Hawker, C. J. *Polym. Chem.* **2017**, *8*, 689-697.

29. Zoppe, J. O.; Ataman, N. C.; Mocny, P.; Wang, J.; Moraes, J.; Klok, H.-A. *Chem. Rev.* **2017**, *117*, 1105−1318.

30. Tsujii, Y.; Ohno, K.; Yamamoto, S.; Goto, A.; Fukuda, T. *Adv. Polym. Sci.* **2006**, *197*, 1−45.

Chapter 4 A photo-selective chain-end modification of polyacrylate-iodide and its application to patterned polymer brush synthesis

Abstract

A photo-selective chain-end modification of polyacrylate-iodide (polymer-I) was developed. In the presence of functional primary amine (NH_2-R-X with an X functionality) and formic acid, by simply switching the ultraviolet (UV) light on and off, polymer-I was selectively converted to hydrogen-terminated polymer-H and chain-end functionalized polymer-NH-R-X (polymer-X), respectively. The scopes of the amenable functional X groups and polyacrylates are wide, and hence this method may serve as a general and versatile method for the selective chain-end modification. As a useful application, this method was successfully used to fabricate chain-end patterned binary polymer brushes on surfaces. This method is free from metal, amenable to various functionalities, and useful for designing a range of chain-end functionalized polymers and surface-functionalized materials.

4.1 Introduction

Chain-end functionalized polymers are of great interest for their use as building blocks to create architecturally designed polymers.[1–3] They can connect with small molecules and other polymers to produce labelled polymers,[4] block copolymers,[5,6] and bio-conjugates,[7,8] yielding advanced polymer materials such as bio-imaging, drug or gene delivery, self-assembly, and stimuli-responsive materials. The chain-end functionalized polymer brushes on solid surfaces also provide smart surfaces.[9,10]

Living radical polymerization, also termed reversible-deactivation radical polymerization, is a useful approach for synthesizing well-defined polymers possessing a capping agent at the growing chain end.[11–14] Chain-end functionalized polymers are accessible by using functional initiators to give functional groups at the initiating chain end or by the post-transformation of the capping agent to functional groups to give functional groups at the growing chain end.[1]

Besides the functionalization, the removal of the capping agent from the polymer chain end is often required for the long-term stability of the obtained polymers. Hydrogen-terminated polymers (polymer-H) can be obtained *via* photo-redox catalysis in the presence of reducing agents from halide- and thiocarbonate-terminated polymers prepared *via* atom transfer radical polymerization (ATRP) and reversible addition-fragmentation chain transfer (RAFT) polymerization.[15–19] This transformation was used to obtain hydrogen-terminated polymer brushes on surfaces in patterned manners.[19]

Our research group developed reversible complexation mediated polymerization (RCMP) using an alkyl iodide (R–I) as an initiator and an organic molecule as a catalyst, yielding a polymer-iodide (polymer-I) possessing an iodide at the growing chain end.[20–25] Mechanistically, polymer-I reversibly generates the propagating radical (polymer$^{\bullet}$) by the work of the catalyst. The catalysts include organic salts such as tetrabutylammonium iodide ($Bu_4N^+I^-$

(BNI)). The polymerization is metal-free, odor-free, and amenable to a wide range of monomers and polymer structures, which are attractive features. The terminal iodide chain end can be modified using primary amines (NH_2-R-X), converting polymer-I to chain-end functionalized polymers (polymer-NH-R-X) with various functional X groups.[26]

Selective reaction is important in organic synthesis and polymer chemisty.[17,27–31] By applying different external stimuli, the reaction proceeds under different pathways, yielding different products from the same reactants. Our group previously utilized polymer-I and cysteamine ($NH_2CH_2CH_2SH$) to selectively produce polymer-H and a thiol-terminated polymer (polymer-SH) with and without photo-irradiation, respectively.[32] The SH of cysteamine worked as a radical chain transfer agent (a hydrogen donor) with the irradiation to generate polymer-H, while the NH_2 of cysteamine worked as a nucleophile without the irradiation to generate polymer-$NHCH_2CH_2SH$ (polymer-SH). However, this method can give only an SH functional chain end, and a more general method accessible to various functional X chain ends is desirable.

In the present work, we developed the first general method to selectively produce polymer-H and polymer-X with various functional X groups. We co-used formic acid as a hydrogen donor and a primary amine NH_2-R-X as a nucleophile to selectively convert polymer-I to polymer-H and polymer-X (polymer-NH-R-X) with and without photo-irradiation, respectively. The use of primary amines with different functional X groups generates various polymer-X, significantly widening the scope of the X groups. This method is robust and practically attractive, since formic acid is inexpensive and various primary amines are commercially available. We focused on polyacrylates because this amine-based substitution is limited to polyacrylate-iodides (not amenable to polymethacrylate-iodides).[26] As a useful application, this method also enabled a facile preparation of patterned binary polymer brushes with hydrogen and various functional X groups at the chain ends, as described below.

4.2 Results and Discussions

Preparation of PBA-I

We carried out the RCMP of butyl acrylate (BA) using 2-iodo-2-methylpropionitrile (CP-I) as an alkyl iodide initiator and BNI as a catalyst and prepared a poly(butyl acrylate)-iodide (PBA-I) possessing a CP group at the initiating chain end and an iodide at the growing chain end. The polymer was purified by reprecipitation with a mixture of methanol and water (v/v = 50/50) and subsequently by preparative gel permeation chromatography (GPC) to remove trace amounts of impurities, yielding a PBA-I with $M_n = 3700$ and $Đ$ $(= M_w/M_n) = 1.27$, where M_n and M_w are the number- and weight-average molecular weights, respectively, and $Đ$ is the dispersity.

Selective chain-end modification of PBA-I using formic acid and $NH_2CH_2CH_2Ph$

We studied the selective chain-end modification of the obtained PBA-I (1 eq, 20 wt%) in the presence of formic acid (4 eq, a hydrogen donor) and $NH_2CH_2CH_2Ph$ (20 eq, a nucleophile) in *N*,*N*-dimethylformamide (DMF) (solvent) at room temperature in the dark and under a UV irradiation (365 nm wavelength) for 2 h. After the reaction, the obtained polymer was purified by reprecipitation and preparative GPC.

In the dark, PBA-I was selectively converted to PBA-$NHCH_2CH_2Ph$ *via* the substitution after 2 h. Figures 4.1a and 4.1b show the matrix-assisted laser desorption/ionization time-of-flight mass spectrometry (MALDI-TOF-MS) spectra before and after the reaction. We used *trans*-2-[3-(4-tert-butylphenyl)-2-methyl-2-propenylidene]malononitrile (DCTB) and CF_3COONa as a matrix and an additive salt, respectively. The polymers contain ^{12}C and ^{13}C atoms. For simplicity, the theoretical molecular weights discussed below and the experimental values given in the figures are the polymers possessing only ^{12}C atoms. In Figure 4.1b, we observed a predominant peak with the experimental molar mass value 2900.85, which matches the theoretical molar mass value 2900.88 of PBA-$NHCH_2CH_2Ph$ (n = 21), where n is the degree of polymerization of PBA (the chemical formula of PBA-$NHCH_2CH_2Ph$ with 21 BA repeating units with CP (C_4H_6N) at the initiating chain and $NHCH_2CH_2Ph$ ($C_8H_{10}N$) at the growing chain end is $C_{159}H_{268}O_{42}N_2$ (Figure 4.1). The theoretical molecular molar mass value (with the additive cation Na^+) without ^{13}C atom is given by 159 × 12 (C) + 268 × 1.00783 (H) + 42 × 15.99491 (O) + 2 × 14.00307 (N) + 22.98977 (Na) = 2900.88). This result suggests that the substitution product was predominant. A minor series of peak (experimental molar mass value = 2925.91) was also observed and belongs to a side product hydroxyl-terminated PBA (PBA-OH) (theoretical molar mass value = 2925.88) generated in the preparation of PBA-I. The ^1H NMR spectra (Figures 4.2a and 4.2b) also confirmed the consumption of PBA-I (peak *c'*, C*H*, 4.3 ppm) and the formation of PBA-$NHCH_2CH_2Ph$ (peak *j*, C_6H_5, 7.1–7.4 ppm) at a high conversion (88%). Figure 4.2a shows the ^1H NMR spectrum of PBA-I. From the peak areas of the terminal monomer unit (peak *c'*, C*H*, 4.3 ppm) and the whole monomer units (peak *d*, OCH_2, 3.8–4.2 ppm), we calculated the degree of polymerization (DP) to be 27. Figures 4.2b and 4.2c show the ^1H NMR spectra of the products obtained in the reactions of PBA-I (1 eq, 20wt%), $NH_2CH_2CH_2Ph$ (20 eq), and HCOOH (4 eq) in the dark and under the UV irradiation, respectively. The products were purified by preparative GPC to remove trace amounts of $NH_2CH_2CH_2Ph$ and other low-molecular-weight species. In the dark, the signal of C_6H_5 (peak *j*, 7.1–7.4 ppm) was clearly observed, demonstrating the introduction of the $NHCH_2CH_2Ph$ moiety. The yield of PBA-$NHCH_2CH_2Ph$ was calculated to be 88% from the relative peak areas of C_6H_5 and the monomer units (peak *d*, OCH_2, 3.8–4.2 ppm) with DP = 27. The intramolecular amidation of PBA-$NHCH_2CH_2Ph$ can yield PBA-lactam-CH_2CH_2Ph possessing a lactam ring with a CH_2CH_2Ph group at the chain end.[26] In the present condition (reacted for 2 h), a small amount of PBA-lactam-CH_2CH_2Ph (theoretical molar mass value = 2826.81) was observed in the MALDI-TOF-MS spectrum (experimental molar mass value = 2826.95) (Figure 4.1b). For a longer reaction time or at a higher reaction temperature, PBA-$NHCH_2CH_2Ph$ would predominantly be converted to PBA-lactam-CH_2CH_2Ph as a thermodynamically stable product.

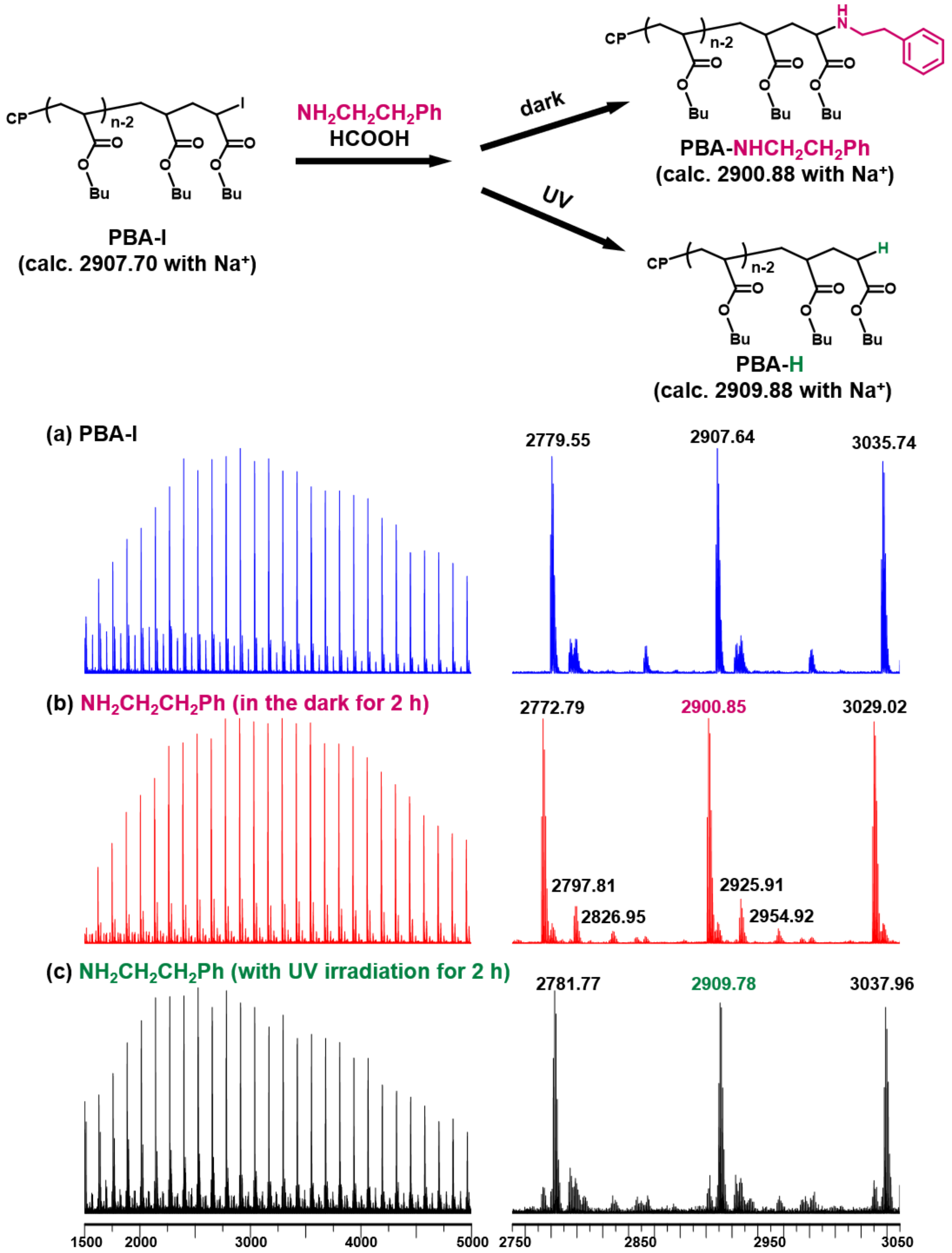

Figure 4.1. MALDI-TOF-MS spectra of (a) PBA-I and the products obtained *via* the reactions of PBA-I (1 eq, 20 wt%), formic acid (4 eq), and $NH_2CH_2CH_2Ph$ (20 eq) in DMF (b) without the UV irradiation after 2 h and (c) with the UV irradiation after 2 h (Table 4.1 (entry 1)).

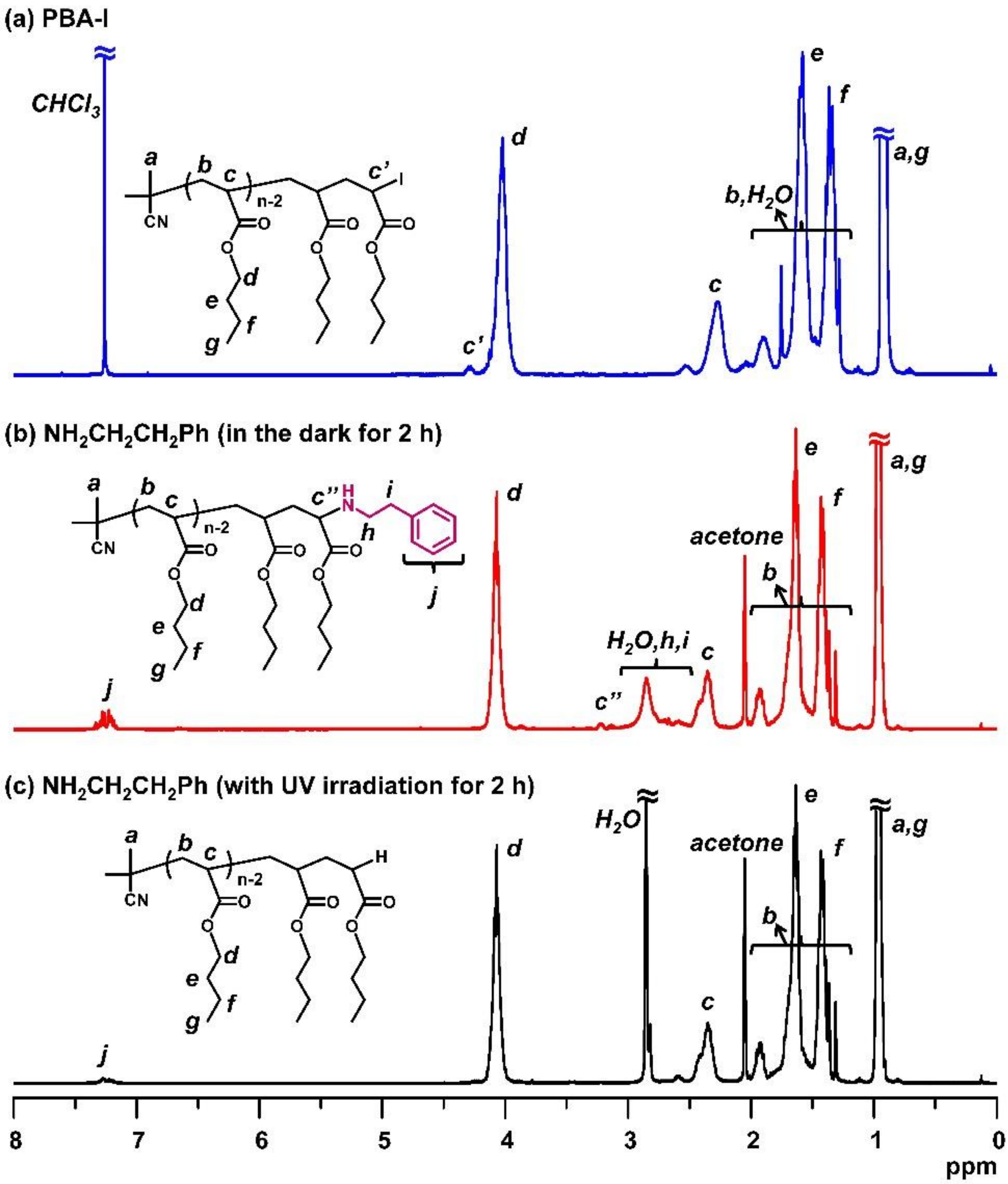

Figure 4.2. ^{1}H NMR (400 MHz) spectra of (a) PBA-I (in $CDCl_3$) and products (in acetone-d_6) obtained *via* the reactions of PBA-I (1 eq, 20wt%), formic acid (4 eq), and $NH_2CH_2CH_2Ph$ (20 eq) in DMF (b) without the UV irradiation after 2 h and (c) with the UV irradiation after 2 h (Table 4.1 (entry 1)).

In contrast, under the UV irradiation, PBA-I was predominantly converted to PBA-H. In the MALDI-TOF-MS spectrum (Figure 4.1c), we observed a single series of the main peak as well as several minor peaks. The experimental molar mass value (2909.78) in the main peak matches the theoretical molar mass value (2909.88) of PBA-H, suggesting that PBA-H was a major product. While the substitution also did occur in a parallel manner, the hydrogenation was much faster in the studied UV condition, resulting in a selective formation of PBA-H. The ^{1}H NMR spectrum (Figure 4.2c) confirmed the generation of PBA-NHCH$_2$CH$_2$Ph (11%) as a minor product and PBA-H (89%) as the main product (assuming that PBA-I was converted to either PBA-NHCH$_2$CH$_2$Ph or PBA-H (100% in total)). These results demonstrate the selective chain-end conversion of PBA-I to PBA-H and PBA-NHCH$_2$CH$_2$Ph with and without photo-irradiation, respectively.

Mechanism study

The photo-induced hydrogenation of alkyl halides using formic acid and amines was previously reported in small molecule systems and polymer systems,[19,33] although the detailed mechanism was not clarified. In the present system, in the absence of amine, PBA-I and formic acid did not give PBA-H, meaning that the reaction is amine-catalyzed. PBA-I and amine would form a PBA-I···amine complex, which facilitates the generation of PBA$^\bullet$ under the UV irradiation (Scheme 4.1a). Subsequently, PBA$^\bullet$ reacts with formic acid to generate PBA-H (Schemes 4.1b and 4.1c). To further probe the mechanism, we used a deuterated formic acid (DCOOH) and tributylamine (TBA) to reduce PBA-I under the UV irradiation. (A primary amine (RNH$_2$) contains two active protons. To avoid the possible proton exchange with DCOOH, we used the tertiary amine (TBA with no active proton) for this mechanistic study purpose. Figure 4.3 shows the MALDI-TOF-MS spectrum of the product obtained in the reaction of PBA-I (20 wt%, 1 eq), DCOOH (4 eq), and TBA (20 eq) in DMF under the UV irradiation at room temperature for 2 h. A minor signal at 2395.72 belongs to an HI elimination product from PBA-I (PBA-ene (theoretical molar mass value = 2395.66 (with the repeating unit n = 18))) without ^{13}C atom. The signal intensity was 2720, which is given in the parenthesis in the figure. The signal at 2397.73 (with the intensity of 23900) belongs to PBA-H (theoretical molar mass value = 2397.68 (n = 18)) without ^{13}C atom and PBA-ene with two ^{13}C atoms (theoretical molar mass value = 2397.67). The signal at 2398.73 (with the intensity of 37000) belongs to PBA-D (theoretical molar mass value = 2398.69 (n = 18)) without ^{13}C atom, PBA-H with one ^{13}C atom (theoretical molar mass value = 2398.68), and PBA-ene with three ^{13}C atoms (theoretical molar mass value = 2398.67). Because all of PBA-ene, PBA-H, and PBA-D have the same number of carbons, the isotopic distribution is the same. The theoretical relative intensities at n = 18 for zero, one, two, and three ^{13}C atoms are given in Figure 4.3. The experimental ratio of PBA-H/PBA-D is calculated as follows:

$$\frac{\text{PBA–H}}{\text{PBA–D}} = \frac{23900 - \frac{2720}{69.008} \times 77.035}{37000 - \frac{23900 - \frac{2720}{69.008} \times 77.035}{69.008} \times 100 - \frac{2720}{69.008} \times 41.637} = 80/20$$

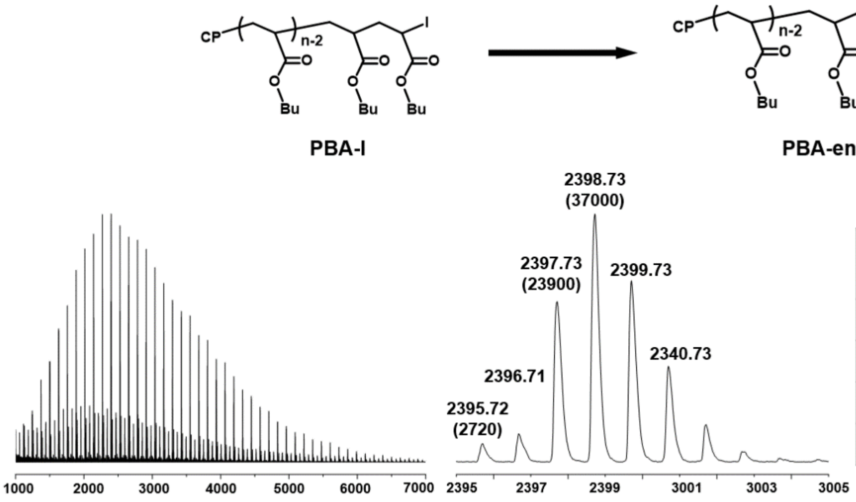

The number of ^{13}C	Theoretical intensity
0	69.008
1	100
2	77.035
3	41.637

Figure 4.3. MALDI-TOF-MS spectrum of the product obtained in a reaction of PBA-I (1 eq, 20 wt%), DCOOH (4 eq), and TBA (20 eq) in DMF under the UV irradiation for 2 h.

Both PBA-D (20%) and PBA-H (80%) were observed in the MALDI-TOF-MS analysis, suggesting that PBA$^{•}$ abstracts the aldehyde deuterium (D) as well as the carboxylic acid proton (H) from DCOOH (Schemes 4.1b and 4.1c). However, it should be noted that the reactivity of aldehyde and carboxylic acid (20/80) may not be quantitative because of possible intramolecular and intermolecular proton exchange of DCOOH during the reaction. PBA$^\bullet$ may also abstract H from TBA. However, without formic acid (namely, in a reaction of PBA-I and TBA only), no PBA-H was observed, meaning that PBA$^\bullet$ did not significantly abstract H from TBA.

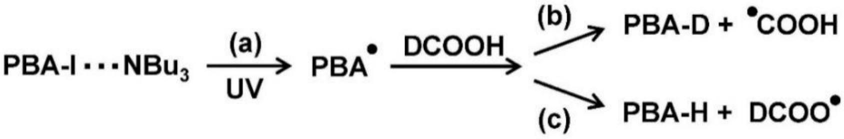

Scheme 4.1. (a) PBA-I···amine complex generates PBA$^\bullet$. PBA$^\bullet$ abstracts (b) the aldehyde deuterium (D) or (c) the carboxylic acid proton (H) from DCOOH.

Expansion of chain-end functionality and polymer scopes

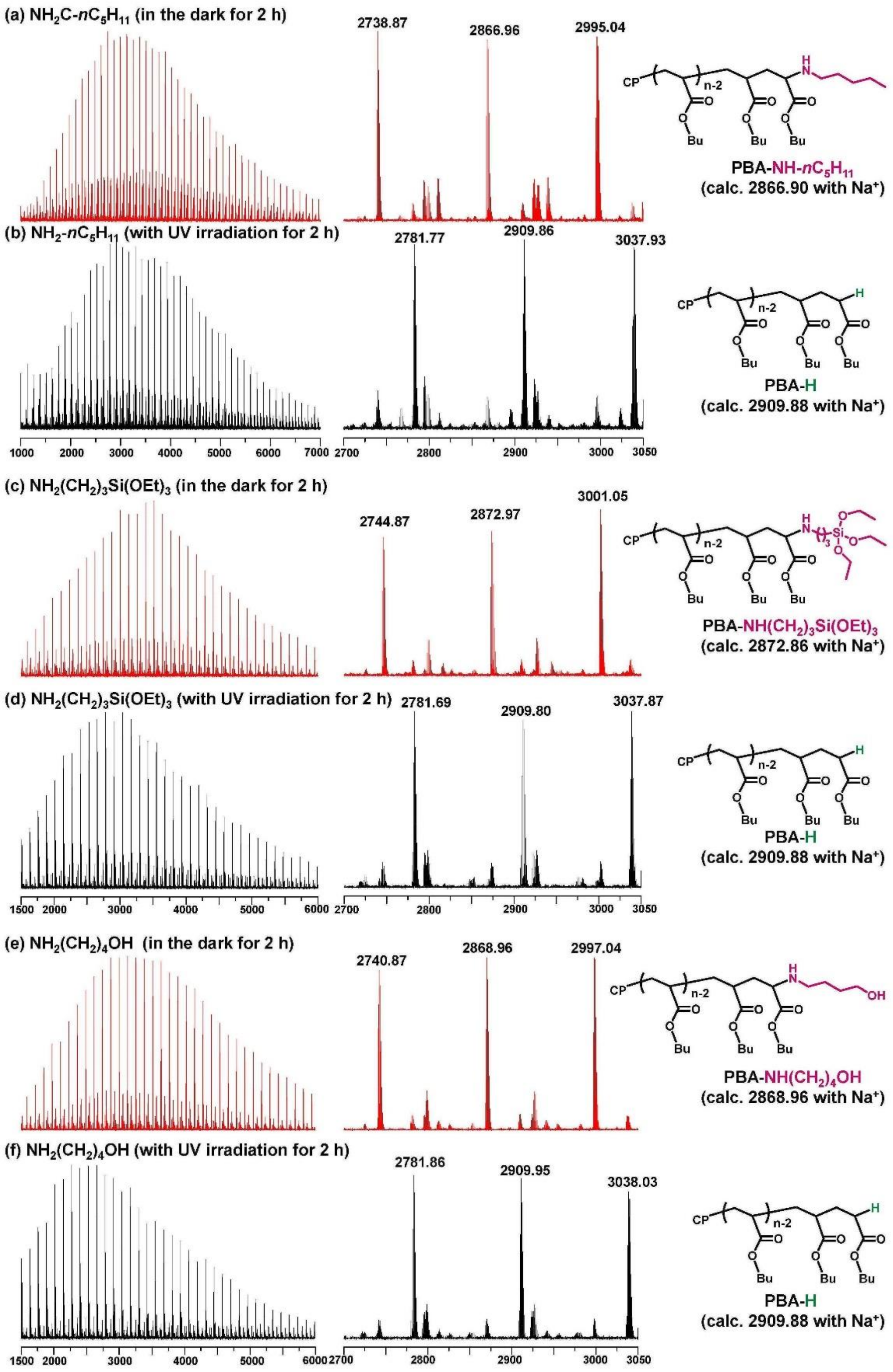

Figure 4.4 MALDI-TOF-MS spectra of the products obtained *via* the reactions of PBA-I (1 eq, 20wt%), formic acid (4 eq), and different amines NH_2-R-X (20 eq) in DMF with and without the UV irradiation after 2 h (Table 4.1 (entries 2−4)). The amine and condition (with or without UV) are given in the figure.

Table 4.1. Reaction of PBA-I (1 eq) with formic acid (4 eq) and an amine (20 eq) in the dark and under UV irradiation for 2 h.

Entry	Amine	Product (%) (with 10% error)	
		In the dark	Under UV irradiation
		PBA-X[a]	PBA-H[b]
1	$NH_2(CH_2)_2Ph$	88	89
2	$NH_2\text{-}n C_5H_{11}$	89	92
3	$NH_2(CH_2)_4OH$	84	85
4	$NH_2(CH_2)_3Si(OEt)_3$	~100	92
5	$NH_2CH_2C{\equiv}CH$	57	97

[a]The amount of PBA-X (PBA-NH-R-X) was determined with ^{1}H NMR. [b]The amount of PBA-X (PBA-NH-R-X) was determined with ^{1}H NMR. Assuming 100% of the total amount of PBA-X and PBA-H, the amount of PBA-H was calculated.

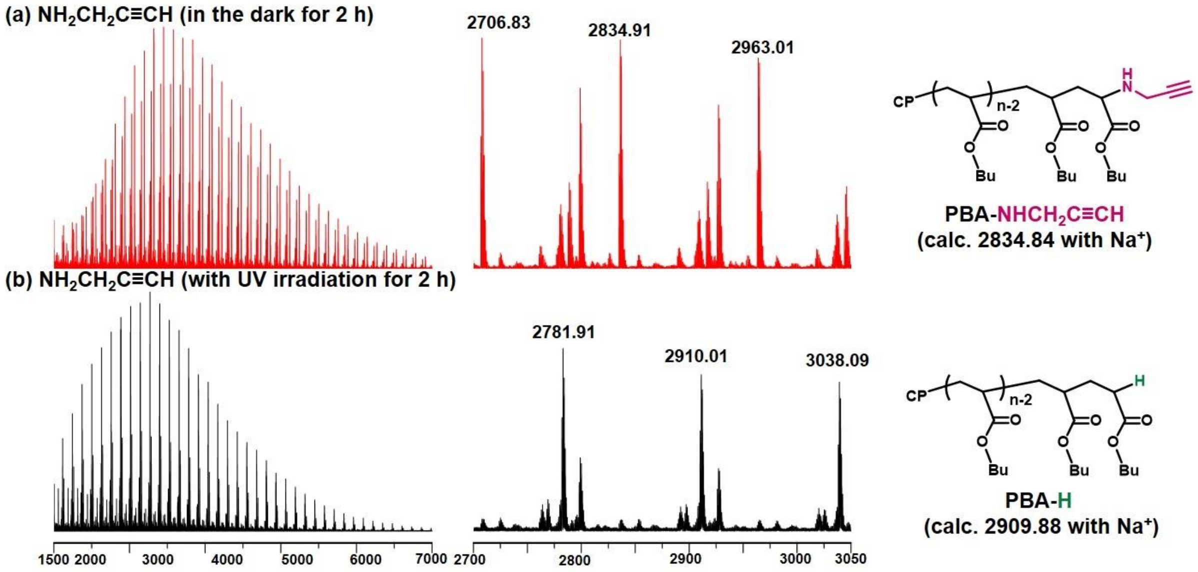

Figure 4.5 MALDI-TOF-MS spectra of the products obtained in the reactions of PBA-I (1 eq, 20wt%), formic acid (4 eq), and $NH_2CH_2C{\equiv}CH$ (20 eq) in DMF (a) in the dark after 2 h and (b) with the UV irradiation after 2 h (Table 4.1 (entry 5)).

We widened the scope of this reaction to other amines (NH_2-R-X) and polymer. The MALDI-TOF-MS spectra (Figures 4.4 and 4.5) confirmed the selective formation of PBA-X (PBA-NH-R-X) and PBA-H in the dark and under the UV irradiation, respectively, for 2 h, with X = alkyl, hydroxyl, triethoxysilyl, and alkynyl functional groups. The reaction yields determined with ^{1}H NMR (Figure 4.6) were high for both PBA-X (57−100%) and PBA-H (85−97%) in all cases (Table 4.1). In the dark, the yield of PBA-X with X = alkynyl (57%) was lower than those with other X groups (84−100%). The reason is unclear at the moment. Under the UV irradiation, not only the reduction to give PBA-H (85−97%) but also the substitution to give PBA-X (3−15%) occurred. Because they are parallel reactions, the results suggest that the reduction was 6−30 times faster than the substition in the studied conditions.

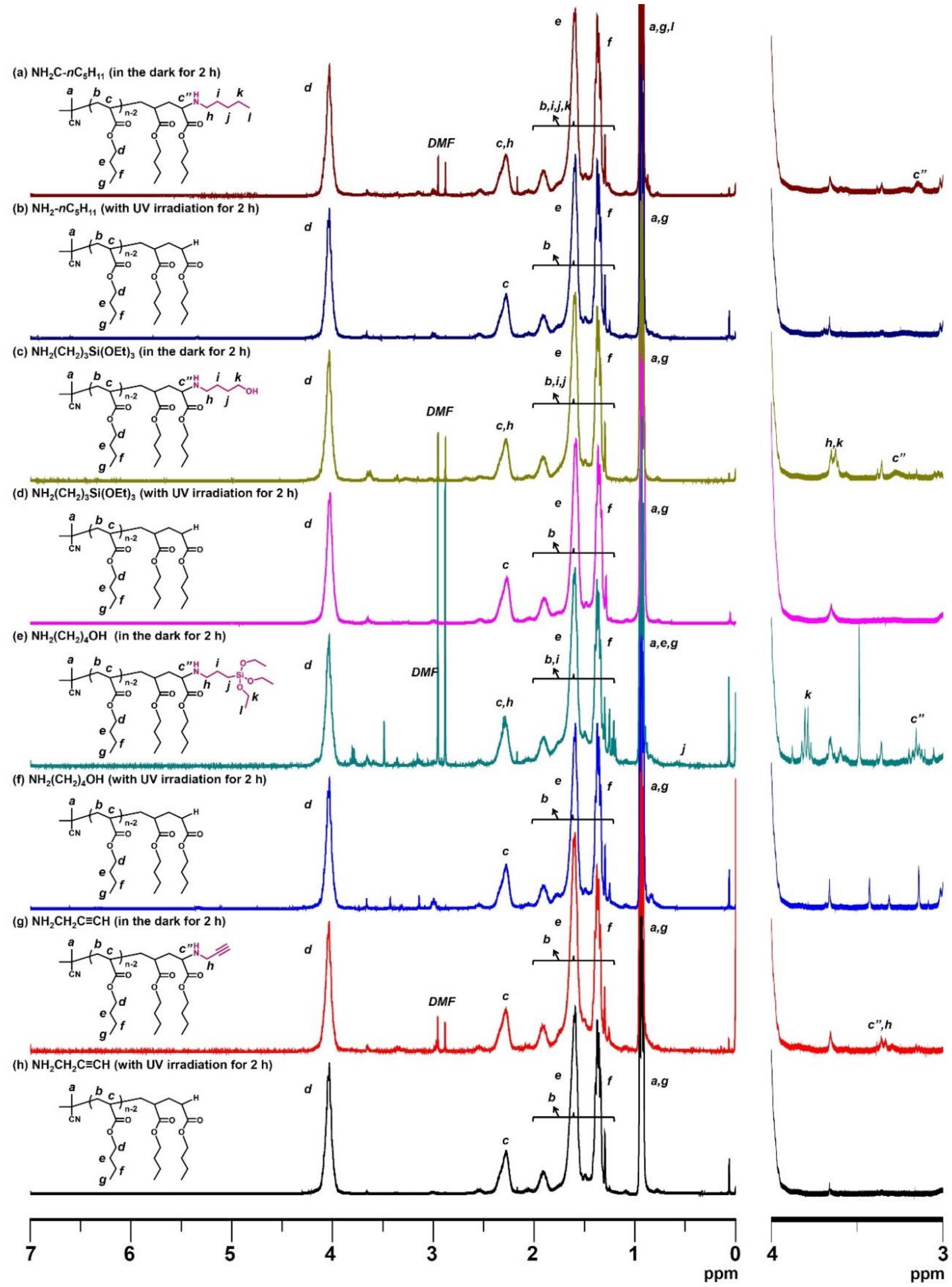

Figure 4.6 ^{1}H NMR spectra of the product (in CDCl$_3$) obtained via reactions of PBA-I (1 eq, 20wt%), formic acid (4 eq), and different amines NH$_2$-R-X (20 eq) in DMF with and without UV after 2 h (Table 4.1 (entries 2-5)). The amine and condition (with or without UV) are given in the figure.

Besides PBA-I, we also selectively converted a biocompatible polyacrylate, i.e., poly(methoxyethyl acrylate)-iodide (PMEA-I), to PMEA-H and PMEA-Ph with and without the UV irradiation, respectively (Figure 4.7). These results demonstrate that this method serves as a versatile method to selectively convert polymer-I to polymer-H and polymer-X with various functional X groups for various polyacrylates. (In the case of PMEA, PMEA-NHCH$_2$CH$_2$Ph was first generated. The intramolecular amidation subsequently yielded a relatively large amount of PMEA-lactam-CH$_2$CH$_2$Ph (Figure 4.7).

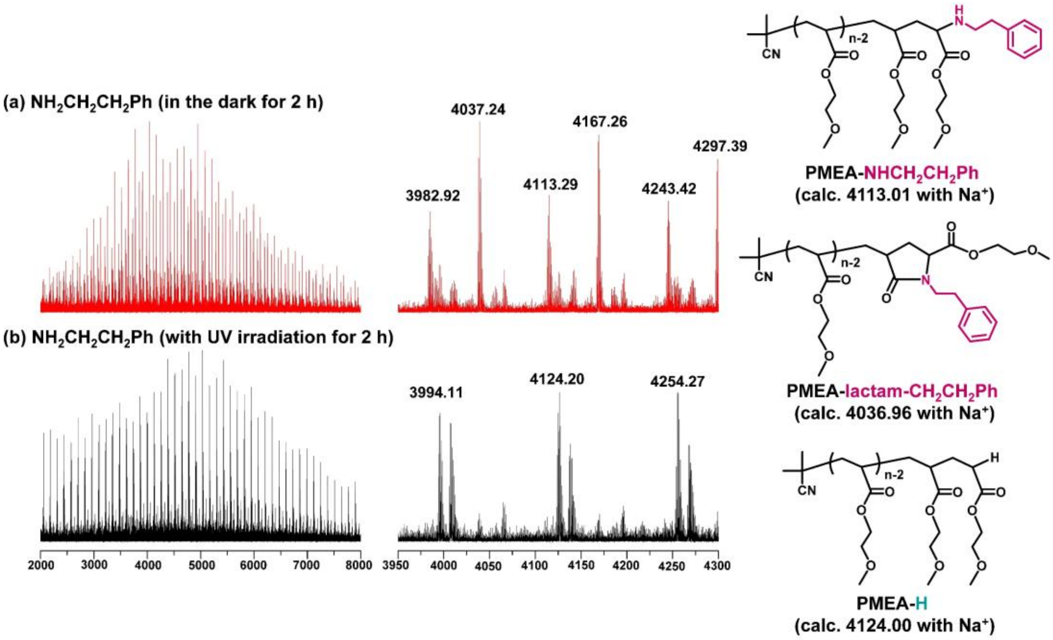

Figure 4.7 MALDI-TOF-MS spectra of the products obtained in the reactions of PMEA-I (1 eq, 20wt%), formic acid (4 eq), and NH$_2$CH$_2$CH$_2$Ph (20 eq) in DMF (a) in the dark after 2 h and (b) with the UV irradiation after 2 h.

Chain-end patterned polymer brushes

An interesting application of this universal selective chain-end modification is to create chain-end patterned polymer brushes on surfaces. The fabrication of polymer brushes on surfaces can dramatically alter the surface properties such as thermodynamic, optical, and biological properties.[34] Surface-initiated living radical polymerization is a useful approach to prepare concentrated polymer brushes with high graft densities.[35] Patterned polymer brushes on surface with multiple polymers and different brush thicknesses have widely been prepared,[36,37] finding applications in, *e.g.*, peptide arrays and smart sensors for environmental changes.[38] However, the preparation of chain-end patterned polymer brushes is still limited. In the present work, we applied our method to obtain chain-end patterned polymer brushes. For the concentrated polymer brushes, because of the steric hindrance of the neighboring chains, the polymer chains are forced to extend, and the growing polymer chain ends tend to be localized at the outermost surface in solution. We used a photomask under the UV irradiation and converted the iodide chain ends of polymer brushes to hydrogen and various functional groups in patterned manners.

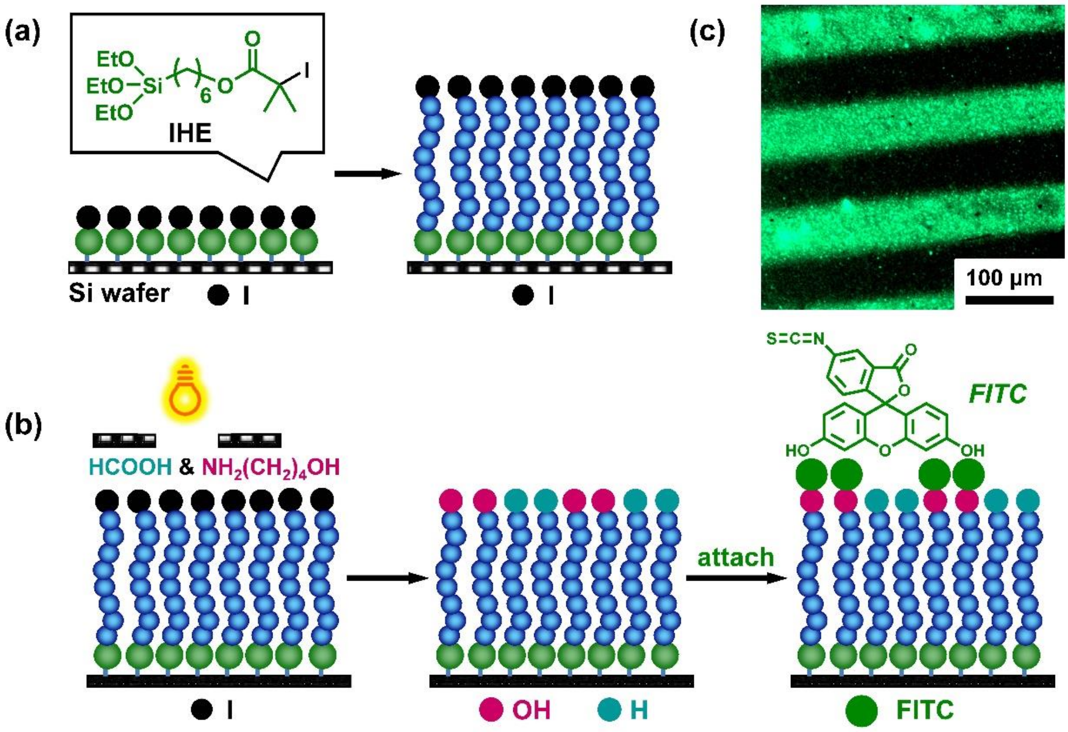

Figure 4.8. (a) Synthesis of PBA-I brush *via* surface-initiated RCMP. (b) Surface patterning of H and OH chain-end functionalized PBA brushes and attachment of FITC. (c) Fluorescence microscope image of FITC-attached patterned PBA brush.

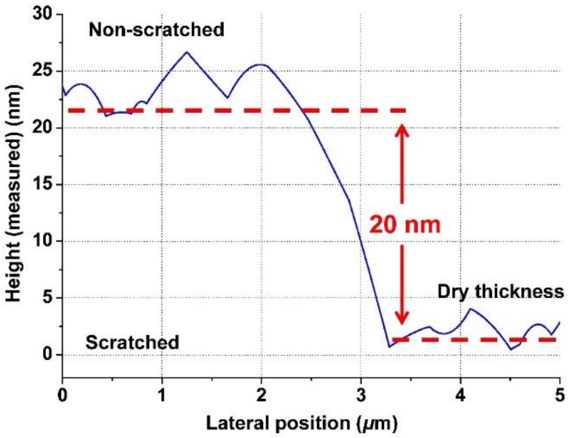

Figure 4.9 AFM height profile in the scratched and non-scratched areas of the PBA-I brush.

Figure 4.8a illustrates the fabrication of a polymer brush with the iodide chain end on a silicon wafer in a uniformed (non-patterned) manner *via* surface-initiated RCMP. A concentrated PBA-I brush (σ^* = approximately 0.45) with a thickness of 20 nm were prepared (Figure 4.9). A DMF solution of HCOOH (1 eq, 1wt%) and $NH_2(CH_2)_4OH$ (4 eq) was dropped on the polymer brush, which was subsequently covered with a cover glass. A stripe photomask was placed on the cover glass. After the UV irradiation for 2 h, the chain-end iodine was modified to an OH functionality in the masked area and was reduced to an H atom in the unmasked area (Figure 4.8b). The formation of the patterned surface was confirmed by labelling the OH functionality with a fluorescence molecule, i.e., fluorescein 5-isothiocyanate (FITC), through an isothiocyanate-hydroxyl addition (Figure 4.8b).[39] A clear fluorescence pattern was observed in the fluorescence microscope image (Figure 4.8c), demonstrating the successful fabrication of the chain-end patterned binary polymer brush. The secondary anime of PBA-$NH(CH_2)_4OH$ may also react with FITC. However, because of the large steric hindrance at the NH moiety, FITC most probably reacted with the OH group rather than the secondary amine moiety. The unreacted PBA-I brush, if any present, may react with FITC. As a control experiment, we tested a reaction of non-immobilized PBA-I with FITC. A DMF solution of non-immobilized PBA-I (20 wt%, 0.075 mM, 0.5 eq), FITC (5.7 wt%, 0.15 mM, 1 eq), TBA (0.15 mM, 1 eq), and 4-dimethylaminopyridine (DMAP) (0.15 mM, 1 eq) was heated in a reaction tube at 60 °C for 12 h. The polymer was purified with preparative GPC. Figure 4.10b shows the ^{1}H NMR spectrum of the obtained polymer. The signals of the monomer units (peaks a-g, 0.8–4.2 ppm) and FITC (peak *a'*-*f'*, 6.5–8.2 ppm) were observed. The yield of PBA-FITC was calculated to be 9% from the relative peak areas of the monomer units (peak *d*, $OC\mathit{H}_2$, 3.8–4.2 ppm) (DP = 27) and FITC (peak *d'*, *e'* and *f'*, 6.5–7.0 ppm), showing that the generation of PBA-FITC was insignificant. The concentrations of FITC, TBA, and DMAP (0.15 mM for all) in this reaction (using non-immobilized PBA-I) were 5.7 times higher than those (0.026 mM for all) in the reaction on surface (using surface-immobilized PBA-I) in Figure 4.8, meaning that the generation of PBA-FITC was even less significant in the reaction studied for polymer brush on surface (Figure 4.8). The result means that the observed labeling proceeded through the addition of the OH group with FITC.

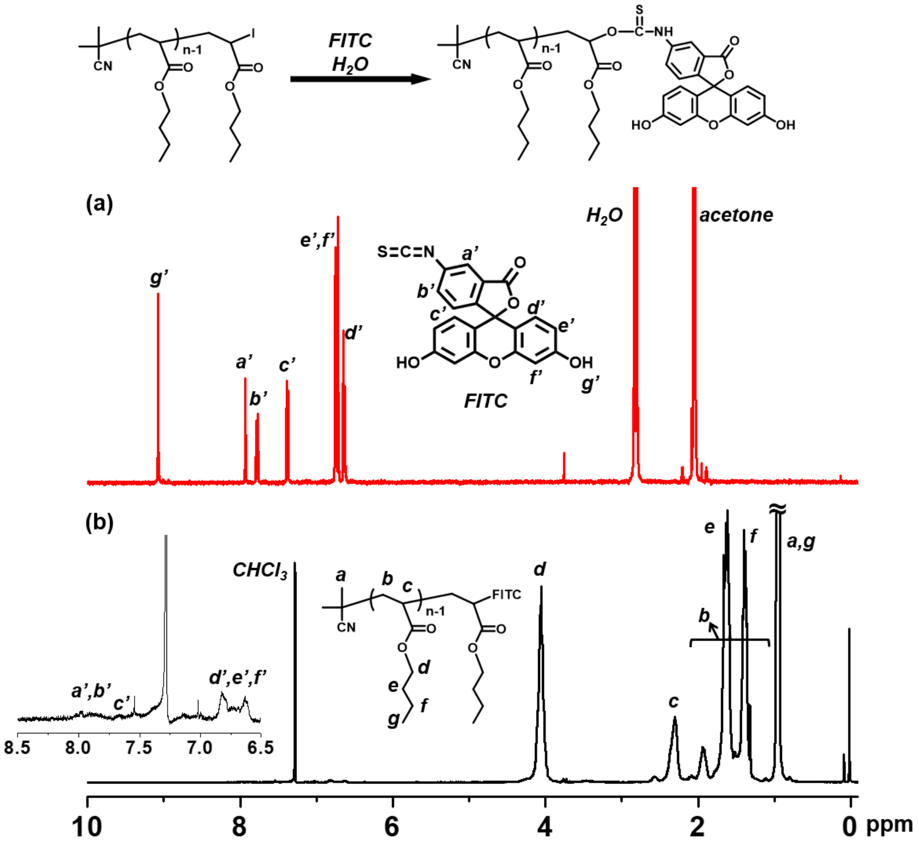

Figure 4.10. ^{1}H NMR spectra of (a) FITC (in acetone-d_6) and (b) the polymer (in $CDCl_3$) obtained in a reaction of PBA-I (20 wt%, 0.075 mM, 0.5 eq), FITC (5.7 wt%, 0.15 mM, 1 eq), TBA (0.15 mM, 1 eq), and DMAP (0.15 mM, 1 eq) in DMF at 60 °C for 12 h.

We also successfully used a different functional group and a different photomask. A patterned PBA brush with an H atom and an alkynyl functional group was synthesized using HCOOH and $NH_2CH_2C\equiv CH$ using a well-shaped photomask. The alkynyl functionality is useful to attach various small molecules and polymers through so-called click reactions.[40] After the chain-end patterning, the alkynyl group was labelled with a fluorescence molecule 7-diethylamino-3-(4-((3-(2-mercaptoethyl)thio)succinimido)phenyl)-4-methylcoumarin (CPS-SH) (Figure 4.11a) *via* a thiol-yne click reaction. A clear well-shaped fluorescence pattern was observed (Figure 4.11), demonstrating the successful fabrication of the hydrogen and alkyne chain-end patterned polymer brush.

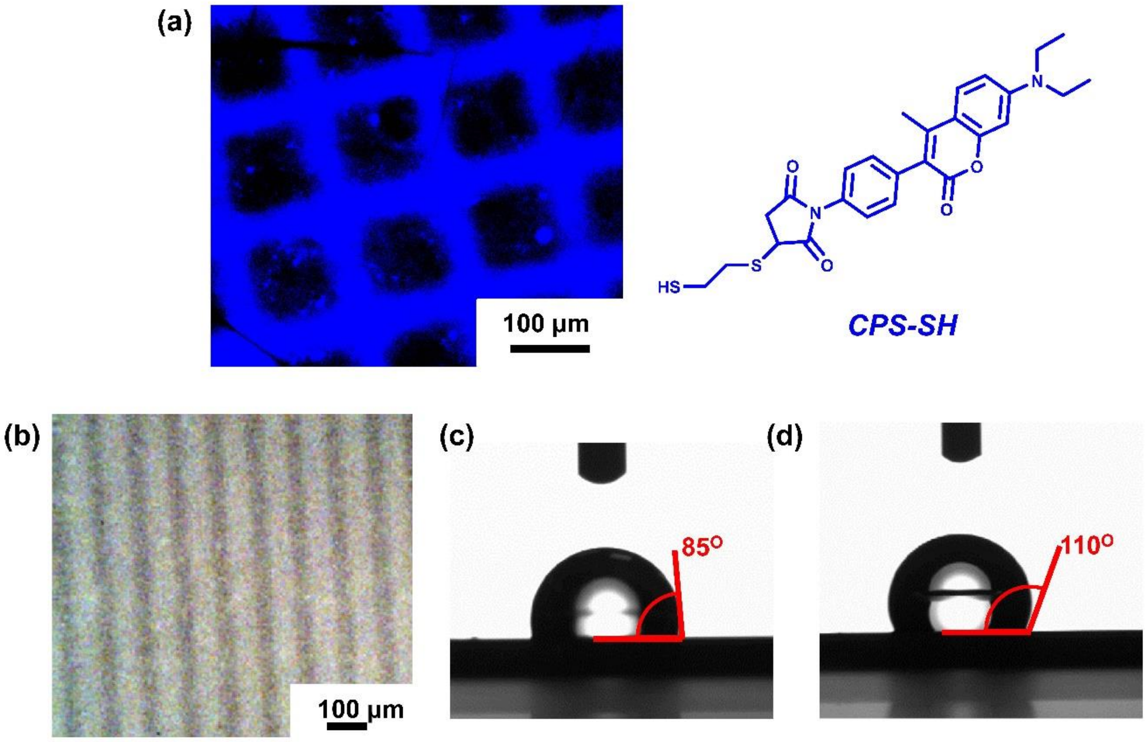

Figure 4.11 (a) Fluorescence microscope image of CPS-attached patterned polymer brushes. The structure of CPS-SH is given in the figure. (b) Microscope image of binary patterned PNFHA-*b*-PBA and PBA-H brushes. Contact angle analysis of (c) binary patterned PBA-$C\equiv CH$ and PBA-H brushes and (d) binary patterned PNFHA-*b*-PBA and PBA-H brushes.

The fabrication of the alkyne chain end was also used to alter a physical property of the polymer brush. A hydrogen and alkyne chain-end patterned PBA brush with a stripe pattern was prepared. Alkynes can react with radicals, although the reactivities of alkynes with radicals are generally much lower than those of alkenes. We immersed the wafer with the stripe pattern in a solution of a fluorinated acrylate (1*H*,1*H*,2*H*,2*H*-nonafluorohexyl acrylate (NFHA)), CP-I (16 mM), BNI (128 mM), and carried out the radical polymerization at 110 °C. A super-hydrophobic NFHA polymer (PNFHA) was grafted through the alkyne chain end of the PBA brush. An optical microscope image (Figure 4.11b) showed a stripe pattern due to the different refractive indexes of PNFHA and PBA, where the darker and lighter stripes correspond to PNFHA-*b*-PBA and original PBA brushes, respectively. A binary patterned PNFHA-*b*-PBA (squares) and PBA (wells) brush was prepared. Figure 4.12 shows the microscope image. The squares (PNFHA-*b*-PBA) were darker than the wells (PBA). This means that, in Figure 4.11b, the darker and lighter stripes correspond to PNFHA-*b*-PBA and PBA, respectively. Figures 4.10c and 4.10d show the contact angle analyses on the brush surfaces before and after the graft polymerization of NFHA, respectively. The contact angle increased from 85° to 110° after the polymerization of NFHA, showing the successful alteration of the surface hydrophobicity by the post-functionalization of the alkyne chain end.

The fabrication of the chain-end patterned polymers using the selective chain-end modification is very useful. But there are still some limitations. The use of the UV light source and photomask limits the resolution of the chain-end patterning. Additionally, this chain-end modification method can be only employed to polyacrylate-iodide, thus this patterning is limited to polyacrylate-iodide brushes.

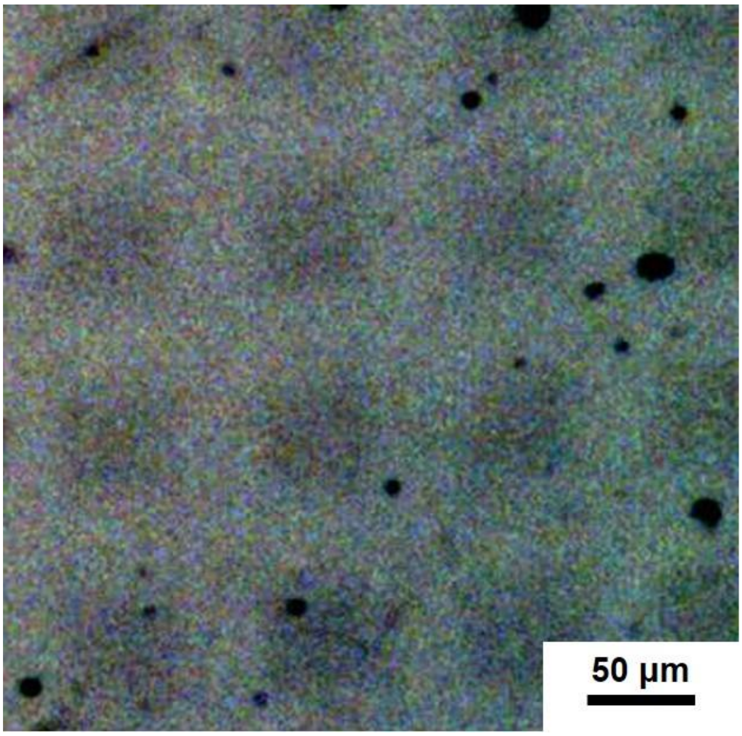

Figure 4.12 Optical microscope image of binary patterned PNFHA-*b*-PBA and PBA-H brush using a well-shaped photomask.

4.3 Conclusions

In summary, we developed a selective chain-end modification method of polymer-I to polymer-H and polymer-X with various functional X groups, using commercially available formic acid and primary amines. By simply switching the UV light on and off, polymer-H and polymer-X were selectively produced, respectively. This method is metal-free, and the scopes of the functional X groups and polyacrylates are wide. This method also enabled the fabrication of chain-end patterned binary polymer brushes. This method may serve as a platform technique for designing chain-end functionalized polymers and surface-functionalized materials for possible applications to, *e.g.*, molecular recognitions, sensors, and biomolecular arrays.

4.4 Experimental

Materials. 2-Iodo-2-methylpropionitrile (CP-I) (>95%, Tokyo Chemical Industry (TCI), Japan), butyl acrylate (BA) (>97%, TCI), 2-methoxyethyl acrylate (MEA) (>98%, TCI), 1*H*,1*H*,2*H*,2*H*-nonafluorohexyl acrylate (NFHA) (> 98%, TCI), tetrabutylammonium iodide (BNI) (>98%, TCI), 2-phenylethylamine (>98%, TCI), 1-amylamine (>98%, TCI), 3-aminopropyltriethoxysilane (>98%, TCI), 4-amino-1-butanol (>98%, TCI), propargylamine (>97%, TCI), *N*,*N*-dimethylformamide (DMF) (>99.5%, Kanto Chemical, Japan), methanol (>99%, International Scientific, Singapore), tetrahydrofuran (THF) (>99.5%, Kanto Chemical), triethylamine (TEA) (>99%, TCI), tributylamine (TBA) (>98%, TCI), 4-dimethylaminopyridine (DMAP) (>99%, TCI), fluorescein 5-isothiocyanate (FITC) (>90%, Sigma-Aldrich, United States), 1,2-ethanedithiol (>99%, TCI), 2-hydroxy-4'-(2-hydroxyethoxy)-2-methylpropiophenone (Irgacure D-2959) (98%, Sigma-Aldrich), 7-diethylamino-3-(4-maleimidophenyl)-4-methylcoumarin (CPM) (>95%, Sigma-Aldrich), formic acid (>98%, TCI), ammonia solution (28% in water, TCI), *trans*-2-[3-(4-t-butylphenyl)-2-methyl-2-propenylidene]malononitrile (DCTB) (>99%, Fluka Chemicals, UK) and sodium trifluoroacetate (NaTFA) (>98%, TCI) were used as received. 6-(2-Iodo-2-isobutyloxy)hexyltriethoxysilane (IHE) was provided through the courtesy of Godo Shigen (Japan) and was used as received. Formic-*d* acid (DCOOH) (95wt% in H_2O) (Sigma-Aldrich) was dried by $MgSO_4$ before use. The glass photomasks (Hunan Omnisun Information Materia, China) polished on both sides with a patterned low reflective chrome film on one side were used as received.

Analytical GPC. The GPC analysis was performed on a Shimadzu LC-2030C Plus liquid chromatograph (Kyoto, Japan) equipped with a Shodex (Tokyo, Japan) KF-804L mixed gel column (300 × 8.0 mm; bead size = 7 μm; pore size = 20–200 Å) and a Shodex LF-804 mixed gel column (300 × 8.0 mm; bead size = 6 μm; pore size = 3000 Å). The eluent was THF at a flow rate of 0.7 mL/min. Sample detection was conducted using a Shimadzu differential refractometer RID-20A. The column system was calibrated with standard poly(methyl methacrylate)s (PMMAs).

Preparative GPC. Polymers were purified with a preparative GPC (LC-9204, Japan Analytical Industry, Tokyo) equipped with JAIGEL 1H and 2H polystyrene gel columns (600×40 mm; bead size = 16 μm; pore size = 20-30 (1H) and 40-50 (2H) Å). Chloroform was used as the eluent at a flow rate of 14 mL/min (room temperature).

NMR. The NMR spectra were recorded on a BBFO400 spectrometer (400 MHz) (Bruker, Germany) at ambient temperature; spectral width 4000.00 Hz, acquisition time 8.192 sec, and pulse delay 1.000 sec.

MALDI-TOF-MS. The MALDI-TOF-MS spectra were recorded on a JMS-S3000 Spiral-TOF (JEOL Ltd., Japan) at an accelerating potential of 20 kV in the positive spiral mode. We prepared polymer solution (10 mg/mL in THF), matrix solution (DCTB: 60 mg/mL in THF), and cationization agent solution (NaTFA: 10 mg/mL in THF). The polymer solution, the DCTB solution, and the cationization agent solution were mixed in a ratio of 1/2/1 (v/v/v). Then, 5 μL of the mixed solution was deposited on the target plate spot and dried in the air at room temperature.

Contact Angle. The water-contact angle analysis of the polymer brushes was carried out with a DM-701 contact angle meter (Kyowa Interface Science, Japan).

UV-LED light. The UV-LED light source (C11924-101) (at 365 (± 10) nm) was purchased from Hamamatsu Photonics (Japan). The energy of the irradiating light per area was measured to be 900 mW/cm^2 with a power meter (FieldMate, Coherent, USA).

AFM. The polymer brush thickness was determined with an atomic force microscope (AFM) (Probe Station AFM5000II, Hitachi High-Technologies, Japan) using a cantilever PRC-DF40P.

Preparation of Polymer-I (PBA-I and PMEA-I). A mixture of monomer (BA or MEA) (15 g, 50 eq), CP-I (1 eq), and BNI (4 eq) was heated in a 100 mL flask at 110 °C for 5 h under an argon atmosphere with magnetic stirring. The reaction mixture was diluted with THF, and the polymer was reprecipitated in a non-solvent (methanol/water mixture (v/v = 1/1) for PBA-I and hexane for PMEA-I. The polymer was further purified with preparative GPC.

General Procedure of Photo-Selective Chain-End Transformation of Polymer-I. A DMF solution of polymer-I (20 wt%, 1 eq), formic acid (HCOOH) (4 eq), and a primary amine (20 eq) was stirred in a reaction tube at room temperature in the dark for 2 h or under the UV irradiation for 2 h. The reaction mixture was diluted with chloroform, and then the polymer was purified with preparative GPC.

Reaction of PBA-I with HCOOH. A DMF solution of PBA-I (20 wt%, 1 eq) and HCOOH (4 eq) was stirred in a reaction tube at room temperature under the UV irradiation for 2 h. The reaction mixture was diluted with THF, and then the polymer was reprecipitated in a methanol/water mixture (v/v = 1/1).

Reaction of PBA-I with TBA. A DMF solution of PBA-I (20 wt%, 1 eq) and TBA (20 eq) was stirred in a reaction tube at room temperature under the UV irradiation for 2 h. The reaction mixture was diluted with THF, and then the polymer was reprecipitated in a methanol/water mixture (v/v = 1/1).

Reaction of PBA-I with DCOOH. A DMF solution of PBA-I (20 wt%, 1 eq), formic-*d* acid (DCOOH) (4 eq), and TBA (20 eq) was stirred in a reaction tube at room temperature under the UV irradiation for 2 h. The reaction mixture was diluted with THF, and then the polymer was reprecipitated in a methanol/water mixture (v/v = 1/1).

Preparation of PBA-I Brush. The IHE-immobilized silicon wafer was heated in a mixture of BA (10 g, 1000 eq), CP−I (1 eq), and BNI (8 eq) in a Schlenk flask at 110 °C under argon atmosphere for 24 h. The M_{n} and values of the non-immobilized polymer produced from CP−I were 23000 and 1.34, respectively. The M_{n} and $Đ$ values are PMMA-calibrated GPC values. After the polymerization, the wafer was rinsed with acetone, sonicated in acetone for 30 min twice, and dried under nitrogen flow. The thickness (h) of the polymer brush in the dry state was determined by atomic force microscope (AFM) to be 20 nm. We scratched the brush and measured the height gap between the scratched and unscratched areas. Assuming that the M_{n} value of the polymer brush is 23000 (179 monomer units), the contour length of the polymer brush chain is 45 nm (= 0.25 nm (length of the monomer unit) x 179 units). (For the sp^3 carbon linkage, the C-C distance is 1.53 Å and the bond angle is 109.5°. The alternate C-C-C distance (length of the monomer unit) is thus calculated to be 0.25 nm.) The surface occupancy (σ^*) is calculated to be 0.45 (= 20 nm (brush thickness) / 45 nm (contour length of the polymer chain)). This σ^* value is viewed as an approximation, because we assume that the M_{n} value of the polymer brush is the same as that of the non-immobilized polymer and use the PMMA-calibrated M_{n} value.

Preparation of OH and Alkyne Chain-End Patterned Brushes. A DMF solution of HCOOH (1 eq, 1 wt%) and a primary amine (5 eq) ($NH_2(CH_2)_4OH$ or $NH_2CH_2C{\equiv}CH$) was dropped onto the silicon wafer fabricated with the PBA-I brush. A cover glass was placed to form a thin layer of the solution between the cover glass and the wafer. Then, a photomask was placed on the cover glass, and UV was irradiated for 2 h. The wafer was cleaned by ultra-sonication in THF for 30 min and dried under nitrogen flow.

FITC Labeling of OH Chain-End Patterned PBA Brush. The OH patterned silicon wafer was heated in a DMF solution of fluorescein 5-isothiocyanate (FITC) (1 wt%, 0.026 mM, 1 eq), TBA (0.026 mM, 1 eq), and 4-dimethylaminopyridine (DMAP) (0.026 mM, 1 eq) in a reaction tube at 60 ^{o}C for 12 h. The wafer was then cleaned by ultra-sonication in THF for 30 min and dried under nitrogen flow. The fluorescence image was taken with Zeiss Observer Z1 (Germany) using the filter set 38 under autoexposure.

Reaction of PBA-I with FITC. A DMF solution of non-immobilized PBA-I (20 wt%, 0.075 mM, 0.5 eq), FITC (5.7 wt%, 0.15 mM, 1 eq), TBA (0.15 mM, 1 eq), and DMAP (0.15 mM, 1 eq) was stirred in a reaction tube at 60 ^{o}C for 12 h. The reaction mixture was diluted with THF, and then the polymer was reprecipitated in a methanol/water mixture (v/v = 1/1). The polymer was further purified with preparative GPC.

Preparation of Fluorescence Molecule CPS-SH. A dichloromethane solution of CPM (0.0034 g, 0.035 mM, 1 eq), 1,2-ethanedithiol (2 eq), and triethylamine (TEA) (1.4 eq) was stirred at room temperature for 2 h. The crude solution was then purified by chromatography (dichloromethane/methanol (v/v = 40/1)), yielding 7-diethylamino-3-(4-((3-(2-mercaptoethyl)thio)succinimido)phenyl)-4-methylcoumarin (CPS-SH) (yellow powder). ^{1}H and ^{13}C NMR spectra of CPS-SH (dimethyl sulfoxide (DMSO)-d_6) are given in Figure 4.13.

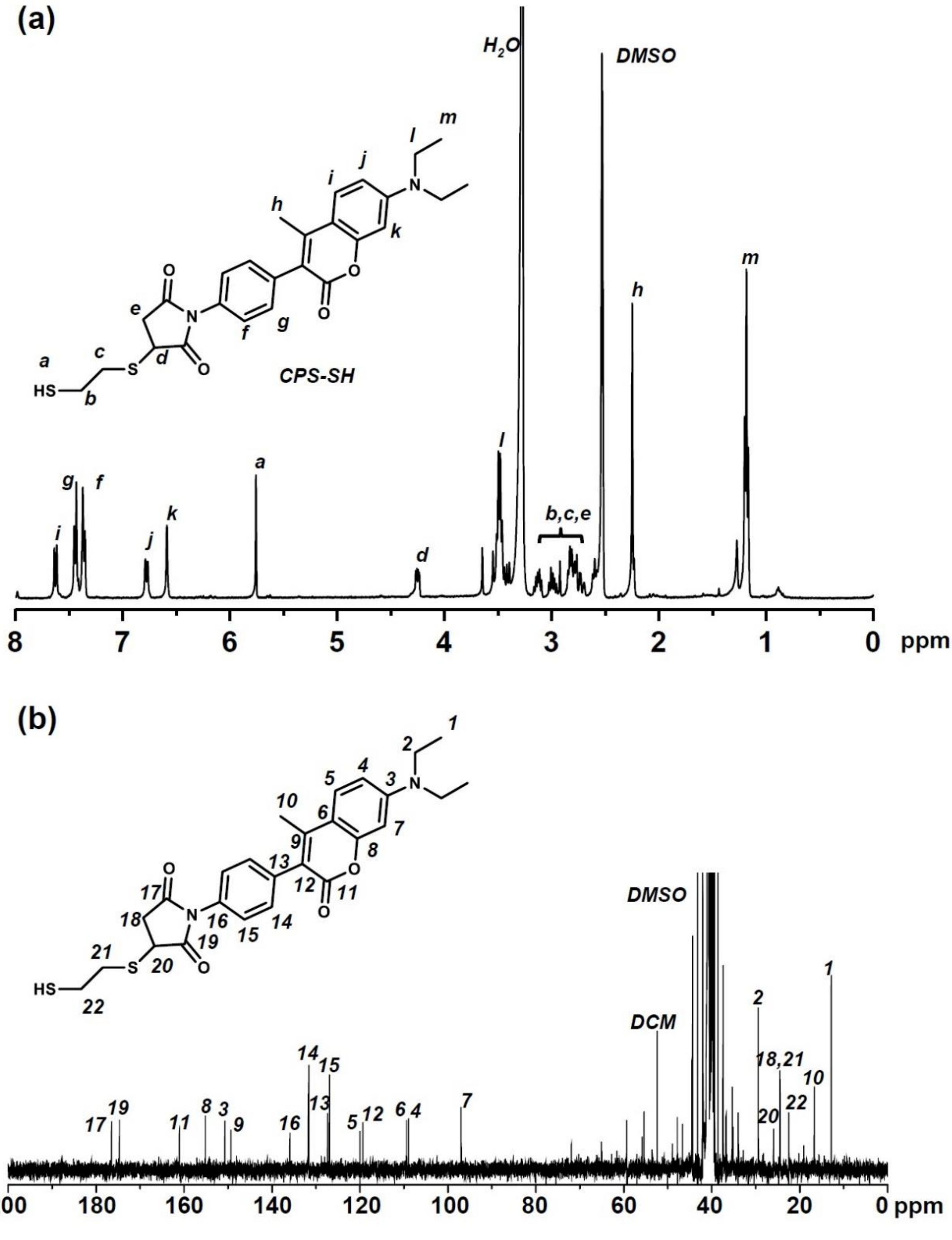

Figure 4.13. (a) ^{1}H and (b) ^{13}C NMR spectra (DMSO-d_6) of CPS-SH.

CPS Labeling of Alkyne Chain-End Patterned PBA Brush. A DMF solution of CPS-SH (1wt%) and 2-hydroxy-4’-(2-hydroxyethoxy)-2-methylpropiophenone (Irgacure D-2959) (1wt%) was dropped onto the silicon wafer with the alkyne chain-end patterned PBA brush. A cover glass was placed to form a thin layer of the solution between the cover glass and the wafer. The wafer was irradiated with UV for 20 min and was cleaned by ultra-sonification in THF for 30 min. The fluorescence image was taken with Zeiss Observer Z1 using the filter set 49 under autoexposure.

Attaching Hydrophobic Polymer Chain to Alkyne Patterned PBA Brush. The silicon wafer with the alkyne chain-end patterned PBA brush was heated in a mixture of 1*H*,1*H*,2*H*,2*H*-nonafluorohexyl acrylate (NFHA) (10 g, 500 eq), CP−I (1 eq), and BNI (8 eq) in a Schlenk flask at 110 ^{o}C under argon atmosphere for 24 h. The wafer was rinsed with acetone (a good solvent of the NFHA polymer), sonicated in acetone for 30 min twice, and dried under nitrogen flow.

4.5 References

1. Tasdelen, M. A.; Kahveci, M. U.; Yagci, Y. *Prog. Polym. Sci.* **2011**, *36*, 455−567.
2. Lunn, D. J.; Discekici, E. H.; Read de Alaniz, J.; Gutekunst, W. R.; Hawker, C. J. *J. Polym. Sci. Part A: Polym. Chem.* **2017**, *55*, 2903−2914.
3. Anastasaki, A.; Willenbacher, J.; Fleischmann, C.; Gutekunsta, W. R.; Hawker, C. J. *Polym. Chem.* **2017**, *8*, 689−697.
4. Beija, M.; Charreyre, M.-T.; Martinho, J. M. G. *Prog. Polym. Sci.* **2011**, *36*, 568−602.
5. Goldmann, A. S.; Glassner, M.; Inglis, A. J.; Barner-Kowollik, C. *Macromol. Rapid Commun.* **2013**, *34*, 810−849.
6. Golas, P. L.; Matyjaszewski, K. *Chem. Soc. Rev.* **2010**, *39*, 1338−1354.
7. Nicolas, J.; Mantovani, G.; Haddleton, D. M. *Macromol. Rapid Commun.* **2007**, *28*, 1083−1111.
8. Dehn, S.; Chapman, R.; Jolliffe, K. A.; Perrier, S. *Polymer Reviews* **2011**, *51*, 214–234.
9. Jiang, H.; Xu, F.-J. *Chem. Soc. Rev.* **2013**, *42*, 3394–3426.
10. Escorihuela, J.; Marcelis, A. T. M.; Zuilhof, H. *Adv. Mater. Interfaces* **2015**, *2*, 1500135.
11. Matyjaszewski, K. *Adv. Mater.* **2018**, *30*, 1706441.
12. Matyjaszewski, K.; Tsarevsky, N. V. *J. Am. Chem. Soc.* **2014**, *136*, 6513−6533.
13. Keddie, D. J.; Moad, G.; Rizzardo, E.; Thang, S. H. *Macromolecules* **2012**, *45*, 5321−5342.
14. Nicolas, J.; Guillaneuf, Y.; Lefay, C.; Bertin, D.; Gigmes, D.; Charleux, B. *Prog. Polym. Sci.* **2013**, *38*, 63−235.
15. Carmean, R. N.; Figg, C. A.; Scheutz, G. M.; Kubo, T.; Sumerlin, B. S. *ACS Macro Lett.* **2017**, *6*, 185−189.
16. Gutekunst, W. R.; Anastasaki, A.; Lunn, D. J.; Truong, N. P.; Whitfield, R.; Jones, G. R.; Treat, N. J., Abdilla, A.; Barton, B. E.; Clark, P. G.; Haddleton, D. M. *Macromol. Chem. Phys.* **2017**, *218*, 1700107.
17. Discekici, E. H.; Shankel, S. L.; Anastasaki, A.; Oschmann, B.; Lee, I.-H.; Niu, J.; McGrath, A. J.; Clark, P. G.; Laitar, D. S.; Read de Alaniz, J.; Hawker C. J.; Lunn, D. J.; *Chem. Commun.* **2017**, *53*, 1888−1891.
18. Alagi, P.; Hadjichristidis, N.; Gnanou, Y.; Feng, X. *ACS Macro Lett.* **2019**, *8*, 664−669.
19. Mattson, K. M.; Pester, C. W.; Gutekunst, W. R.; Hsueh, A. T.; Discekici, E. H.; Luo, Y.; Schmidt, B. V.; McGrath, A. J.; Clark, P. G.; Hawker, C. J. *Macromolecules* **2016**, *49*, 8162−8166.

20. Goto, A.; Ohtsuki, A.; Ohfuji, H.; Tanishima, M.; Kaji, H. *J. Am. Chem. Soc.* **2013**, *135*, 11131−11139.

21. Ohtsuki, A.; Lei, L.; Tanishima, M.; Goto, A.; Kaji, H. *J. Am. Chem. Soc.* **2015**, *137*, 5610−5617.

22. Wang, C.-G.; Hanindita, F.; Goto, A. *ACS Macro Lett.* **2018**, *7*, 263−268.

23. Wang, C.-G.; Chen, C.; Sakakibara, K.; Tsujii, Y.; Goto, A. *Angew. Chem. Int. Ed.* **2018**, *130*, 13692−13696.

24. Liu, X.; Wang, C.-G.; Goto, A. *Angew. Chem. Int. Ed.* **2019**, *131*, 5654−5659.

25. Wang, C.-G.; Oh, X. Y.; Liu, X. Goto, A. *Macromolecules* **2019**, *52*, 2712−2718.

26. Chen, C.; Xiao, L.; Goto, A. *Macromolecules* **2016**, *49*, 9425−9440.

27. Discekici, E. H.; St. Amant, A. H.; Nguyen, S. N.; Lee, I. H.; Hawker, C. J.; Read de Alaniz, J. *J. Am. Chem. Soc.* **2018**, *140*, 5009−5013.

28. Hernandez, J. G.; Bolm, C. *J. Org. Chem.* **2017**, *82*, 4007−4019.

29. Peterson, B. M.; Kottisch, V.; Supej, M. J.; Fors, B. P. *ACS Centr. Sci.* **2018**, *4*, 1228−1234.

30. Wang, C.-G.; Goto, A. *J. Am. Chem. Soc.* **2017**, *139*, 10551−10560.

31. Zheng, J.; Wang, C.-G.; Yamaguchi, Y.; Miyamoto, M.; Goto, A. *Angew. Chem. Int. Ed.* **2018**, *130*, 1568−1572.

32. Chen, C.; Wang, C.-G.; Xiao, L.; Goto, A. *Chem. Comm.* **2018**, *54*, 13738−13741.

33. Discekici, E. H.; Treat, N. J.; Poelma, S. O.; Mattson, K. M.; Hudson, Z. M.; Luo, Y.; Hawker, C. J.; de Alaniz, J. R. *Chem. Commun.* **2015**, *51*, 11705−11708.

34. Zoppe, J. O.; Ataman, N. C.; Mocny, P.; Wang, J.; Moraes, J.; Klok, H. A. *Chem. Rev.* **2017**, *117*, 1105−1318.

35. Tsujii, Y.; Ohno, K.; Yamamoto, S.; Goto, A.; Fukuda, T. *Adv. Polym. Sci.* **2006**, *197*, 1−45.

36. Chen, T.; Amin, I.; Jordan, R. *Chem. Soc. Rev.* **2012**, *41*, 3280−3296.

37. Fors, B. P.; Poelma, J. E.; Menyo, M. S.; Robb, M. J.; Spokoyny, D. M.; Kramer, J. W.; Waite, J. H.; Hawker, C. J. *J. Am. Chem. Soc.* **2013**, *135*, 14106-14109.

38. Yu, Q.; Ista, L. K.; Gu, R.; Zauscher, S.; López, G. P. *Nanoscale* **2016**, *8*, 680−700.

39. Nielsen, L. J.; Eyley, S.; Thielemans, W.; Aylott, J. W. *Chem. Comm.* **2010**, *46*, 8929-8931.

40. Lowe, A. B. *Polymer*, **2014**, *55*, 5517-5549.

Chapter 5 Chain-end modification of polymer iodide using thiols and the applications to patterned polymer brushes and rewritable polymer brushes

5.1 Introduction

Chain-end functionalized polymers are of great importance in polymer science as they can produce designed polymers with complex architectures and advanced polymer materials.[1,2] They can connect with small molecules, other polymers, and biomacromolecules, yielding labeled polymers, block copolymers, and bio-conjugates.[3,4]

Surface modification by using polymer brushes is a useful method to efficiently tune the surface properties and has been widely employed in material science and engineering.[5] To fabricate polymer brushes on surfaces, grafting-to and grafting-from methods have been developed. The grafting-to method anchors pre-synthesized polymers on surfaces.[6,7] The grafting-from method is a bottom-up polymer growth approach from the initiator anchored on the surface, and polymer brushes with higher graft density can be prepared.[8,9]

Controlled radical polymerization (CRP) is a useful technique to synthesize chain-end functionalized polymers.[1,2] By using functional initiators or by post-modifying the chain-end capping agent, variuos functional groups can be introduced at the initiating or the growing chain ends, respectively. Apart from functionalization, removal of the active chain-end capping agent is also desirable to confer the high thermal and optical stabilities of the polymeric materials. In the presence of reductant, the polymers obtained from ATRP and RAFT polymerization, i.e., polymers with halide or thiocarbonylthio groups at the chain end, respectively, can be transferred to hydrogen-terminated polymers (polymer-H) through photo-redox catalysis.[10-12] Recently, Prakash and coworkers achieved a fast and quantitative removal of the capping agent of RAFT-synthesized polymer.[12] The method was free from catalyst, but an expensive trialkylborane was used as the reductant (hydrogen donor).

Our research group developed an organocatalyzed CRP (termed as reversible complexation mediated polymerization (RCMP)) using an alkyl iodide (R–I) as an initiator and organic molecules as catalysts, yielding a polymer-iodide possessing an iodide at the growing chain end.[13-16] In Chapter 2, the chain end iodine was successfully transformed into hydroxyl, alkyl, phenyl, thiol, and triethoxysilyl groups via the substitution reaction with primary amines (R-NH_2) with functional R groups.[17] The conversion was quantitative, but a long reaction time (~ 12 h) is required.

In Chapter 5, we developed rapid and complete chain-end functionalization and chain-end reduction methods of polyacrylate-iodide (polymer-I) by using commercially available thiols (R-SH) to generate polymer-SR and polymer-H, respectively. In order to obtain polymer-SR, the substitution of polyacrylate-halide with R-SH was previously studied using polyacrylate-bromide (polymer-Br) synthesized by ATRP.[18] However, relatively long reaction time was required (~ 12 h) to convert the bromide chain end to functional groups. The present polymer-I has higher reactivity than polymer-Br due to the weaker C-I bond at the terminal chain end. Therefore, the substitution reaction was much faster, and a quantitative chain-end modification was achieved in a short time (~ 10 min), as describe below.

Under UV irradiation, the C-I bond was cleaved to generate a carbon-centered radical (polymer$^\bullet$). Thiols are good hydrogen donors, which can react with polymer$^\bullet$ to give polymer-H quantitatively. In Chapter 5, this chain-end reduction was employed to fabricate patterned polymer brushes. Concentrated polymer-I brushes were prepared via surface-initiated RCMP. Due to the steric hindrance of the neighbouring chains, polymer chains are forced to extend, and the C-I bonds at the growing chain end tend to be localized at the outermost surface of the polymer brush. The chain-end iodide was spatially reduced to hydrogen by using UV light and a photomask for generating a hydrogen and iodine chain-end patterned polymer brush, which was further subject to surface-initiated RCMP to furnish a patterned block copolymer brush.

Most of the polymer brushes previously reported had irreversible functionalities. Polymer brushes with dynamic and reusable functionalities may provide smart surfaces.[19-21] In Chapter 5, we fabricated rewritable polymer brushes that can anchor (write), de-anchor (erase), and re-anchor (re-write) external molecules on the surfaces. An SH group on the surface was reversibly linked with an SH group of an external molecule via a disulphide linkage. The reversible formation and cleavage of the disulphide bond enabled the writing, erasing, and rewriting of the external molecules on the surface.

5.2 Results and Discussion

5.2.1 Chain-end functionalization of polymer-I using thiols

Poly(butyl acrylate) iodide (PBA-I) was synthesized by RCMP using 2-iodo-2-methylpropionitrile (CP-I) as an initiator and tetrabutylammonium iodide (BNI) as a catalyst. The PBA-I was reprecipitated in a mixture of water/methanol (v/v = 1/1) and further purified by preparative GPC to remove trace amounts of impurities. The M_n and dispersity ($Đ$) of the purified PBA-I were 3400 and 1.29, respectively.

PBA-I was reacted with R-SH to generate PBA-SR in the presence of a base. We mixed PBA-I (1 eq, 20 wt%), diisopropylamine ($^iPr_2NH$) (4 eq), and R-SH (20 eq) in dimethylformamide (DMF) with magnetic stirring for 10 min. Figure 5.1a shows the matrix-assisted laser desorption/ionization time-of-flight mass spectrometry (MALDI-TOF-MS) spectrum of the product using $C_{12}H_{25}SH$. The *trans*-2-[3-(4-tert-butylphenyl)-2-methyl-2-propenylidene]malononitrile (DCTB) was used as a matrix and CF_3COONa was used as an additive salt. All the polymer samples possess both ^{12}C and ^{13}C atoms. To simply analysis of the results, all the molecular weight values (theoretical and experimental) discussed in this chapter are calculated or given only considering the polymers with ^{12}C atoms. In Figure 5.1a, we observed a predominant peak with the experimental molar mass value 2853.80, which matches the theoretical molar mass value 2853.90 of PBA-$SC_{12}H_{25}$ (n = 20), where n is the degree of polymerization of PBA. The result shows a high yield (90%) of PBA-$SC_{12}H_{25}$. Figures 5.1b-i show the MALDI-TOF-MS spectra of the products by using various functional thiols, i.e., $(EtO)_3Si(CH_2)_3SH$, 2-phenylethanethiol ($Ph(CH_2)_2SH$), 4-chlorobenzyl mercaptan ($ClC_6H_4CH_2SH$), 2-mercaptoethanol ($HOCH_2CH_2SH$), 2-propene-1-thiol ($CH_2{=}CHCH_2SH$), thioglycolic acid ($HSCH_2COOH$), DL-dithiothreitol ($HSCH_2CH(OH)CH(OH)CH_2SH$) (DTT), and 1,2-ethanedithiol ($HSCH_2CH_2SH$). The yields of PBA-SR were high (61-98%) in all cases, as summarized in Table 5.1.

The base ($^iPr_2NH$) was required in the substitution reaction to deprotonate (active) R-SH to a more reactive RS^- and to neutralize the generated HI. Tributylamine (TBA) was too strong base to use. The use of TBA mainly converted PBA-I to PBA-H instead of the desired PBA-SR, because PBA-I and TBA formed a PBA-I ⋯ NBu_3 complex, which facilitated the generation of $PBA^\bullet$. $PBA^\bullet$ then abstracted a hydrogen from R-SH to yield PBA-H. $^iPr_2NH$ is a weaker base and also steric hindrance and hence would not significantly generated the complex (and hence PBA-H).

In Chapter 2, we reported the substitution reaction between PBA-I and cysteamine ($NH_2CH_2CH_2SH$), from which PBA-$NHCH_2CH_2SH$ was generated as the main product. In the case of $NH_2CH_2CH_2SH$, a mixed solvent (diglyme/1-butanol = 1/1 w/w) with low polarity was used, in which the deprotonation of SH is difficult ($NH_3^+CH_2CH_2S^-$ should reprecipitate in the mixed solvent). So the $-NH_2$ worked as nucleophile but not SH.

Table 5.1. Reaction of PBA-I (1 eq) with $^iPr_2NH$ (4 eq) and functional thiols for 10 min

Entry	**Thiol**	**PBA-SR (%)[a]**
1	$n C_{12}H_{25}SH$	90
2	$(EtO)_3Si(CH_2)_3SH$	86
3	$Ph(CH_2)_2SH$	95
4	$ClC_6H_4CH_2SH$	97
5	$HOCH_2CH_2SH$	95
6	$CH_2=CHCH_2SH$	98
7	$HSCH_2COOH$	84
8	DTT	73
9	$HSCH_2CH_2SH$	61

[a] percentages are rough estimate from MALDI-TOF-MS spectra with 10% estimate error

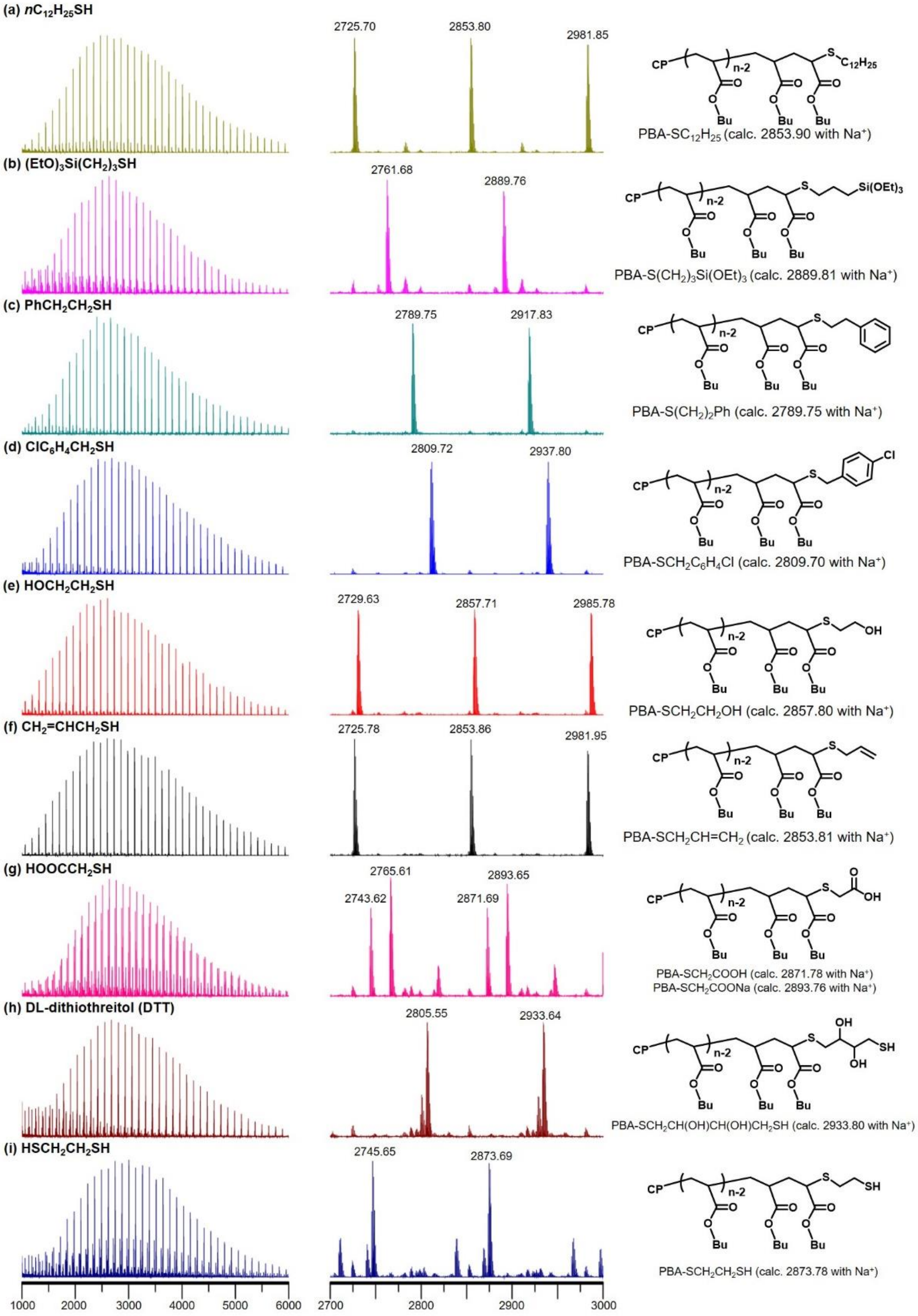

Figure 5.1. MALDI-TOF-MS spectra of the products from the reaction of PBA-I (1 eq, 20 wt%), ${}^{i}Pr_2NH$ (4 eq) and different thiols (R-SH, 20 eq) in DMF for 10 min (Table 5.1). The thiols are given in the figure.

5.2.2 Chain-end reduction of polymer-I using thiols

PBA-I (1 eq, 20 wt%) and 1-dodecanethiol ($C_{12}H_{25}SH$) were dissolved in DMF under UV irradiation at room temperature. The stoichiometric amount of thiol for the chain-end reduction is two equivalents. The chain end C-I was cleaved under UV irradiation to generate $PBA^•$ and $I^•$, which abstract hydrogens from two $C_{12}H_{25}SH$ molecules to generate PBA-H, HI and $C_{12}H_{25}S^•$. Two molecules of $C_{12}H_{25}S^•$ subsequently combine to form $C_{12}H_{25}SSC_{12}H_{25}$. We used different amounts of the thiol, i.e., a stoichiometric amount (2 eq, Table 5.2, entry 1) and an excess amount (20 eq, Table 5.2, entry 2). A high conversion (88-90%) of PBA-I to PBA-H was achieved in 30 min using 2 equivalents of $C_{12}H_{25}SH$ and in even a shorter time of 10 min using 20 equivalents. Figure 5.2 shows the MALDI-TOF-MS spectrum of the product prepared by using 20 equivalents of $C_{12}H_{25}SH$ for 10 min. A single series of repeated peaks was observed, and the experimental molar mass value (2781.77) matched the theoretical molar mass value (2781.81) of PBA-H.

Table 5.2. Chain-end reduction of PBA-I

Entry	**Amount of $C_{12}H_{25}SH$**	**Time**	**Conversion (%)[a]**
1	2	30 min	88
		1 h	86
		2 h	87
		4 h	87
2	20	5 min	86
		10 min	90
		20 min	90
		30 min	90
		1 h	93

[a] Estimated from the peak heights in the MALDI-TOF-MS spectra with 10% estimate error.

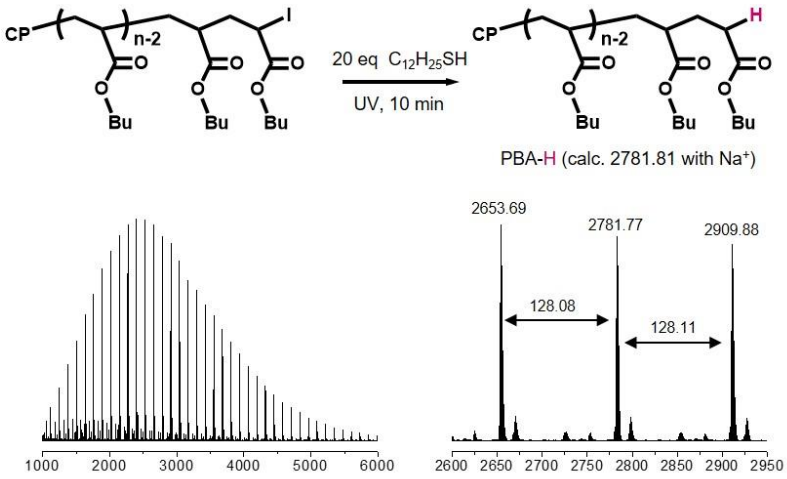

Figure 5.2. MALDI-TOF-MS spectrum of the product from the reaction of PBA-I (1 eq, 20 wt%), $C_{12}H_{25}SH$ (20 eq) in DMF under UV for 10 min.

Instead of UV irradiation, thermal heating was also able to cleave the chain-end C-I bond for generating $PBA^{\bullet}$, which abstracted hydrogen from $C_{12}H_{25}SH$ to generate PBA-H. We heated a mixture of PBA-I (1 eq, 20 wt%) and $C_{12}H_{25}SH$ (20 eq) in DMF at 100 °C for 1 h. The MALDI-TOF-MS spectrum of the obtained product was shown in Figure 5.3, demonstrating the predominant formation of PBA-H.

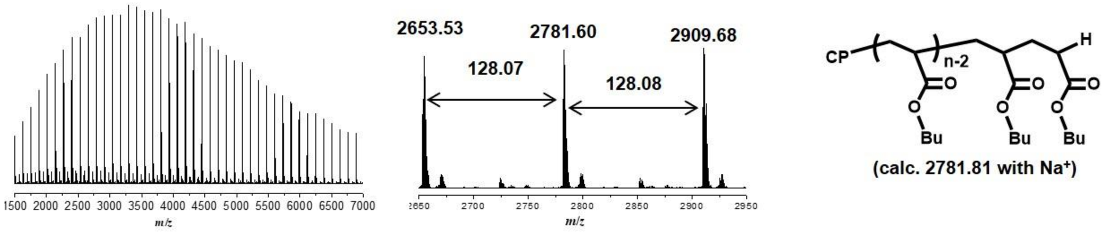

Figure 5.3. MALDI-TOF-MS spectrum of the product from the reaction of PBA-I (1 eq, 20 wt%) and $C_{12}H_{25}SH$ (20 eq) in DMF at 100 ^{O}C for 1h.

As well as PBA-I, the chain-end reduction was effective to polystyrene-iodide (PSt-I). A PSt-I (M_n = 4400 and $Đ$ = 1.27) (1 eq, 20 wt%) was reacted with $C_{12}H_{25}SH$ (20 eq) in the presence of BNI (5 eq), 2.2′-azobis(2-methylpropionitrile) (AIBN) (5 eq), and TBA (5 eq) in DMF at 120 °C for 8 h. BNI worked as a catalyst to activate PSt-I to produce $PSt^{\bullet}$, which subsequently reacted with $C_{12}H_{25}SH$ yielding PSt-H. AIBN was used to accelerate the generation of PSt$^{\bullet}$ via the degenerative chain transfer. TBA was used to neutralize the generated HI. Figure 5.4 shows the MALDI-TOF-MS spectrum of the product. For polystyrene, CF_3COOAg was used as the additive salt instead of CF_3COONa. Only a single series of peak was observed. The experimental molar mass value (2881.56) matched the theoretical molar mass value (2881.69), showing that the chain-end reduction method was applicable to PSt-I.

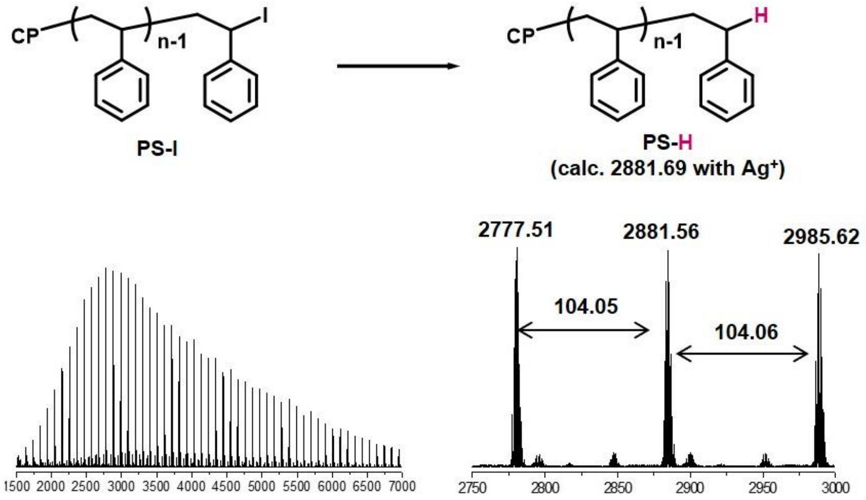

Figure 5.4. MALDI-TOF-MS spectrum of the product from the reaction of PSt-I (1 eq, 20 wt%), $C_{12}H_{25}SH$ (20 eq), BNI (5 eq), AIBN (5 eq) and TBA (5 eq) at 120 ^{O}C for 8 h.

The chain-end reduction method was applied to furnish patterned polymer brushes. Previously, patterned reduction of the chain-end bromide of polymer brushes synthesized via ATRP was studied.[15] The reduction took a relatively long reaction time (around 6 h). In the present study, patterned polymer-H and polymer-I brushes was obtained in 10 min, as described below.

Uniform PBA-I brushes were synthesized on a silicon wafer via surface-initiated RCMP (Figure 5.5). Concentrated PBA-I brushes (surface occupancy (σ^*) > 10%) with different thicknesses (6-30 nm) were prepared (Table 5.3). The thicknesses of the polymer brush in the dry state were measured by AFM. The brush was scratched, and the height gap was measured between the scratched and unscratched areas. The M_n and $Đ$ of the non-immobilized polymers generated from a non-immobilized CP-I and the height and surface occupancy (σ^*) of the obtained PBA brushes are summarized in Table 5.3.

Table 5.3. M_n and $Đ$ of the non-immobilized polymers generated from a non-immobilized alkyl iodide initiator (CP-I) and the thickness and surface occupancy (σ^*) of the obtained PBA brushes.

Entry	First block					Second block				
	Monomer	M_n	$Đ$	Thickness (nm)	σ^*	Monomer	Pattern	M_n	$Đ$	Thickness (nm)
1	BA	12000	1.41	6	0.25	BA	circle	50000	1.83	24
2	BA	51000	1.44	20	0.20	BA	grid	59000	1.98	15
3	BA	18000	1.54	10	0.28	HFBA	stripe	122000[a]	-	-
4	BA	56000	1.71	20	0.18	HFBA	grid	83000[a]	-	-
5	BA	94000	2.11	30	0.16	HFBA	square	150000[a]	-	-

[a] The M_n of non-immobilized PHFBA generated from CP-I was calculated by ^{1}H NMR.

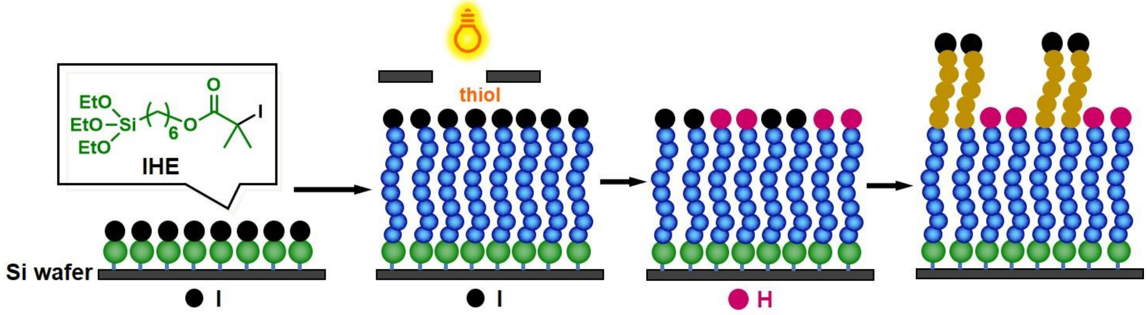

Figure 5.5. Syntheses of PBA-I brushes and patterned block polymer brushes.

A thin PBA-I brush (6 nm, Table 5.2, entry 1) was studied first. On the prepared polymer brushes, a DMF solution of $C_{12}H_{25}SH$ (5 wt%) was dropped. A cover glass was then covered to form a thin solution layer, on which a photomask containing repeating circle was placed. After UV irradiation for 10 min, the iodide at the brush chain end was reduced to hydrogen in the unmasked area, while the iodide remained in the masked area. We subsequently carried out surface-initiated RCMP of butyl acrylate (BA) (8 M) from this chain-end patterned PBA brush in the presence of CP-I (8 mM) and BNI (64 mM) at 110 °C for 18 h to grow PBA from the PBA-I brush chains (chain extension), giving a patterned PBA brush with two different thicknesses. A clear patterned image with repeating circles was observed with an optical microscope (Figure 5.6a). A patterned PBA with a thin first block (6 nm) and a thick second block (24 nm) (Table 5.3, entry 1) was observed. We also used a different photomask with a grid (well-shaped) pattern and prepared a patterned PBA brush with a thicker first block (20 nm) and a relatively thinner second block (15 nm) (Table 5.3, entry 2 and Figure 5.6b).

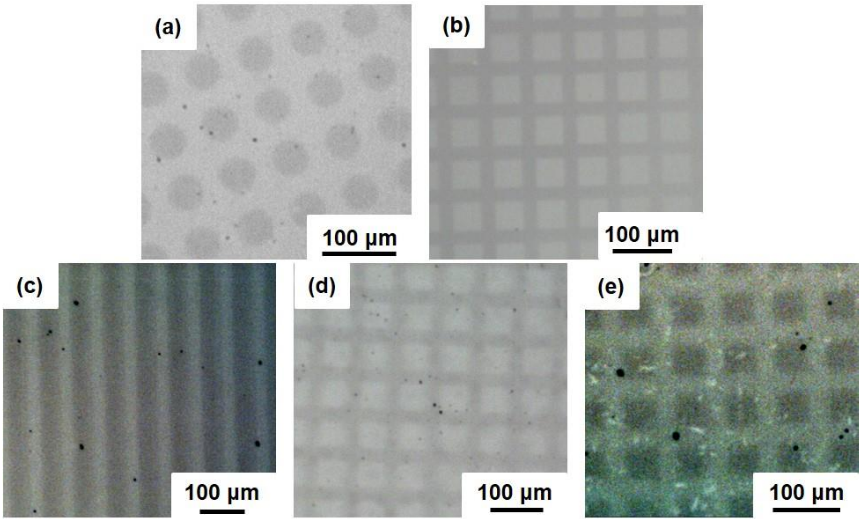

Figure 5.6. Optical microscope images of patterned PBA brushes (Table 5.3, entries (a) 1, (b) 2) and patterned PHFBA-*b*-PBA and PBA brushes (Table 5.3, entries (c) 3, (d) 4 and (e) 5).

The surface energy (contact angle) was also tuned by using a different monomer. We prepared three patterned hydrogen- and iodine-terminated PBA brushes with different thicknesses and different (stripe, grid and square) patterns (Table 5.3, entries 3-5). The prepared PBA brushes were immersed in a mixture of 2,2,3,4,4,4-hexafluorobutyl acrylate (HFBA, 1000 eq), CP-I (1 eq), and BNI (8 eq) and heated at 110 °C. PHFBA chains grew from the iodine-terminated PBA brush chains, generating patterned PHFBA-*b*-PBA and PBA brushes. Clear images with stripe (Figure 5.6c), grid (Figure 5.6d), and square (Figure 5.6e) patterns were clearly observed with an optical microscope. Figure 5.7a and 5.7b show the contact angle analyses of patterned PBA brushes (Table 5.1, entry 2 and Figure 5.6b) (99.5°) and patterned

PHFBA-*b*-PBA and PBA brushes (Table 5.1, entry 4 and Figure 5.6d) (106.0°), respectively. The different contact angles demonstrate the tuning of the surface energy with this patterning.

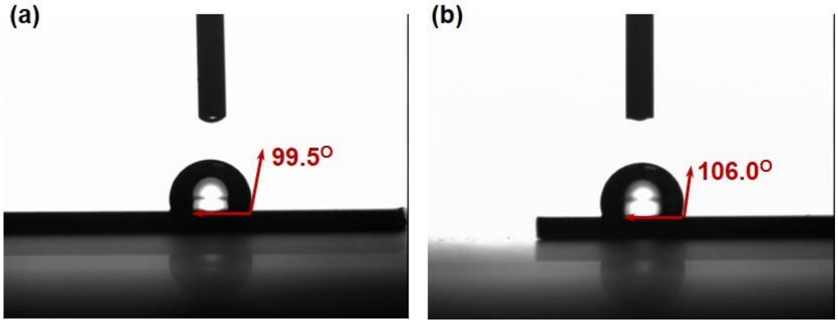

Figure 5.7. Contact angle analysis of (a) patterned PBA brushes and (b) patterned PHFBA-*b*-PBA and PBA brushes.

5.2.3 Hetero-coupling via thiol-disulphide exchange reaction

Thiol-terminated polymer (polymer-SH) is of significant interest since it can connect with other polymers and biomolecules via thiol-ene/yne click reactions and thiol-disulphide exchange reactions, giving block copolymers, star polymers, hyper-branched polymers as well as bio-conjugates.[22-25] Polymer-SH can be tethered on a solid surface to give a polymer brush on the surface.[26] The disulphide bond can reversibly be cleaved to generate the thiols by using reducing agents.

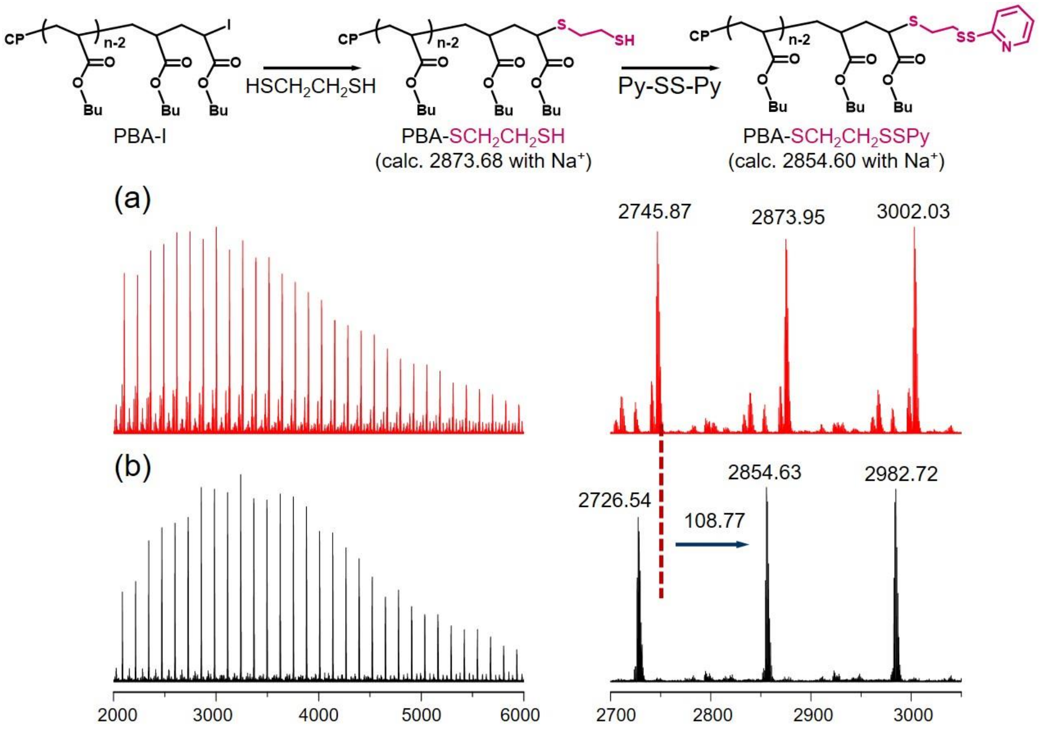

Figure 5.8. MALDI-TOF-MS spectra of the prepared (a) PBA-SCH_2CH_2SH (PBA-SH) and (b) PBA-SCH_2CH_2SSPy (PBA-SSPy).

A thiol-terminated PBA (PBA-SH) was prepared via a reaction of PBA-I (M_n = 4000 and $Đ$ = 1.29) (20 wt%, 1 eq), $HSCH_2CH_2SH$ (20 eq) and $^{i}Pr_2NH$ (4 eq) in DMF at room temperature for 10 min. The polymer was purified with reprecipitation from a mixture of water and methanol (v/v = 50/50) and subsequently by preparative GPC, yielding a PBA-SH with M_n = 4600 and $Đ$ = 1.28. Figure 5.8a shows the MALDI-TOF-MS analysis of the prepared product.

We observed a predominant peak with the experimental molar mass value 2873.95, which matched the theoretical molar mass value 2873.68 of PBA-SCH_2CH_2SH (PBA-SH).

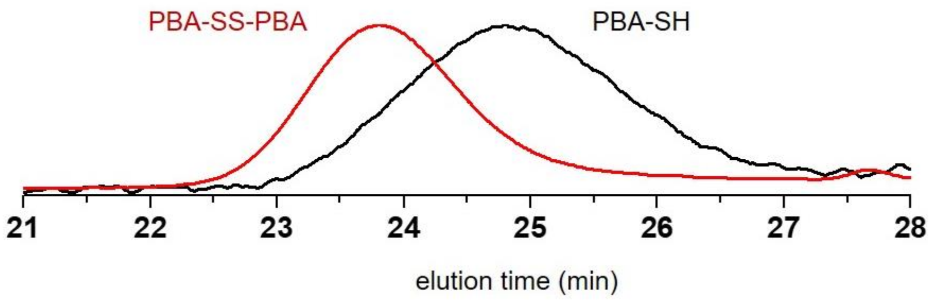

Figure 5.9. GPC traces of PBA-SH (black) and PBA-SS-PBA (red line) obtained from the reaction of PBA-SH (20 wt%), I_2 (2 eq) and TBA (2 eq) in DMF.

The obtained PBA-SH is highly reactive to generate a homo-coupling product with a disulphide linkage (PBA-SS-PBA) in the presence of an oxidant. We mixed the obtained PBA-SH (20 wt%), I_2 (2 eq) (an oxidant) and TBA (2 eq) (a base to neutralize the generated HI) in DMF with magnetic stirring for 12 h. The GPC curve (Figure 5.9, red line) show that a predominant fraction of PBA-SH extended to a homo-coupling product. The molecular weight increased from 4600 to 8400, showing the efficient generation of PBA-SS-PBA.

Hetero-coupling products with a disulphide linkage are attractive since it is useful in the preparation of amphiphilic block copolymers towards drug delivery applications, for example. To synthesize a hetero-coupling product from two different thiol-functionalized polymers (polymer-SH and polymer'-SH), we pre-functionalized one of the two polymers (polymer-SH) to polymer-SSPy, where the pyridylthio group (SPy) is a good leaving group. A hetero-coupling product (polymer-SS-polymer’) can be prepared via the reaction of polymer-SSPy and polymer’-SH, where the homo-coupling products can be avoided.

We mixed PBA-SH (1 eq, 20 wr%) and Py-SS-Py (5 eq) in DMF for 4 h to obtain PBA-SSPy. The MALDI-TOF-MS analysis of the product (Figure 5.8b) confirmed the conversion of PBA-SH to PBA-SSPy nearly quantitatively.

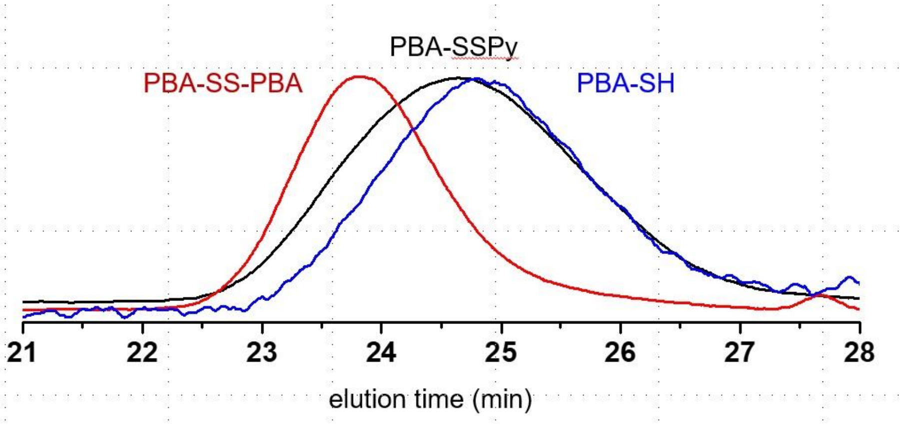

Figure 5.10. GPC traces of PBA-SSPy (black line), PBA-SH (blue lie) and PBA-SS-PBA (red line) obtained from the reaction of PBA-SSPy (1 eq, 10 wt%), PBA-SH (1 eq, 10wt%) and TBA (5 eq) in DMF for 12 h.

A mixture of PBA-SSPy (M_n = 5000 and $Đ$ = 1.31) (1 eq, 10 wt%), PBA-SH (M_n = 4600 and $Đ$ = 1.28) (1 eq, 10wt%) and TBA (5 eq) in DMF was placed at room temperature with magnetic stirring for 12 h. Figure 5.10 shows the GPC traces before (black (PBA-SSPy) and blue (PBA-SH) lines) and after (red line) the reaction. A smooth GPC peak shift was observed, showing the efficient formation of the coupling product PBA-SS-PBA, as also confirmed with MALDI-TOF-MS (experimental molar mass value = 5594.43 and theoretical molar mass value = 5594.81) (Figure 5.11).

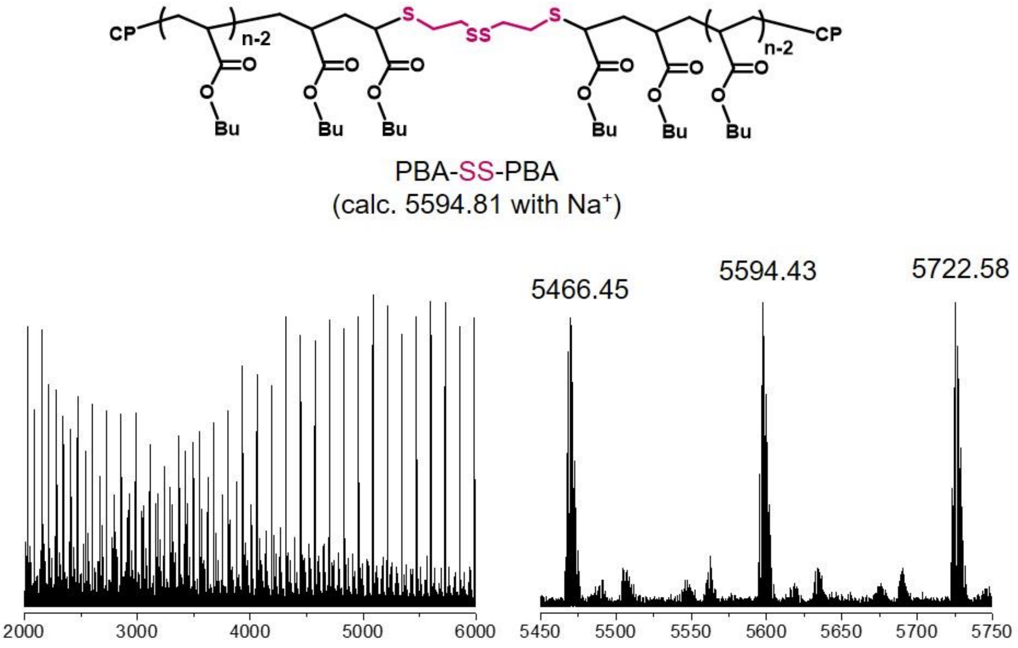

Figure 5.11. MALDI-TOF-MS spectrum of the product from the reaction of PBA-SSPy (1 eq, 10 wt%), PBA-SH (1 eq, 10wt%) and TBA (5 eq) in DMF for 4 h.

As a control experiment, we mixed PBA-SSPy (1 eq, 10 wt%) and TBA (5 eq) in DMF for 12 h. Figure 5.12 shows the GPC curves before (black) and after (red line) the reaction. The GPC peaks did not shift to higher molecular weight area, suggesting that the homo-coupling of PBA-SSPy cannot occur. This result demonstrates the GPC peak shift observed in Figure 5.10 was due to the thiol-disulphide exchange reaction between PBA-SSPy and PBA-SH (not homo-coupling of PBA-SSPy or PBA-SH).

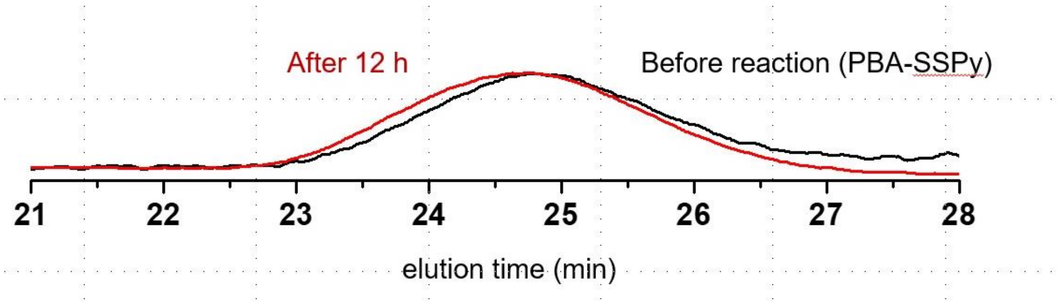

Figure 5.12. GPC traces of PBA-SSPy (black line) and the reaction mixture (red line) of PBA-SSPy (1 eq, 10 wt%) and TBA (5 eq) in DMF for 12 h.

5.2.4 Rewritable polymer brushes on the surface

This efficient thiol-disulphide exchange (hetero-coupling) reaction was employed to fabricate rewritable polymer brushes. We used $(EtO)_3SiCH_2CH_2CH_2SH$ and anchored SH group on a silicon wafer (Figure 5.13d). The thiol-functionalized wafer was immersed in a DMF solution of Py-SS-Py (5 wt%) for 24 h, giving an SSPy-immobilized wafer (Figure 5.13a). Pre-synthesized PBA chains were anchored on the silicon wafer via a reaction of PBA-SH and the SSPy group on the surface, giving a PBA brush on the surface (Figure 5.13b) (writing process). The contact angle (Figure 5.13) significantly changed from 77.9° (anchored with SSPy group) to 98.2° (anchored with PBA). The disulphide bond was able to cleave by using a reducing agent, i.e., DTT (5 wt%) in DMF for 24 h, generating the original SH-immobilized surface (Figure 5.13d) with the contact angle of 87.6° (erasing process). DTT could be employed to cleave the disulphide bond in biomacromolecules, such as DNA and proteins. We may find possible applications in biomaterials. The surface with the same contact angle was obtained, demonstrating the complete erase of the attached polymer chain.

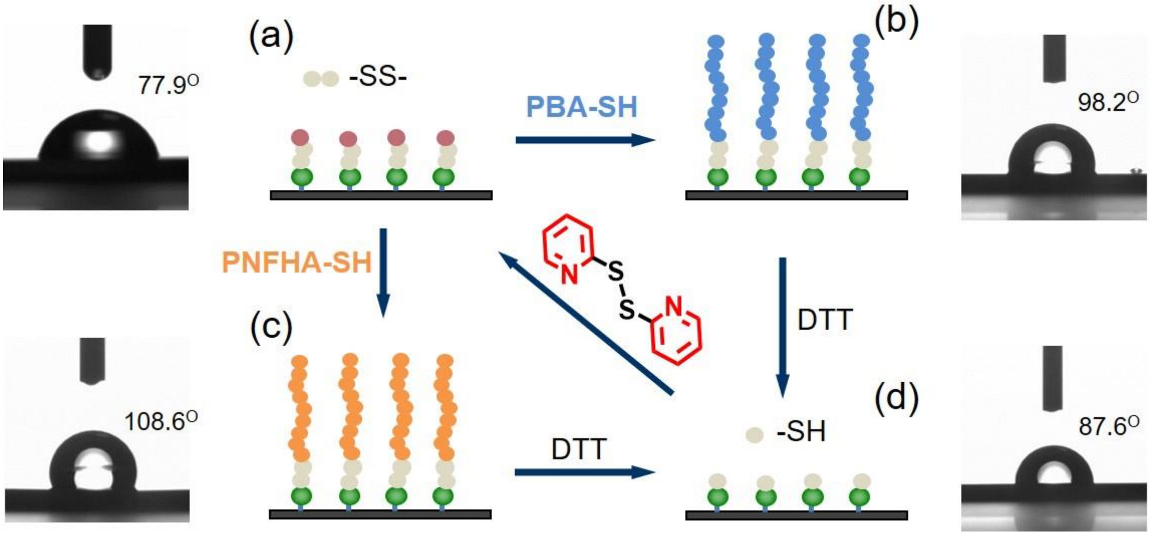

Figure 5.13. Fabrication of pyridyl disulphide group modified silicon water and reversible surface modification by using polymer-SH.

We anchored the SSPy group again and then another (super-hydrophobic) polymer, i.e., thiol-terminated poly(1*H*,1*H*,2*H*,2*H*-nonafluorohexyl acrylate) (PNFHA-SH), giving a PNFHA brush (Figure 5.13c) (rewriting process). The contact angle of the surface increased from 77.9° (anchored with SSPy group) to 108.6° (anchored with PNFHA). The PNFHA brush can also be erased by DTT (Figure 5.13d). The results demonstrate a rewritable surface using the thiol-disulphide exchange reaction.

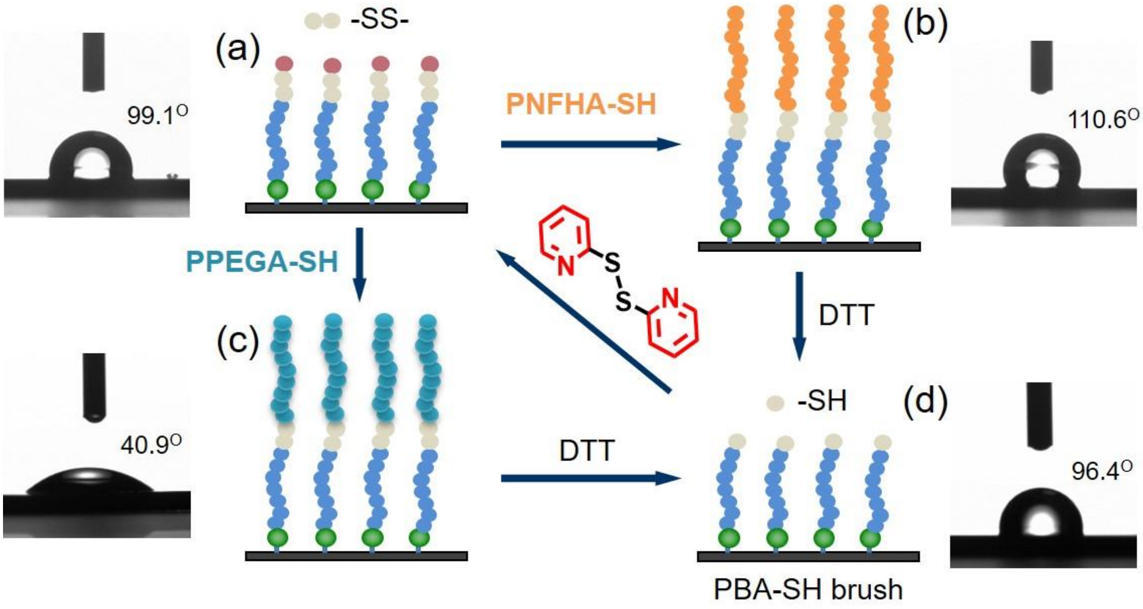

Figure 5.14. Reversible modification of PBA brushes using polymer-SH via a thiol-disulphide exchange reaction.

We also studied the reversible surface modification of polymer brushes. A polymer brush with a thiol group at the outermost surface can generate a block copolymer brush via a coupling reaction with an external polymer (Figure 5.14). A PBA-SH brush (Figure 5.14d) was prepared via post-modification of a PBA-I brush using $HSCH_2CH_2SH$, which subsequently reacted with Py-SS-Py to generate a PBA-SSPy brush (Figure 5.14a). Two different polymer chains, i.e., PNFHA (hydrophobic) (Figure 5.14b) and thiol-terminated poly(poly(ethylene glycol) methyl ether acrylate) (PPEGA-SH) (hydrophilic) (Figure 5.14c), were successfully attached on the

PBA-SSPy brush, providing hydrophobic (contact angle = 110.6°) and hydrophilic (contact angle = 40.9°) surfaces, respectively (writing process). In both cases, the anchored polymer chains are erasable, regenerating the original PBA-SH brush (contact angle = 96.4°) (Figure 5.14).

The anchored polymer can also be erased in a patterned manner (Figure 5.15). On a PNHFHA-*b*-PBA brush with a disulphide linkage, a mixture of DTT (5 wt%) and a photo-initiator Irgacure D-2959 (1 wt%) in DMF was dropped. A cover glass was placed to form an ultrathin solution layer, on which a photomask with a stripe pattern was placed. After UV irradiation for 5 min, the wafer was immersed in a DMF solution of a fluorescent molecule 7-diethylamino-3-(4-maleimidophenyl)-4-methylcoumarin (CPM) (Figure 5.15) (1 eq, 0.5 wt%) and TBA (2 eq) for 1 min. CPM molecule was attached on the surface via a thiol-ene Michael-addition. A clear fluorescence image with a stripe pattern was observed (Figure 5.15b), demonstrating the successful removal of the hydrophobic PNHFHA chains.

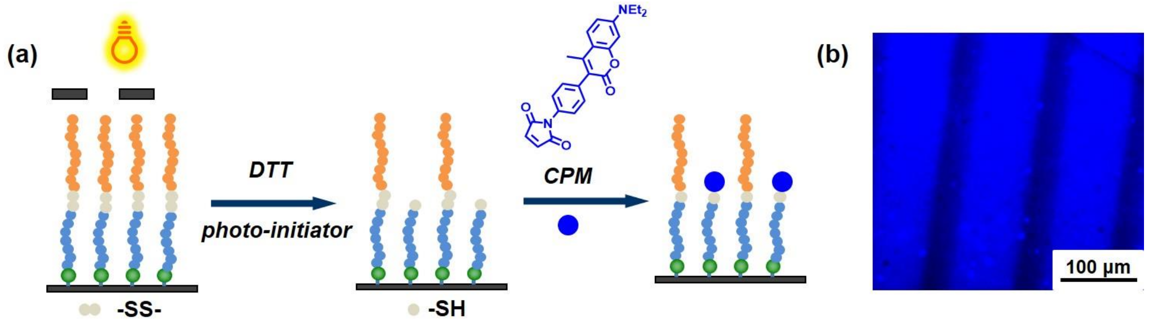

Figure 5.15. (a) Spatial erasure of the PNFHA chains and the attachment of CPM molecule. (b) Fluorescence microscope image of CPM-attached polymer brush.

5.3 Conclusions

We developed the chain-end reduction and chain-end functionalization methods of polymer-I by using commercially available thiols. Under UV irradiation, polymer-I was reduced yielding polymer-H in a rapid and nearly quantitative manner. The chain-end reduction was employed to fabricate patterned polymer brushes. In the masked area, the chain end still remained active and underwent block polymerization to give patterned polymer brushes. Patterned polymer brushes with different thicknesses and different patterns were prepared. In the dark condition using $HSCH_2CH_2SH$, polymer-SH could be obtainable, which could reversibly couple with the SSPy group on the surface via a disulphide linkage. Taking advantage of the reversible nature, we developed a writable, erasable, and rewritable surface, which may serve as a smart surface.

5.4 Experimental

Materials. butyl acrylate (BA) (>97%, Tokyo Chemical Industry (TCI), Japan), 2-Iodo-2-methylpropionitrile (CP-I) (>95%, TCI), 1*H*,1*H*,2*H*,2*H*-nonafluorohexyl acrylate (NFHA) (> 98%, TCI), poly(ethylene glycol) methyl ether acrylate (PEGA) (M_n = 480, Sigma-Aldrich, United States), tetrabutylammonium iodide (BNI) (>98%, TCI), 1,2-ethanedithiol (>99%, TCI), (3-Mercaptopropyl)triethoxysilane (>96%, TCI), 2-phenylethanethiol (98%, Sigma-Aldrich), 4-chlorobenzyl mercaptan (>98%, TCI), 2-mercaptoethanol (>99%, TCI), 2-propene-1-thiol (60%, Sigma-Aldrich), thioglycolic acid (98%, Sigma-Aldrich), DL-dithiothreitol (DTT) (>98%, TCI), methanol (>99%, International Scientific, Singapore), tetrahydrofuran (THF) (>99.5%, Kanto Chemical), tributylamine (TBA) (>98%, TCI), 2-hydroxy-4'-(2-hydroxyethoxy)-2-methylpropiophenone (Irgacure D-2959) (98%, Sigma-Aldrich), 7-diethylamino-3-(4-maleimidophenyl)-4-methylcoumarin (CPM) (>95%, Sigma-Aldrich), silver trifluoroacetate (AgTFA) (>98%, Sigma-Aldrich), *trans*-2-[3-(4-t-butylphenyl)-2-methyl-2-propenylidene]malononitrile (DCTB) (>99%, Fluka Chemicals, UK), and sodium trifluoroacetate (NaTFA) (>98%, TCI) were used as received. Formic-*d* acid (DCOOH) (95wt% in H_2O) (Sigma-Aldrich) was dried by $MgSO_4$ before use. The glass photomasks (Hunan Omnisun Information Materia, China) polished on both sides with a patterned low reflective chrome film on one side were used as received.

MALDI-TOF-MS. In this work, the same MALDI-TOF-MS machine was used with previous chapters. The THF solution of polymer (10 mg/mL), matrix (DCTB) (60 mg/mL), and cationization agent (AgTFA for PSt and NATHA for other polymers) (10 mg/mL) were prepared. We mixed polymer solution, the DCTB solution and the cationization agent solution in a ratio of 1/2/1 (volume ratio). Then, 5 µL of the mixed solution was dropped on the analysis plate, which was subsequently dried at the ambient condition.

UV-LED light. The UV-LED light source (C11924-101) (at 365 (± 10) nm) was purchased from Hamamatsu Photonics (Japan). The energy of the irradiating light per area was measured to be 900 mW/cm^2 with a power meter (FieldMate, Coherent, USA).

AFM. The polymer brush thickness was determined with an atomic force microscope (AFM) using a cantilever PRC-DF40P. We used the same AFM with previous chapters (see Chapter 4).

Syntheses procedures of Polymer-I (PBA-I, PPEGA-I and PNFHA-I). We mixed CP-I (1 eq), monomer (BA, PEGA or NFHA) (15 g, 50 eq), and BNI (4 eq) in a 100 mL flask with magnetic stirring, which was subsequently heated at 110 at 110 °C for a predetermined time (5h for PBA-I, 7.5 h for PPEGA-I, or 12 h for PNFHA-I) under an argon atmosphere. THF was then added to dilute the reaction mixture, and the THF solution was reprecipitate in a non-solvent (for PBA, methanol/H_2O (1/1, v/v); for PPEGA, hexane/diethyl ether (1/1, v/v); for PNFHA, chloroform). The obtained PBA-I and PPEGA-I was further purified by using preparative GPC to remove the remaining impurities.

Preparation of PS-I. We mixed St (10 g (8 M)), CP-I (160 mM), AIBN (60 mM), and Bu_4NI (40 mM) in a 100 mL flask under an argon atmosphere, which was subsequently heated at 80 °C for 9 h with magnetic stirring. THF was then added to dilute the reaction mixture, and the THF solution was reprecipitated in methanol. The polymer was further purification with preparative GPC to remove the remaining impurities.

General syntheses procedures of chain-end functionalization for polymers. A mixture of polymer-I (1 eq, 20 wt%), a thiol (20 eq), and $^iPr_2NH$ (4 eq) was dissolved in a good solvent (DMF for PBA and PPEGA, diethyl ether for PNFHA) in a reaction tube, and was stirred at room temperature in the dark for a predetermined time (10 min for PBA, 2 h for PPEGA and PNFHA). THF was added to dilute the reaction mixture, and then the THF solution was reprecipitated in a non-solvent (for PBA, methanol/H_2O (1/1, v/v); for PPEGA, hexane/diethyl ether (1/1, v/v); for PNFHA, chloroform). The chain-end functionalized PBA and PPEGA were further purified with preparative GPC to remove the remaining impurities.

General syntheses procedures of UV-induced chain-end reduction for PBA-I. A mixture of PBA-I (1 eq, 20 wt%) and a thiol (2 or 20 eq) in DMF was stirred under UV irradiation for a predetermined time. THF was added to dilute the reaction mixture, and then the THF solution was reprecipitated in a methanol/water mixture (1/1, v/v).

Chain-end reduction of PBA-I at 100 °C. We dissolved PBA-I (1 eq, 20 wt%) and $C_{12}H_{25}SH$ (20 eq) in DMF, and the mixture was heated at 100 °C with magnetic stirring for 1 h. The reaction mixture was diluted by THF, and then the polymer was reprecipitated in a methanol/water mixture (1/1, v/v).

Chain-end reduction of PSt-I. We dissolved PSt-I (1 eq, 20 wt%), $C_{12}H_{25}SH$ (20 eq), AIBN (5 eq), BNI (5 eq) and TBA (5 eq) in DMF, and the mixture was heated at 120 °C for 8 h with magnetic stirring. The reaction mixture was diluted by THF, and then the polymer was reprecipitated in methanol.

Preparation of IHE-immobilized and thiol-immobilized silicon wafer. A silicon wafer (0.8 cm × 0.8 cm) was rinsed with acetone and was sonicated in acetone for 30 min; The wafer was subsequently rinsed with chloroform and was sonicated in chloroform for 30 min; Then, the silicon wafer was rinsed with isopropanol and was sonicated in isopropanol for 30 min. The silicon wafer was dried with nitrogen flow, and further cleaned by using am ozone cleaner for 30 min. The silicon wafer was placed in a solution of IHE (for IHE-immobilized silicon wafer) (1 wt%) or $(EtO)_3SiCH_2CH_2CH_2SH$ (for thiol-immobilized silicon wafer) (1 wt%), aqueous ammonia solution (11 wt%), and ethanol (89 wt%) for 24 h. The modified silicon wafer was washed with ethanol (with sonification for 30 min), and then dried by using nitrogen, giving silicon wafers immobilized with IHE or thiol.

Preparation of PBA-I Brushes. In a Schlenk flask, we mixed CP−I (1 eq), BA (10 g, 1000 eq), and BNI (4 eq), and the IHE-immobilized silicon wafer was immersed in the solution under argon atmosphere. The mixture was then heated at 110 °C for a predetermined time. The silicon wafer was washed by using THF, and was sonicated in THF for 30 min. The silicon wafer was dried with nitrogen, giving a PBA-I brush immobilized silicon wafer. We used an AFM to determine the thickness (dry state) of the obtained polymer brush. The polymer brush was scratched, and the thickness is determined by the height gap between the scratched brush and the non-scratched brush. The M_n and $Đ$ of the non-immobilized polymers generated from CP-I (non-immobilized alkyl iodide initiator) and the height and surface occupancy (σ^*) of the obtained PBA brushes are summarized in Table 5.3.

Preparation of hydrogen and iodine patterned PBA brushes. We dissolved $C_{12}H_{25}SH$ (5 wt%) in DMF, and we dropped the solution on the prepared PBA-I brushes. Then, the silicon wafer was covered with a cover glass forming an ultrathin solution layer between the silicon wafer and the cover glass. We subsequently placed a photomask on the glass, and irradiated the silicon wafer by using a UV LED light (irradiation power = 900 mW/cm^2) for 10 min. After reaction, the silicon wafer was washed with THF and sonicated in THF form 30 min. After drying with nitrogen, the chain-end patterned (hydrogen and iodine) PBA brushes were obtained.

Preparation of patterned PBA brushes and patterned PBA and PBA-*b*-PHFBA brushes. In a Schlenk flask, we mixed CP−I (1 eq), monomer (BA for patterned homopolymer, HFBA for patterned block copolymer) (1000 eq), and BNI (8 eq). The hydrogen and iodine patterned PBA brushes were immersed in the solution under argon atmosphere. The mixture was heated at 110 ^{o}C for 24 h. The silicon wafer was washed with THF, and was sonicated in THF for 30 min. After dried by nitrogen, the patterned PBA or patterned PBA and PBA-*b*-PHFBA was obtained.

Preparation of PBA-SSPy. We dissolved PBA-SH (1 eq, 20 wt%) and Py-SS-Py (5 eq) in DMF in a reaction tube, and the solution was then stirred at ambient condition for 4 h. We added THF to dilute the reaction mixture, and the reaction mixture was then reprecipitated in a mixture of methanol/water (1/1, v/v). We further purify the product by using a preparative GPC to remove remaining impurities.

Oxidization of PBA-SH using iodine. We dissolved PBA-SH (1 eq, 20 wt%), iodine (2 eq) and TBA (2 eq) in DMF in a flask, the solution was then stirred in the dark for 12 h at ambient condition. We added THF to dilute the reaction mixture, and the reaction mixture was then reprecipitated in a mixture of methanol/water (1/1, v/v). We further purify the product by using a preparative GPC to remove remaining impurities.

Coupling reaction of PBA-SH and PBA-SSPy. We dissolved PBA-SH (1 eq, 10 wt%), PBA-SSPy (1 eq) and TBA (5 eq) in DMF in a reaction tube, and the solution was stirred in the dark for 12 h at ambient condition. We added THF to dilute the reaction mixture, and the reaction mixture was then reprecipitated in a mixture of methanol/water (1/1, v/v). We further purify the product by using a preparative GPC to remove remaining impurities.

Preparation of PBA-SH Brushes. We prepared a DMF solution of $HSCH_2CH_2SH$ (1 eq, 5 wt%) and iPr_2NH (0.2 eq), and we immersed a silicon water fabricated with PBA-I brush in the solution for 10 min at dark. The silicon wafer was then washed by THF, and sonicated in THF for 30 min. After dried by nitrogen, a PBA-SH brush was obtained.

Preparation of silicon wafer with pyridylthio groups. We prepared a DMF solution of Py-SS-Py (1 eq, 5 wt%), and we immersed a thiol-immobilized silicon wafer or a PBA-SH fabricated silicon water in the solution for 12 h at dark. The silicon wafers were then washed by THF, and was sonicated in THF for 30 min. After dried by nitrogen, the silicon wafers with pyridylthio groups were obtained.

General procedures for anchoring polymer-SH on surfaces via thiol-disulphide exchange reaction. A silicon wafer fabricated with pyridylthio groups was immersed in a solution of polymer-SH (10 wt%) (PBA-SH and PPEGA-SH in DMF, PNFHA in diethyl ether) and TBA (2 wt%) for 24 h. The silicon wafers were then washed by THF, and was sonicated in THF for 30 min. After dried by nitrogen, the silicon wafer fabricated with polymer brush was obtained.

Removal of the polymer chains on surfaces. The silicon wafers fabricated with polymer brushes with the disulphide linkage were immersed in a solution of DTT (5 wt%) (PBA-SH and PPEGA-SH in DMF, PNFHA in diethyl ether) and TBA (5 wt%) for 24 h. The silicon wafers were then washed by THF, and was sonicated in THF for 30 min. The silicon wafers were then dried by using nitrogen.

Spatially removal of PNFHA chains from PNFHA-*b*-PBA brush. We dissolve Irgacure D-2959 (1wt%) and DTT (5 wt%) in DMF, and we dropped the solution on the prepared PNFHA-*b*-PBA brush. Then, the silicon wafer was covered with a cover glass forming an ultrathin solution layer between the silicon wafer and the cover glass. We subsequently placed a photomask on the glass, and irradiated the silicon wafer by using a UV LED light (irradiation power = 900 mW/cm^2) for 5 min. After reaction, the silicon wafer was washed with THF and sonicated in THF form 30 min. The silicon wafer was then dried by using nitrogen.

CPM Labeling of patterned PBA and PNFHA-*b*-PBA brush. The patterned PBA and PNFHA-b-PBA brush were immersed in a mixture of CPM (0.5 mg/mL, 1 eq), TBA (2 eq), and DMF for 1 min in the dark at ambient condition. The silicon wafer was washed with THF, and was sonicated in THF form 30 min. The silicon wafer was then dried with nitrogen. A fluorescence picture was taken by using a fluorescence microscope (same with previous chapter).

5.5 References

1. Section 4.5, ref. 1.
2. Section 4.5, ref. 2.
3. Section 4.5, ref. 4.
4. Section 4.5, ref. 6.
5. Section 1.8, ref. 58.
6. Zdyrko, B.; Luzinov, I. *Macromol. rapid Comm.*, **2011**, *32*, 859-869.
7. Hansson, S.; Trouillet, V.; Tischer, T.; Goldmann, A. S.; Carlmark, A.; Barner-Kowollik, C.; Malmström, E. *Biomacromolecules* **2012**, *14*, 64-74.
8. Section 1.8, ref. 61.
9. Edmondson, S.; Osborne, V. L.; Huck, W. T. *Chem. Soc. Rev.* **2004**, *33*, 14-22.
10. Section 4.5, ref. 15.
11. Section 3.5, ref. 22.
12. Section 4.5, ref. 18.
13. Section 1.8, ref. 54.
14. Section 1.8, ref. 55.
15. Section 3.5, ref. 25.
16. Section 4.5, ref. 24.
17. Section 3.5, ref. 27.
18. Anastasaki, A.; Willenbacher, J.; Fleischmann, C.; Gutekunsta, W.R.; Hawker, C.J. *Polym. Chem.* **2017**, *8*, 689−697.
19. Du, X.; Li, J.; Welle, A.; Li, L.; Feng, W.; Levkin, P. A. *Adv. Mater.* **2015**, *27*, 4997-5001.
20. Li, L.; Feng, W.; Welle, A.; Levkin, P. A. *Angew. Chem. Int. Ed.* **2016**, *55*, 13765-13769.
21. Blinco, J. P.; Trouillet, V.; Bruns, M.; Gerstel, P.; Gliemann, H.; Barner-Kowollik, C. *Adv. Mater.* **2011**, *23*, 4435-4439.
22. Lowe, A. B. *Polym. Chem.* **2010**, *1*, 17-36.
23. Section 4.5, ref. 40.
24. Section 3.5, ref. 18.
25. Nagy, P. *Antioxid. Redox Sign.* **2013**, *18*, 1623-1641.
26. Section 3.5, ref. 20.

Chapter 6 Conclusions

Polymer-I with narrow molecular weight distribution and high chain-end fidelity was synthesized via RCMP. Chain-end modification methods, in which the polymer-I was converted to either chain-end functionalized polymers or chain-end reduced polymers, were successfully developed. Novel chain-end patterned polymer brushes were firstly reported via selective chain-end modification methods. Patterned polymer brushes and rewritable polymer brushes on the surface were also successfully synthesized.

In Chapter 2, polymer-I was converted to chain-end functionalized polymers via the substitution reaction of polymer-I and primary amines. Several functional groups, such as SH, OH, phenyl, alkyl, and $Si(OEt)_3$, were successfully introduced at the polymer chain end. The chain-end functionalization of PBA-I and PSt-I were studied in detail by using different primary amines. In the case of PBA-I, a ring-closure occurred to generate a 5-member lactam following the substitution reaction of PBA-I and primary amines. By controlling the amount of $NH_2CH_2CH_2OH$ (stoichiometric amount (2 eq) or excess amount (20 eq)), one OH group or two OH groups can be selectively introduced at the PBA chain end respectively. At different temperatures, i.e., high temperature (100 °C) or room temperature, the reaction of PBA-I with $NH_2CH_2CH_2SH$ underwent a radical process or substitution reaction to generate PBA-H or PBA-SH, respectively. The chain-end functionalization is quantitative, easy to operate, and free from metal, which are attracting features and may find promising biomedical applications.

In Chapter 3, a selective modification method of polymer-I was developed by using biocompatible cysteamine. By controlling the light on and off, the polymer-H and polymer-SH were quantitatively synthesized. This selective modification is facile and amenable to the presence of moisture and oxygen, which are attractive for practical uses. This photo-induced selective modification method was applied to prepare novel chain-end patterned polymer brushes on the surface in a single step. The chain-end patterned brushes with thiol (reactive) and hydrogen (inert) groups may find useful applications, such as biomolecular and ionic recognitions.

In Chapter 4, the selective modification of polymer-I was developed by co-using formic acid and primary amines (NH_2-R-X), and the scope of the functional groups was broadened from the only thiol to various functionalities, such as hydroxyl, alkynyl, and triethoxysilyl groups. With and without photo irradiation, polymer-I underwent an amine-catalyzed reduction and a substitution reaction to generate polymer-H and various chain-end functionalized polymers (polymer-NH-R-X), respectively. This selective chain-end modification is metal-free and amenable to a broad range of functional groups and polyacrylates. Different chain-end patterned polymer brushes, i.e., OH and H patterned polymer brushes and alkyne and H patterned polymer brushes, were fabricated by employing this selective chain-end modification method. This selective chain-end modification method can be utilized as a platform technique to prepare chain-end patterned polymer brushes with designed functionalities.

In Chapter 5, chain-end modification methods of polymer-I using primary thiols (RSH) were developed. A broad range of chain-end functionalized polymers (polymer-SR) were successfully prepared in a quantitative and rapid manner (10 min). A broad scope of primary thiols with various functional groups are commercially available. This fast chain-end functionalization is facile to perform, which is favored for practical uses. Thiol-terminated polymers (polymer-SCH_2CH_2SH) were successfully synthesized by using 1,2-ethanedithiol ($HSCH_2CH_2SH$), which were reversibly attached on a solid surface via a thiol-disulphide reaction giving rewritable polymer brushes as an interesting application.

The polymer-I was also thermally and photochemically reduced to polymer-H by using thiol as a good hydrogen donor. Under UV irradiation, the chain-end reduction is quantitative and swift (with 10 min). This UV-induced chain-end reduction was employed to fabricate patterned homopolymer brushes and patterned block copolymer brushes on the surface.

Efficient and quantitative chain-end modification methods were developed to produce several chain-end functionalized polymers. Developing the application of the chain-end functionalized polymers will be interesting to study in the future. They can be anchored on solid surfaces to produce composite materials, such as silicon, titanium oxide, and glass substrates. Polymer brushes with designed functionalities are also attractive to produce stimuli-responsive materials. Polymer brushes with thiols at the chain ends can be reversibly oxidized to disulphide among the polymer chains, from which polymer brushes with a complex loop structure can be obtained (Figure 6.1a). The architectural transformation could be also achieved in a patterned manner (Figure 6.1b). Stimuli-responsive sensor materials and polymer brushes with complicated architectures could be designed through introducing specific functionalities at the chain ends of the polymer brushes.

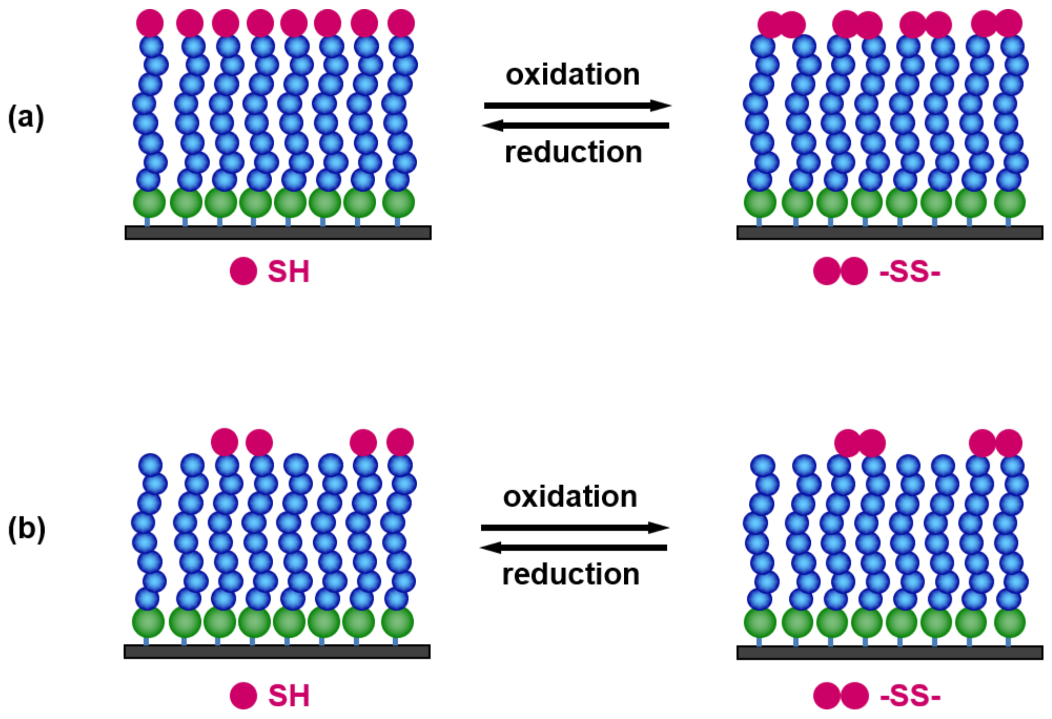

Figure 6.1. Reversible fabrication of polymer brushes with a loop structure.